FIXATION AND STABILIZATION OF HEAVY METALS IN A PRODUCT COMPOSED OF FLY ASH AND INDUSTRIAL ACIDIC WASTES

A Thesis Submitted to
the Graduate School of Engineering and Sciences of
İzmir Institute of Technology
in Partial Fulfillment of the Requirements for the Degree of

DOCTOR OF PHILOSOPHY

in Chemical Engineering

by
Berna ÜZELYALÇIN ÜLKÜ

July 2010
İZMİR

We approve the thesis of **Berna ÜZELYALÇIN ÜLKÜ**

_____
Prof. Dr. Mehmet POLAT
Supervisor

_____
Prof. Dr. Hürriyet POLAT
Co-supervisor

_____
Prof. Dr. Devrim BALKÖSE
Committee Member

_____
Prof. Dr. Mustafa DEMİRCİOĞLU
Committee Member

_____
Assoc. Prof. Dr. Alper BABA
Committee Member

_____
Assoc. Prof. Dr. Selahattin YILMAZ
Committee Member

07 July 2010

_____
Prof. Dr. Mehmet POLAT
Head of the Department of
Chemical Engineering

_____
Assoc. Prof. Dr. Talat YALÇIN
Dean of the Graduate School
of Engineering and Sciences

ACKNOWLEDGEMENTS

ABSTRACT

FIXATION AND STABILIZATION OF HEAVY METALS IN A PRODUCT COMPOSED OF FLY ASH AND INDUSTRIAL ACIDIC WASTES

Large quantities of fly ash are produced in the world while only a very small portion of it finds utilization as a product. Since even larger quantities of fly ash should be expected to be generated in an increasingly energy-hungry world, finding new, smart pathways towards fly ash utilization carries its own weight in achieving sustainable development. Manufacturing light-weight fly ash aggregates which could also be used as sinks for other wastes with acceptable environmental foot-print and possible added value is exactly one such pathway.

This thesis comprises of the studies where a fly ash sample from a large Thermal Power Plant (Soma fly ash) is used to stabilize an extremely acidic industrial waste in an aggregate structure with the aim that the aggregates produced had acceptable environmental impact and possible product value.

The study is divided into several parts. Initial chapters contain the characterization studies of both the fly ash from Soma, Manisa Thermal Power Plant and the highly acidic industrial waste from a metal stripping factory in Cigli-Izmir. Later chapters contain the methodology and the experimental parts of the work. The acidity of the aggregates was also optimized keeping in mind the present environmental regulations. Solid/liquid ratio, effect of aging of the aggregates, effect of leaching from the aggregates and their mechanical strengths were the main experimental parameters investigated. Mineralogical composition of the aggregates was compared with the raw fly ash to shed light on the fixation mechanism.

The fly ash was rich in especially Si, Al and Ca and some heavy metals in trace amounts whereas the acidic waste contained huge amounts of Zn, Fe and other heavy metals. This study demonstrated conclusively that the acidic waste was not only neutralized by the fly ash to disposable levels, but also that the leaching of both the major and minor elements from the aggregate body into the water was below the environmental limits in force both in Europe and Turkey today. The produced aggregates were also observed to possess the low-strength-material properties which open the possibility for their utilization in construction applications.

ÖZET

AĞIR METALLERİN UÇUCU KÜL VE ENDÜSTRİYEL ATIKLARDAN OLUŞMUŞ BİR ÜRÜN BÜNYESİNDE SABİTLENMESİ VE STABİLİZASYONU

Dünyada her yıl büyük miktarlarda uçucu kül üretilmesine rağmen, bunun çok az bir bölümü bir ürüne dönüştürülebilmektedir. Her gün artan enerji ihtiyacına karşılık ileride çok daha fazla uçucu kül üretimi olacağı düşünüldüğünde, uçucu külleri değerlendirmede yeni ve akılcı yollar bulmak, sürdürülebilir kalkınma açısından büyük önem taşımaktadır. Bünyesinde farklı atıkları barındıran, çevreye dost ve katkı değeri yüksek olan düşük dayanımlı agrega malzemelerin üretimi, bu yollardan biri olarak gösterilebilir.

Bu tez, uçucu kül kullanılarak yapılan bir çalışmadır. Soma Termik Santrali uçucu külü, son derece asidik endüstriyel bir atığı bir agrega malzeme bünyesinde sabitleştirerek, çevresel olarak kabul edilebilir ve ürün değeri olan bir malzeme üretmek üzere kullanılmıştır.

Çalışma birkaç kısımdan oluşmaktadır. İlk bölümlerde Soma-Manisa Termik Santrali uçucu külü ve Çiğli-İzmir'de bulunan bir metal işleme fabrikasından alınan asidik atığın karakterizasyonu çalışmaları yer almaktadır. Sonraki bölümlerde çalışmanın yöntemi ve deneysel detayları yer almaktadır. Agregaların asitliği, şu an geçerli olan çevre yönetmeliklerinde yer alan standartlar doğrultusunda optimize edilmiştir. Katı/sıvı oranı, agrega kurutma süresinin etkisi, özütleme zamanının agregalar üzerine etkisi ve agreganın mekanik özellikleri, incelenen bellibaşlı deneysel parametrelerdir. Uçucu külün ve agregaların mineralojik yapıları, elementlerin tutunma mekanizmalarını açıklamak üzere incelenmiştir.

Uçucu kül yüksek oranda Si, Al, Ca ve iz olarak ağır metaller içerirken, asidik atık olağanüstü miktarda Zn, Fe ve diğer toksik elementleri içermektedir. Bu tez çalışması sonuç olarak, asidik atığın çevreye bırakılabilir şekilde nötralize edilebildiğini göstermekle kalmayıp, agrega bünyesinden suya özütlenen major ve minör elementlerin miktarlarının Türkiye ve Avrupa çevresel limitlerinin altında olduğunu da göstermiştir. Üretilen agrega malzemelerin ayrıca düşük dayanımlı dolgu malzemesi olarak belirlenmesi, bu malzemenin inşaat uygulamalarında kullanılabilirliğine de fırsat vermektedir.

to my mother

TABLE OF CONTENTS

LIST OF TABLES

LIST OF FIGURES

LIST OF SYMBOLS/ABBREVIATIONS

AG	Aggregate
AOIZ	Atatürk Organized Industrial Zone
ASTM	American Society for Testing of Materials
AMD	Acidic Mine Drainage
AW	Acidic Waste
A/W	Aggregate/water ratio
CEN	European Comitee for Standardization
DTA	Differential Thermal analysis
E	Ultimate stress
EDX	Energy Dispersive X-ray Analyzer
EPA	Environmental Protection Agency
FTIR	Fourier Transform Infrared Spectrometry
ICP-AES	Inductively Coupled Plasma-Atomic Emission Spectrometry
ICP-MS	Inductively Coupled Plasma-Mass Spectrometry
SFA	Soma Fly Ash
MeOH	Metal hydroxide
S/L	Solid/liquid ratio (Fly ash/Acidic Waste)
SEM	Scanning Electron Micrograph
TCLP	Toxicity Characteristic Leaching Procedure
TGA	Thermogravimetric Analysis
XRD	X-ray Diffraction
σ_u	Young's modulus

CHAPTER 1

INTRODUCTION

1.1. Problem Definition

Controlling or elimination of large amounts of industrial wastewater is an expensive activity (Wang and Viraraghavan, 1997; Gupta and Torres, 1998). Effluents from metal plating, mining, metallurgy, tanneries and painting industries are laden with heavy metals and hazardous compounds and must be disposed off properly to prevent risks to soil and groundwater (Papandreou et al., 2007). Such wastewaters can be treated by chemical, physicochemical and biological methods (Üzelyalçın and Polat, 2004). Neutralization is a convenient chemical method that can be used to easily neutralize the industrial wastes. Neutralization of industrial effluents elimination of toxic metal ions by low cost adsorbents such as "fly ash" have been suggested by numerious studies in the literature (Theis and Wirth, 1977; Talbot et al., 1978; Viraraghavan and Rao, 1991; Jackson et al., 1999; Gupta, 2000; Hequet et al., 2001; Ricou et al., 2001; Lin and Chang, 2001; Bayat, 2002; Polat et al., 2002a,b, Polat et al., 2007).

Fly ash is a by-product from coal-fired electric power generating plants and contains metal oxides, silicates, sulfur compounds and many other chemical pollutants in its structure. EPA (Environmental Protection Agency) of United States defines fly ash as non-combustible residual particles expelled by flue gas. The coal fly ash has many potential uses in the industry; portland cement and grouts (Sheng et al., 2003; Krishnamoorthy et al., 2002), embankments and structural fill (Singh et al., 2008; Horiuchi et al., 2000), waste stabilization and solidification (Kumpiene et al., 2007; Camacho and Munson Mc-Gee, 2006), raw feed for cement clinkers (Bouzoubaa et al., 1997), mine reclamation (Ciccu et al., 2003), wastewater treatment (Cho et al., 2005), mineral fill in asphaltic concrete (Zoorob et al., 2000), cellular concrete (Brylicki and Lagosz, 1997), geopolymers (Andini et al., 2008), glass ceramic tiles (Leroy and Ferro, 2001), metal castings (Deng and Tikalsky, 2008), and filler in wood and plastic products (Potgieter-Vermaak et al., 2005) are to name only a few. Annual production of fly ash in the world is 450 million tones and only 6% of this amount is re-utilized. In

Turkey, 11 coal consuming power plants produce 15 million tonnes of fly ash and not a negligible part is used in industrial applications (Ülkü et al., 2008).

Studies present in the literature, where heavy metal-rich and extremely acidic wastes were scrubbed and neutralized using fly ashes from Turkey and Israel. At proper fly ash/waste ratios, the fly ash in the aggregate structure acted as neutralizer for the acidic waste due to its basic nature and the leaching of heavy metals from the aggregates was below the environmental limits within a pH range between 3 and 9 (Polat et al., 2002a; Polat et al. 2002b; Polat, et al., 2007). Heavy metals in the metals seemed to be are physically and chemically "fixed" in produced stabilized material structure. This means that the mobility of metals is significantly reduced in the aggregates, compliant with the environmental regulations. Moreover, the utilization of the produced aggregates is feasible in construction applications with adequate stress-strain properties (Dermatas et al., 2003).

1.2. Scope and Objectives of Study

The major objective of this study is to explore the possible utilization of a coal fly ash from Soma Thermal Power Plant for managing extremely acidic/toxic waste from Atatürk Organized Industrial Zone (AOIZ). The specific objectives of this research and the tasks performed in order to achieve these objectives are;

i.   *to evaluate and determine if coal fly ash collected from the Soma Thermal Power Plant has suitable geotechnical and geoenvironmental properties required for use in industrial acidic waste treatment.*

In order to achieve this above sub-objective, the following specific tasks were performed:

i. Characterize the physicochemical and mineralogical properties of fly ash collected from Soma Thermal Power Plant;

ii. Evaluate and compare the acid neutralization capacity of Soma fly ash;

iii. Assess the potential environmental impacts associated with the utilization of Soma fly ash by examining the leaching behavior of metals.

ii. *to evaluate the potential use of coal fly ash to neutralize extremely acidic waste*

In order to achieve the above objective, the following specific tasks were performed:

    i. Characterize the industrial acidic wastes collected from AOIZ;

    ii. Evaluate the level of acidity of industrial acidic waste;

    iii. Study the theoretical and experimental neutralization capacity of coal fly ash and industrial acidic waste with preliminary tests.

iii. *to fix the metals exist in these wastes (ash and acidic waste) in the structure of produced aggregate.*

In order to achieve the above objective, the following specific tasks were performed:

    i. Production of aggregates as pellets by mixing the raw pulverized fly ash with acidic waste in pre-determined liquid/solid ratios under various operating conditions;

    ii. Determination of amount of release of toxic metals, pH variations within time, neutralization potential of the ashes, effect of the drying time, solid/liquid ratios and liquid/water ratios.

iv. *to characterize the resulting solid aggregate to determine the mechanisms of neutralization and fixation.*

In order to achieve the above objective, the following specific tasks were performed:

    i. Determination of the mechanism of neutralization and stabilization of heavy metals in aggregate structure by detecting the minerals precipitating out during the process;

    ii. Study the mechanical properties of aggregates to evaluate the use of produced aggregates for construction applications.

1.3. Thesis Outline

The thesis consists of six chapters, the contents of which are as follows:

Chapter 1 introduces the theme of the thesis, outlines the scope and objectives of the research, and states the contributions of the study to the research on coal fly ash utilization for industrial acidic waste management.

Chapter 2 reviews available literature on coal fly ash and industrial acidic waste treatment problems. Chemistry and formation of fly ash and acidic waste, current technologies implemented or under investigation to prevent and treat wastes were investigated.

Chapter 3 presents results of the engineering and geo-chemical characterization of Soma fly ash with respect to acidic waste treatment applications. The solubility characteristics of toxic elements associated with fly ash and their possible environmental impacts are discussed.

Chapter 4 examines the materials and experimental methods used in the thesis.

Chapter 5 presents and discusses the results of characterization of Soma Fly ash, industrial acidic waste and the aggregate characterization to evaluate the fixing and stabilization mechanism of major ions and trace elements in aggregate structure. The mechanical properties of the solid product are also investigated for use of it in industrial applications.

Chapter 6 presents the overall summary and conclusions made from the findings of the research as well as some recommendations for further research and possible improvements for the use of coal fly ash in acidic waste management.

1.4.   Originality of the Thesis and Major Contributions

The work described in this study involved field sampling, laboratory experiments, and theoretical analysis using geochemical modeling. Based on the results obtained, this thesis presents the following important contributions to knowledge:

i.   The thesis presents comprehensive laboratory techniques used to identify suitable geotechnical and geoenvironmental properties of coal fly ash that is important for environmental applications such as acidic waste management.

ii.   It also assesses the potential utilization of coal fly ash and an acidic waste to produce an aggregate material and attempts to ascertain the major chemical and mineralogical changes that occurred in the aggregates during neutralization and stabilization processes.

iii.   One other major contribution of this thesis is designing an experimental program to stabilize industrial acidic wastewater using coal fly ash. Equilibrium modelling was used to determine the optimum conditions to prevent the release of heavy metals from the aggregate structure.

CHAPTER 2

LITERATURE REVIEW

2.1. Fly Ash

Fly ash is a fine powdery particulate material which is produced from the burning of pulverized coal in a coal-fired boiler and carried off in the flue gas. Some electrostatic or mechanical collection devices are used to collect the fly ash in flue gas by means of electrostatic precipitators, bag houses, or cyclones. Coal-fired boiler furnaces used in industry are three types; dry-bottom boilers, wet-bottom boilers, and cyclone furnaces. The dry-bottom furnace is the most common type. Pulverized coal is combusted in a dry-ash, dry-bottom boiler and approximately 80 percent of all the ash leaves the furnace as fly ash (Hall and Livingston, 2001).

Fly ash, which is a coal combustion residue, is a complex heterogeneous material. Because of the poor combustion efficiency of the combustors, lack of proper quality control in maintaining the particle size of the pulverised coal feed etc, the fly ash has a wide distribution of char, semi-coke or coked carbon matters of large dimension (90–300 μm). It is irregularly shaped, containing vesicular, alumino-siliceous matter of complex composition and fine solid/hollow alumino-siliceous spheres (Sarkar et al., 2006). The chemical composition of fly ash varies depending upon the type of coal used in combustion, combustion conditions and removal efficiency of air pollution control device.

The fly ash chemical composition directly depends on the source of coal. For example the lignitic and subbituminous coals of western region in Turkey are rich in calcium and bituminous and anthracites coals of eastern region are rich in silica and alumina (Apak et al., 1998; Querol et al., 1999; Polat et al., 2002a; Polat et al., 2002b; Bayat, 2002; Ural, 2005; Vassileva et al., 2005; Karayiğit et al., 2005; Doğan and Kobya, 2006; Eren and Acar, 2007). Utilization of fly ash can be in the form of an alternative to another industrial resource, process, or application. Some of these processes are addition to cement and concrete products, structural fill and cover material, waste stabilization/solidification, roadway and pavement utilization, addition

to construction materials as a light-weight aggregate, infiltration barrier and underground void filling, and soil, water and environmental improvement (Manz, 1999, Mohapatra and Rao, 2001; Iyer and Scott, 2001; Hall and Livingston, 2001).

2.1.1. Utilization of Fly Ash in the World

Fly ash is a pozzolanic by-material produced in coal-burning thermal power plants, that is annually generated by the coal industry in gigascale quantities (Marthur et al., 2003). This class of industrial by-product material, if not utilized, is generally 'landfilled' as part of daily management practices. Worldwide, China-India axis is currently the largest producer of fly ash followed by Russia and USA. According to the report released by Coal Industrial Society of China in January 2009, China produced 1.09 billion tons of coal and generated 81.8% of the total electricity in 2005 (Zhou et al., 2006). The total amount of coal burned was about 2.716 billion tons in 2008 which was 7.65% higher than last year (Dai, 2010). Meanwhile, 293 million tons of coal combustion residues were generated by Chinese power plants in 2005 (Zhou et al., 2006). This amount is expected to increase every year. Presently about 110 million tonnes of coal-ash is generated in India in more than 70 thermal power plants (Sarkar et al, 2005). By the year 2012 this is predicted to increase to 170 million tones per annum. In India, at present, the major portion of fly ash produced goes for disposal in ash ponds and landfills and only a small fraction of it is utilized (Bhattacharjee et al., 2002). The utilization rate (13%) is far below the global utilization rate (25%) (Iyer et al., 2001; Sushil and Batra, 2006).

On a worldwide basis, 450 million of metric tons of fly ash are produced annually; only a small portion e.g., 20 to 40% of the fly ash is re-utilized for industrial applications such as an additive or stabilizer in cement. The remaining amount of fly ash is disposed to controlled landfills or held for future use (Landman, 2003).

The disposal of these vast quantities of fly ash is costly, for that reason, new, innovative and environmentally safe utilization techniques are developed (Shackelford et al., 2000).

Fly ash is generated in large amounts in the countries where the electricity production depends on coal-powered power plants. For example, in Turkey, every year about 15 million tons of fly ash is discarded into environment with close to zero re-use

ratios. Manz (1999), searched the production and utilization of fly ashes especially in concrete in the world and documented the information country by country. According to this article, about 91 000 tons of this amount are used in blended cement.

In 1994, approximately 6.74 million metric tons (7.42 million short tons) of coal fly ash was used in the United States in cement and concrete products. The amount of fly ash in typical structural concrete applications ranges from 15 to 35 wt%, with amounts of up to 70 wt% for mass concrete in dams, walls, and girders and for roller compacted concrete pavements and parking areas (Manz, 1999).Worldwide, specifications for fly ash use in Portland cement concrete are the most common compared to stabilization, structured fill, and other uses.

The ECOBA (European Coal Combustion Products Association) member countries account for 90% of CCP (Coal Combustion Products) in Europe, producing 37.14 million tonnes of fly ash and utilizing about 48% of it (Kalyoncu, 2001).

It has been estimated that total amount of ash produced in Europe in 1997 was 63 million tons (Hall et al., 2001).

2.1.2. Overview of Production, Use and Disposal of Fly Ash in Turkey

Turkey produces more than 15 million tons of fly ash annually but only a small amount is utilized. The reasons for low utilization are; high transportation costs, (90% of the transportation is by highways), availability of raw materials within a 50 km range and conventional construction techniques of which the 28 days compressive strength requirement is above 20 MPa. The amount utilized is realized by blended cement production and some local facility constructions. Another reason is that the engineering performance of fly ash varies in a very large scale depending on the production and handling procedures followed. The necessity of continuous process during fly ash utilization (which results in providing sufficient storage for fly ash with adequate quality) and the necessity to continuous property analysis are the other reasons for increased cost. Also, the use of fly ash utilization methods requires the medium technical skills, so the use of it in applications is not preferred (Vassilev et al., 2004).

The preliminary studies (Karayigit et al., 2000) have shown that some industrial Turkish coals have trace element contents higher than the world average for coals and in

some cases concentrations even above the recorded maximums for World coals (Swaine, 1990).

2.1.3. Background of Coal Fly Ash Properties

Fly ash consists of fine, powdery particles that are predominantly spherical in shape, either solid or hollow, and mostly glassy (amorphous) in nature. The carbonaceous material in flyash is composed of angular particles. The particle size distribution of most bituminous coal fly ashes is generally similar to that of silt (less than a 0.075 mm or No. 200 sieve). Although subbituminous coal fly ashes are also silt-sized, they are generally slightly coarser than bituminous coal fly ashes.

The specific gravity of fly ash usually ranges from 2.1 to 3.0, while its specific surface area (measured by the Blaine air permeability method) may range from 0.17 to 1.0 m^2/gram (Mohapatra and Rao, 2001).

Depending on the amount of unburned carbon in the ash, the color of fly ash can vary from tan to gray to black. If the carbon content is low, color of the fly ash turns to lighter. Lignite or subbituminous fly ashes are usually light tan to buff in color, indicating relatively low amounts of carbon as well as the presence of some lime or calcium. Bituminous fly ashes are usually some shade of gray, with the lighter shades of gray generally indicating a higher quality of ash.

Fly ash has a characteristic structure which consists of spherical microscopic spheres (Figure 2.1). The spheres, if they are empty, are referred to as cenospheres. As the molten droplets of inorganic coal residues cool down fly ash particles solidify and separate out as spheres, with those solidifying around a trapped gas bubble being hollow. Cenospheres can easily be isolated using flotation and many industrial applications. The content of cenosopheres in fly ash is related to the furnace temperature and coal composition; fly ashes from fuel oil combustion consist almost entirely of cenospheres. Spherical and irregular-fused particles of pulverized fly ash are of good quality and are suitable for cementitious building materials (Mohapatra and Rao, 2001). The phase-mineral composition of cenospheres includes mostly aluminosilicate glass, mullite, quartz, calcite, Fe oxides, and Ca silicates and sulphates (Vassilev et al., 2004).
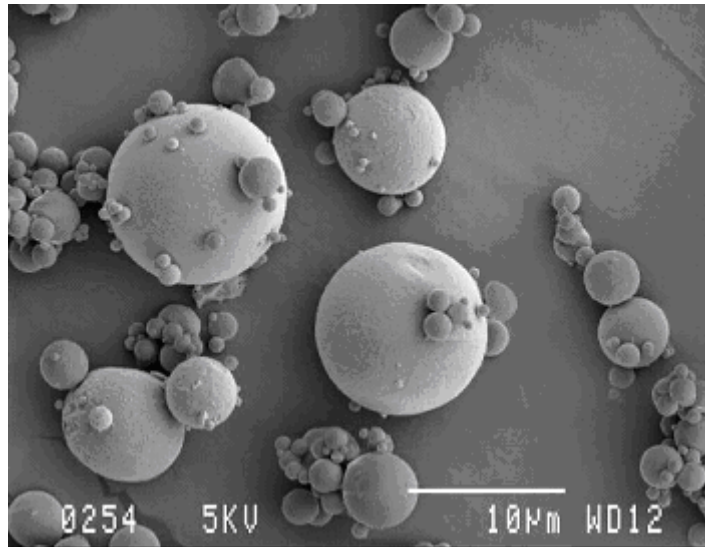
Figure 2.1. Spherical microstructure of fly ash

The resultant physical properties of the ash, such as moisture content, particle mass, glass composition and the portion of unburned carbon, will depend on the combustion temperature at which the coal was fired, the air/fuel ratio, coal pulverization size and rate of combustion. ASTM (American Society for Testing of Materials) standard C 618-95 defines two classes of ash, F and C ashes. The chemical differences that ASTM standard C 618-95 uses to differentiate between class F and C ash compositions are detailed in Table 2.1 (Scheetz and Earle, 1998). Beside them Class F fly ash contains less than 10% lime (CaO). On the other hand, Class C fly ash will harden and gain strength over time and generally contains more than 20% lime.

.

Table 2.1. ASTM Standard C 618-95 Chemical Requirements for Fly Ash Class

Chemical differences (%)	F	C
Silicon dioxide (SiO_2)+aluminum oxide (Al_2O_3)+ iron oxide (Fe_2O_3), min	70.0	50.0
Sulfur trioxide (SO_3), max	5.0	5.0
Moisture content, max	3.0	3.0
Loss on ignition, max	6.0	6.0
Available alkalis (as Na_2O) max	1.5	1.5

Fly ash can be approximated as an aluminosilicate and can be used like other minerals. The amorphous aluminosilicate nature of fly ash makes the chemical structure of fly ash difficult to characterize, but also very versatile, since the glassy phase reacts first before the crystalline phase, and also goes into solution first (Landman, 2003).

As the coal is combusted, mineral matter transforms to fix ash and is thermally altered into different forms, many of which are by themselves chemically very reactive or which can be chemically activated. The term used to describe this behavior is 'pozzolanic'. Fly ash has found many uses which are based upon both the bulk chemical and mineralogical make-up of the ash and upon the physical size distribution and shape of the ash (Vassilev et al., 2004).

The mineralogy of fly ash can be described using X-ray diffraction and in many sources the mineralogy of fly-ash relates to the minerals in the coal. The main phases are glass, mullite, quartz, magnetite, hematite and anhydrate. Although fly ash contains many potentially toxic trace elements, leaching tests have shown that these are relatively stable within the aluminosilicate matrix. Accordingly fly ash is not classified as a hazardous waste in America. The only element that might pose a problem is hexavalent chromium. During combustion, the mineral matter in coal structure transforms into other compounds, which are mainly carried with the flue gases as fly ash. The primary components of power station fly ash are silica (SiO_2), alumina (Al_2O_3) and iron oxides (Fe_2O_3), calcium as lime (CaO) or gypsum ($CaSO_4$) and whether strong basic oxides such as MgO, Na_2O, K_2O and a portion of unburnt carbon. X-ray diffraction studies revealed quartz (SiO_2), mullite ($3Al_2O_3 \cdot 2SiO_2$) and frequently hematite (Fe_2O_3), magnetite (Fe_3O_4), calcium sulphate ($CaSO_4$), calcium oxide (CaO) and periclase (MgO) in crystalline phases in the fly ash (Corigliano et al., 1997).

Trace elements which associate with coal during and following coalification are further enriched in the ash upon burning. Fly ash may contain from 20 to 50 trace elements (Scheetz and Earle, 1998). Some are found in an aluminosilicate matrix (Ti, Na, K, Mg, Hg, Fe), some are determined at the surface (As, Se, Mo, Zn, Cd, W, V, U) while others are found in an acid soluble phase (Ca, Sc, Sr, La, rare earth elements, and probably Ni). The elements Mn, Be, Cr, Cu, Co, Ga, Ba and Pb are dispersed between the aluminosilicate matrix and acid soluble phase. Most metals display an association with a certain surface oxide of iron, manganese and aluminum while As, B, Ge, Se, Pb, Mo, Zn and Tl show affinity towards anhydrite ($CaSO_4$) (Hansen and Fisher, 1980).

The composition of the fly ashes in different locations was determined by many scientists; Polat et al. investigated the minor and major element concentrations in Turkish fly ashes (Soma and Yatağan). The composition of the two fly ashes with respect to major and trace elements are given in Table 2.2 (Polat et al., 2002a).

Table 2.2. Composition of Soma and Yatağan fly ashes for major and trace elements

Element (as oxides)	Weight%		Element	ppm	
	Soma	Yatağan		Soma	Yatağan
SiO_2	33.4	36.4	Co	104	96
Al_2O_3	16.1	15.4	Cu	172	164
BaO	0.2	0.2	Pb	420	392
Fe_2O_3	6.0	7.8	Cd	40	32
CaO	33.8	23.5	Cr	64	92
MgO	6.1	8.8	Mo	72	81
Na_2O	1.0	1.1	Zn	116	120
K_2O	0.7	0.8	Mn	404	284
SO_3	2.8	6.8	Ni	152	180

Several authors have discussed the properties of fly ash considering several aspects. Bergeson and Schlorholtz (1992) discussed the physical and physicochemical properties of raw and hydrated fly ash, particularly relating to its use in the construction industry. Sykorora et al. (1997) found the mineral, mineralogical and chemical composition and morphology of fly ash to depend on the reaction conditions, coal quality and size distribution of particles. Haynes et al (1992) studied the factors governing the surface enrichment of the fly ash produced from high temperature coal combustion and found that the submicron particles, constituting only 1% of the total mass, contributed most to the ash surface area. Griest et al. (1984) observed the concentration of carbonaceous particles consisting of uncombusted coal, coal coke. These fractions are more sorptive, have higher levels of organic matter and exhibit higher surface areas than the mineral or magnetic particle-enriched subfractions. Nugteren et al. (1998) studied the composition of fly ashes and concluded that the heavy particles can be separated from fine fractions by physical separation processes. Malek and Roy (1985) studied the zeta potentials of low-Ca fly ashes and found that the point

of zero charge shifted to acidic pH after the fly ash was aged in several solutions containing calcium. Zeta potential values of different types of cement and fly ash at varying pH and ionic strengths indicated Na and K as the potential determining ions for cement in aqueous medium and were in full agreement with the modified Stern-Graham model of the reactive double layer on cement. Naegele (1986), Naegele and Schneider (1988), Alderliesten et al. (1987) observed that the carbon content of the fly ash decreased with increasing fineness of the pulverised coal while the particle size distribution of the fly ash showed a strong correlation with that of the pulverised coal used. Mohapatra and Kanungo (1997) studied the fly ash samples from two thermal power plants with the objective of creating a database for different fly ash samples in the country. They observed that relevant physical properties varied with particle size distribution of the samples. Graham and Hower (1994) observed that combustion byproducts, at power plants with very similar feed coals but different approaches to flue gas desulfurisation, had only minor differences in their chemical, mineralogical and petrographic characteristics. The mineralogical, morphological, physical and chemical properties of seven different fly ashes from eastern, central and western lignite and bituminous coal-fields in Turkey were studied and compared by Bayat (1998).

2.1.4. Coal Fly Ash Applications

Many patents are claimed for the use and beneficiation of fly ash. The most important use of fly ash is in the cement industry, where the presence of fly ash adds strength to concrete. The greatest utilization of fly ash is an additive to cement and concrete (Bergeson and Schlorholtz, 1992). It was claimed that fly ash used as an additive to Portland cement has many adventages on the resulting concrete such as decreasing the water/cement ratio, improvement of the particle size packing, initial freeze thaw durability of the concrete, decrease in cost, increases resistance to corrosion and increasing the strength of concrete.

Use of fly ash as a structural fill or cover materials was accounted for 15.3% of all utilized amount in 1996. The use of fine grained ash fills more void spaces creating a well graded mix of aggregates within the solid mass (Haynes et al., 1992).

The use of fly ash mixtures for hazardous waste stabilization and solidification was accounted for approximately 11.9% in 1996. The process of stabilizing a waste

consists of encapsulating the waste in a solid block whereas a semi-liquid waste transforms to a solid. By the solidification process, a strong, solid structure waste block is produced of which hydration properties are similar to Portland cement at a stabilized pH value.

Another application of fly ash is the addition with cement in grout. This provides the enhancing the binding of the lead contaminated soil, creating an impermeable monolith and achieving a durable structure (Haynes et al., 1992).

Re-utilization of fly ash as a material in the construction of roadways has been a significant outlet for ash during the 1990s. Fly ash has been used in embankment soil stabilization, subgrade base course material, as aggregate filler, a bituminous pavement additive and as mineral filler for bituminous concrete. The combination of all of these uses accounted for the re-utilization of approximately 5.5% of the total fly ash produced in 1996.

Use of fly ash as a by-product aggregate in the manufacture of light weight construction products presents many adventages especially economic saving to the manufacturer. For example, fly ash bricks are lighter than conventional clay-fired bricks and this enables a truck to carry more bricks per load. This reduces the shipping costs and improves profit margins.

Repeated harvesting of foodstuff depletes the trace elements in soil. Although the use of fly ash as soil amendment has been studied, the full scale application of this technology has not been implemented. In future, farmers might use fly ash, rather than lime, to increase the mineral content of the foodstuff (Landman, 2003).

Solidification of waste has existed since Roman times and is practiced mainly in countries with high population densities, where large quantities of waste are produced and shortage of space creates handling difficulties. In most cases it is practiced in countries where the availability of natural aggregates is limited, such as in the Netherlands. It should be noted that most of the studies carried out on stabilization/solidification techniques involved the use of municipal and industrial solid waste, fly ash, etc. (Hytiris and Kapellakis, 2004). The residual fly ash produced by coal combustion in thermoelectric power plants was mixed with acidic water obtained from olive mills. Good mechanical strength; wet strength; high porosity and high specific surface area; good adsorptive properties were achieved (Rovatti et al., 1992).

Fly ash also may be used to remove organic compounds from aqueous solution. In the literature there are a few studies about the adsorption of phenols (Akgerman and

Zardkoohi, 1996, Kumar et al., 1987, Viraraghavan and Demaria, 1998), chlorophenols (Kao et al., 2000), dyes (Gupta et al., 1990, Gupta et al., 1988), low molecular weight organics (Mott and Weber, 1992), o-xylene (Banerjee and Cheremisinoff, 1997) and toluene (Peloso and Rovatti, 1983).

In literature, there are many other studies from all over the world, related to the utlization of fly ash on any other subjects (Swanepoel and Strydom, 2002; Gupta et al., 2000; Landman et al., 2004; Andini et al., 2008; Demirbaş et al., 1995; Sheng et al., 2003; Palmer et al., 2000). Different applications of fly ash are given at Table 2.3 below (Üzelyalçın and Polat, 2004).

Table 2.3. Applications of fly ash

Building industry	Cement and concrete, roof tiles, bricks, panels and boards, grout, patches and roads, binder
Soil Beneficiation	Sewage treatment, soil stabilization, soil stabilization for roads, fertilizer or composting, landfill, sludge stabilization, coagulation and sludge conditioning agents
Filler Material	Foams, phenolic resole foam, polyurethane foam, polypropylene, epoxy resin, polyisocyanurate or polurathane foam, polyester-polyurethane hybrid resin foams, polymers, PVC, polyester, rigid shaped particles based on fly ash and resin, fibreglass
Insulating Material	High and low temperature applications
Ceramic Material	Mineral wool, glass-ceramics, coated cellular glass pellet, glass
Metal and Metal oxide source	Iron, germanium, antimony, vanadium, aluminium, uranium, selenium, thorium, gallium, lead, zinc, chromium, molybdenum, boron, silica, titanium, cobalt
Adsorbent for organics	Chlorophenols, o-xylene, phenol, toluene, oil and tar
Adsorbent for inorganics	SOx, nitrates, cadmium, selenium, radium, strontium, zinc, chromium, nickel, fluoride, NOx, phosphate, lead, mercury, barium, copper, cobalt, caesium, iron and ammonia
Starting Material for Zeolite Synthesis	Zeolite Na-P1, Zeolite P1, Zeolite K-G, ZK19 and Linde A, Merlinoite, nosean, Hydroxy-cancrinite, perlialite, kalsilite, Na-chabazite etc.

2.1.5. Minerals and Trace Elements in Coal and Coal Fly Ash

The mineralogy of the constituents of coal is dependent upon the geology of the surrounding environment of the coal deposits. The most common mineral constituents are the clay minerals, illite and kaolinite; sulfides, such as pyrite and marcasite; carbonates like dolomite, ankerite, calcite and siderite; and quartz. The clay minerals make up 60-90% of the total mineral matter; and quartz is found in almost all coals and can comprise anywhere from 1 to 20% of the inorganic compounds present in the coals Many trace elements are present within coal deposits, ranging from a few percent of the total composition of the coal to a fraction of a part per million (ppm). In addition, the processing and handling/storage of fly ashes can have a significant impact upon their pozzolanic reactivity. Likewise, the combustion process, which the coal goes through, will have a significant impact on the chemical and physical properties of the fly ash. In the former combustion process, thermal alteration of the mineral assemblage at approximately 800°C mainly results in the dehydroxylation of the clays into chemically very reactive meta- forms. When coupled with calcium oxide and anhydrite they readily react to form a plaster-ettringite cementitious system which will continue to react with the meta-clays to form C-S-H (calcium-silicate-hydrate), which will result in long stability of the solidified product. In contrast, pulverized coal combustion at approximately 1450°C results in a nearly identical mineralogical assemblage, minus the lime from the bed support, but with the exception that the clays will be converted into a glass; it is this glass that possesses the pozzolanic character that is responsible for its cementitious reactivity. Pulverized coal fly ashes exhibit a chemical reactivity that is directly correlated to the calcium content of the ash (Querol et al., 1997; Pandian, 2004; De Casa et al., 2007; Koukouzas et al., 2007).

The most common and predominant phases are quartz, mullite, hematite, magnetite and lime apart from other minor constituents. It also depends upon the type of the coal used. Thus, lignite fly ash has predominantly quartz, anorthite, gehlenite, hematite and mullite as major crystalline phases. The low calcium fly ashes contain quartz and mullite as the major crystalline phases, whereas the high calcium fly ashes consist of quartzite, C3A and C4AS (Sarkar et al., 2006).

2.1.6. Adsorption Properties of Fly Ash

The removal capacity has been found to be a strong function of the chemical composition of the fly ash (Hequet et al., 2001). Particularly, the presence of calcium oxide results in alkaline solutions which help precipitation of heavy metal hydroxides and formation of calcium silicate hydrates (Corigliano et al., 1997; Ricou et al., 2001). An aqueous medium of pH 7-8 was most suitable to be efficient for removal of cadmium (Cd), pH 2-3 for chromium (Cr), pH 4 for copper (Cu), pH 5 for zinc (Zn) and pH 5-5.5 for lead (Pb) (Virarghavan et al., 1998). However the effect of possible pH reversal must be considered for such route.

Some researchers modified fly ash to increase its adsorption properties. The modification of the fly ash by treating with 7 M NaOH hydrothermally increased the surface area 8-fold. Hence, the cation exchange capacity of the modified fly ash was increased from 2 meq to 188 meq per gram of ash. Adsorption studies were also done using an anionic dye (alizarin sulfonate) and a cationic dye (methylene blue) and experiments showed that the modified fly ash adsorbed a cationic dye to a much greater extent than an anionic dye. The capacity of the ash for methylene blue had increased 10-fold during modification when compared to the untreated fly ash (Woolard et al., 2002).

The studies on the adsorptive properties of two different Turkish fly ashes for Cd^{2+}, Cu^{2+}, Cr^{6+}, Ni^{2+} and Zn^{2+} are present in literature. The amount of adsorbed metals increased progressively with increasing pH. It should be noted that adsorption seems to start at very low pH values of 3 for these cations. The amount adsorbed reached 80% when the pH was over 5.5 for Cu^{2+}, over 6.5 for Cd^{2+}, over 6.5 for Zn^{2+} and over 7.5 for Ni^{2+}. The adsorption of Cr^{6+} was never above 30% and the maximum adsorption took place in the range of 3.0-4.0. It was observed that the fly ashes utilized were as effective as the activated carbon as adsorbents though the adsorption capacity was a function of the CaO content for the adsorptions Cd^{2+}, Cu^{2+}, Ni^{2+} and Zn^{2+}. However, the desorption test in the same study showed that desorption started at pH around 7 and increased up to 100% as pH was lowered to 3 for Cd^{2+}, Ni^{2+} and Zn^{2+}. For Cu^{2+} it started at around pH 5 and reached only about 30% at pH 3. The results of the researcher do not distinguish between the mechanisms of adsorption and suggests reversible precipitation at first glance (Bayat, 2002).

The fly ash is also used as an adsorbent for organic wastes. Whether this adsorbent nature of fly ash can be ascribed to the porous nature of the silicates or to the activated carbon particles embedded on the surface of the fly ash particle is still a matter for debate. To remove SO_x from gas streams, fly ash is usually mixed with Ca $(OH)_2$. Fly ash is also used for the removal heavy metals from aqueous samples. This property is dramatically enhanced by the formation zeolites from fly ash (Landman, 2003).

2.1.7. Leaching Studies of Fly Ash

When coal is known to concentrate many elements such as B, Cr, Cu, Ni, Mo, S, V etc. during and following coalification, further enrichment of these elements may take place in different forms in the ash. When stored in water, leaching of these elements occurs to produce solutions of varying salinity and composition. The equilibrium concentrations and distribution of dissolved components between the solution and the solid phase vary depending on the conditions of the solution (Polat et al., 2002a; Polat et al., 2002b).

It is known that when low quality lignite is burned, its fly ash contains several toxic elements, such as cadmium (Cd), lead (Pb) and zinc (Zn) which can leach out and contaminate soils as well as surface water and groundwater (Polat et al., 2002a, Baba and Kaya, 2004b). When fly ash is not properly disposed they may come into contact with the terrestrial, aquatic and atmospheric environment, and if leached, these elements cause the contamination of subsurface water (Polat et al., 2002b).

The leaching procedures such as European Committee for standardization (CEN) and toxicity characteristic leaching (TCLP) of the U.S. Environmental Protection Agency (U.S.EPA) are the procedures that are used for the evaluation of leaching of heavy metals. The main difference between these procedures is the pH of the sample prepared. In the U.S. EPA-TCLP procedure, the samples are tested at pH 5.0, but in the EU-CEN, the samples were prepared with distilled water. pH of the solution changes depending on the chemical composition of fly ash, and this affects the leachability of toxic heavy metals. Due to the differing solubility of that metal at different pHs, the heavy metal can be hazardous according to one procedure, but it can not be hazardous according to another procedure (Baba and Kaya, 2004a).

Many important aspects of the leaching behaviour of fly ash have been covered by a number of researchers. Harris and Silberman (1983) measured the rates of leaching of several transition metal ions from coal fly ash by solutions of the chelating agents citric acid, EDTA, hystidine and glycine at pH 7.4. Wasay (1992) performed batch and column experiments at pH 6.0 at different pore volumes to study the leaching of trace elements from fly ash. The metals in the leachate decreased with the average percentage of leachable toxic metals at 44.7% respectively for the batch study. Fliszar-Baranyai et al. (1992) studied the leaching behaviour of four Hungarian fly ashes at pH 4.0 and 2.5 with nitric and sulfuric acids. The leaching behaviour of fly ash was studied by Reardon et al. (1995) and found that the concentration of Na^+, K^+, Cl^-, B^{2+} or Cr^{6+} in the leachate was not controlled by mineral solubility in contrast to Ca^{2+}, SO_4^{2-}, Al^{3+}, Si^{2+}, As^{6+}. Theyconcluded that the elemental concentration could be determined readily with the help of a chemical equilibrium model for mineral solubility and the hydrochemical transport model for the rate of release of metals from fly ash particles.

The leaching studies with water indicated rapid leaching of most of the trace metals (except Cu) from the surface of ash particles in the pH range 6.4-7.5. The leaching rates of most trace metals (except Co and Cd) were relatively slow under acidic conditions (pH=4.5). Calesso et al. (1992) used different leaching methods such as EPA, INSA, and column leaching to study the mobility of elements in the fly ash leachate. Ni, Cu, Co, V, Mo and Cr were found in the acid leachate (EPA method) whereas Ca, Na, K, Mo and Cr were extracted through column leaching.

Mohapatra and Kanungo (1997) correlated the fall in release of metal ions with the formation constants of different hydrolytic species, namely MeOH and $Me(OH)_2$ with increase in pH of the medium. Das and Sanden (1982) studied the leaching and scavenging properties of aqueous fly ash aliquots with a spiked eluent by measuring the specific count rate of the liquid phase as a function of time. Bettoli et al. (1995) compared the leaching behaviour of fly ash with a bottom ash produced from the same combustible material. Khandekar et al. (1996) standardized the leaching condition of fly ash with respect to time and pH of extraction media. The method helps to assess potential risks due to leaching of pollutants from industrial solid waste. Reuss (1983) studied different methods for estimating the leaching of heavy metals from different fly ash samples and discussed the advantages and disadvantages of HNO_3 and HF acids. Berry et al. (1988) studied the influence of HCl leaching on the glassy constituents of a high calcium fly ash. Drakonaki et al. (1998) found that in lignite fly ash due to its

alkaline nature, toxic metal ions were leached in extremely low quantities, only sulfur was released in considerable quantities.

Several workers have considered the usefulness of developing leaching models for fly ash. Leim et al. (1983) predicted a model for metal leaching from coal ash and explained the behaviour of metal leaching by the mass-action law. Roy and Griffin (1984) found an equilibrium relationship between ash and water and presented a qualitative model for the metal leaching of fly ashes. Garavagila and Caramuscio (1994) used measured concentration values to calculate elemental speciation in solution with the geochemical program MINTEQA2 A number of solubility controlling minerals in the pH range 8-12 was found and geochemical reaction models were attributed to predict and control the leaching of elements from fly ashes. Schwab (1995) characterised the leaching of coal fly ash by applying the MINTEQA2 model. Bruggen et al. (1998) also used the MINTEQA2 model to predict metal concentrations in the leach solutions. Lu (1996) presented a mathematical model to predict the quantity and quality of the leachate from incinerator.

2.2. Industrial Waste Characterization

Waste characterization begins with an understanding of the industrial processes that generate a waste. Enough information must be obtained about the process to enable proper characterization of waste, for example, by reviewing process flow diagrams or plans and determining all inputs and outputs. You should also be familiar with other waste characteristics such as the physical state of the waste, the volume of waste produced, and the general composition of the waste. If the total concentration of all the constituents in a waste has been estimated using process knowledge (which could include previous testing data on wastes known to be very similar), estimates of the maximum possible concentration of these constituents in leachate can be made using the dilution ratio of the leachate test to be performed (EPA report, Characterizing Waste).

2.2.1. Environmental Evaluation of Wastes and Wastewater

Industrial, agricultural, and domestic activities of humans have affected the environmental system, resulting in drastic problems such as global warming and the

generation of wastewater containing high levels of pollutants. As water of good quality is a precious commodity and available in limited amounts, it has become highly imperative to treat wastewater for removal of pollutants. In addition, the rapid modernization of society has also led to the generation of huge amount of materials of little value that have no fruitful use. Such materials are generally considered as waste, and their disposal is a problem.

Wastewater treatment is becoming ever more critical due to diminishing water resources, increasing waste-water disposal costs, and stricter discharge regulations that have lowered permissible contaminant levels in waste streams. The treatment of wastewater for reuse and disposal is particularly important for countries, since they occupy one of the most arid regions in the world. The municipal sector consumes significant volumes of water, and consequently generates considerable amounts of waste-water discharge. Municipal waste-water is a combination of water and water-carried wastes originating from homes, commercial and industrial facilities, and institutions.

2.2.2. Industrial Acidic Wastes

Every community produces liquid waste, solid waste and gas emissions. The liquid waste is usually termed wastewater. Wastewater can be a combination of the liquid or the water-carried wastes removed from houses, commercial and industrial establishments, ground water, surface water and storm water (Metcalf and Eddy, 2002). Industrial sources throughout the world are dumping many metallic and organic compounds each year. These compounds need to be properly handled and removed if they cause health problems. Many industrial plants are required to pre-treat their wastewater before dumping it in the wastewater network. The most important physical characteristic of wastewater is its total solids content.

Industrial or commercial wastewaters which originate from numerous sources may contain considerable variety and amounts of contaminants including heavy metals.

There are several processes which are commercially available to remove these contaminants from these waters prior to discharge into environment or recycling back into the process stream. These can be listed in three main categories as chemical, physicochemical and biological. A list of these methods and the contaminants they are traditionally employed to remove is given in Table 2.4 (Üzelyalçın and Polat, 2004).

Table 2.4. Treatment methods of wastewaters and the contaminants removed

Method	Process Used	Contaminants Removed	Reactant
Chemical	Neutralization	Acidic wastes; waters containing HCl, HNO_3, H_2SO_4,CO_2,COOH	Hydrate of lime $(Ca(OH)_2)$, NaOH, limestone($CaCO_3$), partially calcined dolomite,calcined magnesite, cement, soda
	Flocculation	-Coarse and colloidal dispersions, metal ions	Aluminium and iron ions
	Precipitation	-Unsettleable minerals; phosphates, tartaric acid, citric acid and other organics	Chlorides and sulfites of aluminium and iron
	Adsorption	-Coloring, odorous and flavouring substances -Organics such as phenols -Heavy metals	Activated carbon Many low-cost adsorbents
	Extraction by solvents	-Dissolved substances	Benzol, butyl acetate, isopropyl ether and other solvents
	Ion-exchange process	Many metal ions; copper, sodium, cadmium, nickel, chromium etc	Cation exchangers; resins with sulfonic acid and carboxylic acid
		Sulfates, cyanides	Anion exchangers;resins with amino groups
Physico-chemical	Adsorption by activated charcoal	Biological substances, metals, fine suspended solids and colloids	Activated carbon
	Oxidation by ozone	Coloring, odorous and flavouring agents, breaking up detergents	Ozone
	Pond treatment		
	Reverse osmosis (Hyperfiltration)	Many metallic compounds	Cellulose acetate membranes
	Ion exchange methods	Minerals	-Natural (Zeolite) Exchangers -Synthetic resins
	Electrodialysis	Dissolved substances	
Biological	Aerobic decomposition Nitrification Desulfurization Fermentation Biofiltration Sludge activation Anaerobic treatment	Carbohydrates, fats, proteins Organically bound nitrogen Heavy metals	Algae, yeast The bacterium; Nitrosomonas, Nitrobacter etc.

Acidic waste waters from industrial and mining activities constitute a wordwide environmental hazard. 'Acid mine drainage' (AMD) waters are often highly acidic (pH< 4), contain elevated concentrations of sulfate and dissolved metals, and are toxic to most life forms. Trace quantities of many metals are important constituents of most waters. Many of these metals are also classified as priority pollutants, pollutants that can cause cancers. But most of these metals are necessary for the growth of biological life. The presence of any of these metals in excessive quantities will interfere with many beneficial uses of the water because of their toxicity. Therefore, it is desirable to control the concentration of heavy metals when considering reuse options (Tamimi, 2003).

Acidic waste waters can be reacted with fly ash in a pre-determined equilibration time using different solid/liquid ratios to produce neutral or alkaline process waters and remove major and minor elements from solution. The elemental concentration trends with time in the solution can be used to determine which elements have solubility control in the neutralization process.

A summary of the sources of these waters, their pH and the contaminants they may contain are given in Table 2.5 (Üzelyalçın and Polat, 2004).

2.2.3. Formation and Chemistry of Industrial Acidic Waste

Every community produces liquid waste, solid waste and gas emissions. The liquid waste is usually termed wastewater. Therefore, wastewater can be a combination of the liquid or the water-carried wastes removed from residence, institutions, commercial and industrial establishments, ground water, surface water and storm water. Wastewater is generated from domestic and industrial sources. Industrial sources throughout the world are dumping 10,000 new organic compounds each year. These compounds need to be properly handled and removed if they cause health problems.

Many industrial plants are required to pre-treat their wastewater before dumping it in the wastewater network. The most important physical characteristic of wastewater is its total solids, total suspended solids, total dissolved solids, volatile and fixed solids content. Wastewater contains a variety of solid materials varying from rags to colloidal material. In the characterization of wastewater, coarse solids are usually removed before the sample is analyzed for solids.

Table 2.5. Sources of the industrial and commercial wastewaters

Industrial& Commercial Wastewater	Sources	pH	Contaminants
Nonmetallic Minerals Industries	Manufacture of mortar binding agents, glass, concrete Sandy limestone producing plants Cement factories Porcelain factories Other ceramic industries	Strongly basic	-Suspended and dissolved substances and oils -Inorganic substances with dust -Phenol
Metal Processing Industries	Iron works Blast-furnace gases Steel and Rolling Mills Machinery Production Metal Pickling Plants Electroplating Plants	Basic	-Suspended solids, cyanide, H_2S, ammonia -Metal salts; copper, brass, nickel, cadmium, silver, gold, chrome, zinc, lead, aluminium, hexavalent chromium -Sulfuric, hydrochloric or nitric acid -Soluble cooling oils -Soaps, naphthenates, naphthenosulfonates, synthetic detergents, resins, nitrite, phosphates, silicates -$FeCl_2$, $FeSO_4$
Mines and Ore Dressing Plants	Pit Waters Coal Washing and Dressing Hard-Coal Coking Plants Coke-quenching	Wide	-Suspended solids (coal and plastic clay particles) and dissolved substances(sodium chloride, calcium, magnesium and barium chloride) -Metal salts (iron, nickel, magnesium sulfates and arsenic compounds) -Dissolved ammonia, carbolic acid, phenol, organic acids
Chemical Industry	Mineral Acid Production Potash Industry Fertilizer Production	Wide	-Metal particles, , mineral oil, arsenic sludge phenol -CO_2, alkali carbonates, bituminous substance, flue dust, sulphur compounds
Pharmaceutical &Cosmetics Industry	Drug Production Cosmetics Industry	Acidic	-Organic acids, acetone, amyl acetate, dichloroethylene
Dye & Colorant Manufacturing	Inorganic dyes Organic dyes		-Chlorides, iron compounds, cyanogen compounds, lead acetates, lead carbonate, barium, sodium sulfide, hydrogen sulfide, potassium acetate, potassium chromate, alkali sulfate, calcium sulfate, calcium chloride, sodium arsenite, potassium sulfide -Organic solvents, acetic acid residues, nitric acid and its salts
Soap&Detergent Production		Acidic	-Fatty acids, alcohols, ketones
Plastic Industries		Wide	-Formaldehyde, methanol, suspended resin
Textile Industry		Wide	-Dissolved organic substances, hydrogen sulfide, carbon disulfide, free mineral acids, zinc salts
Oil Refining Industry		Wide	-Metal salts,oil and oil emulsions, inorganic acids and alkalis and soda lye, organics such as phenols and naphthenic acid, mercaptans
Food Processing Plants	Dairy Industries Meat Industries Fruit juice industries Mineral water industry Breweries Sugar Industry	Wide	-Lactose, protein -Blood, plasma content, urine -Organic substances, fruit scraps, grain and hop residues, leaves, yeast -Broken glass -Alkalis, dust

Total solids, TS, are defined as the residue remaining after a wastewater sample has been evaporated and dried at a temperature of 103 to 105 ^{o}C. Total Suspended Solids, TSS, are defined as the portion of TS retained on a specific size filter after drying at 105 ^{o}C. Usually the Whatman glass fiber filter with a nominal pore size of 1.58 micron is used. Total Dissolved Solids, TDS, can be defined as the solids that pass through a filter with nominal pore size of 2 microns or less. The TDS can be calculated using the following equation:

$$TDS = (TS - TSS) \qquad\qquad (2.1)$$

Volatile solids (VS) are defined as those solids that can be volatilized and burned off when ignited in a muffle at oven at 500 ± 50°C. They are assumed to be organic matter. Fixed solids (FS) are defined as the residue that remains after a sample has been ignited in a muffle oven. TS, TSS and TDS are comprised of both fixed and volatile solids. The ratio of VS to FS (organic to non-organic matter) is used to characterize the wastewater in respect to amount of organic matter present in the wastewater (Tamimi, 2003).

The source of inorganic nonmetallic constituents in wastewater comes from the water supply and from the addition of highly mineralized water from private wells, ground water and from industrial use. Because concentrations of various inorganic constituents in wastewater can greatly affect the beneficial uses made of the treated effluent, the constituents must be considered separately.

The pH range suitable for the existence of most biological life is typically 6 to 9. Wastewater with an extreme concentration of hydrogen ion is difficult to treat by biological means.

Chloride is a constituent of concern in wastewater because it affects the final reuse application of treated effluent. Conventional methods of wastewater treatment do not remove chloride and hence chloride concentrations are usually high in wastewater, the contributing sources need to be investigated and reduced for a beneficial use to be considered.

Alkalinity can be defined as the ability of wastewater to neutralize acids; it is a measure of buffering capacity against a *pH* drop. Alkalinity results from the presence of the hydroxide [OH^-], carbonate [CO_3^{2-}] and bicarbonate [HCO_3^-] ions in wastewater. These ions can be present with elements such as calcium, magnesium, sodium,

potassium and ammonia. Calcium and magnesium carbonates and bicarbonates are the most common. It should be mentioned here that wastewater is normally alkaline.

Nitrogen, phosphorus and sulfur are essential elements for the growth of microorganisms, plants and animals. Nitrogen is the building block in the synthesis of proteins and hence the quantity in wastewater is essential to be known to determine if the wastewater is present in wastewaters.

Trace quantities of many metals are important constituents of most waters. Many of these metals are also classified as priority pollutants, pollutants that can cause cancers. But most of these metals are also necessary for the growth of biological life. The presence of any of these metals in excessive quantities will interfere with many beneficial uses of the water because of their toxicity. Therefore, it is desirable to control the concentration of heavy metals when considering reuse options. The case of controlling boron concentration when the treated effluent is planned to be used for irrigation agricultural crops is one example.

Organic compounds are usually composed of a combination of carbon, hydrogen, oxygen and nitrogen. Biochemical Oxygen Demand (BOD) is the most widely used parameter of organic pollution applied to both wastewater and surface water. Total Chemical Oxygen Demand (COD) test is used to measure the oxygen equivalent of the organic material in wastewater that can be oxidized chemically using dichromate in an acid solution.

The source of pathogenic organisms found in wastewater can be excreted by human beings and animals who are infected or carriers of a particular infectious disease. There are four categories of pathogenic organisms found in wastewater. These are bacteria, protozoa, helminthes and viruses.

2.2.4. Industrial Wastewater Treatment

Treatment of wastewater produced by an industry takes place in a plant purposely built in the area of production, or after transport in the sewage system by purpose-built structures within the urban waste treatment plant. Moreover, treatment carried out within the area of production can confer those characteristics on the industrial waste that allow it to be deposited directly into the final receiver, or even used again, either completely or partially, in the productive cycle, hence giving the

wastewater the necessary qualities for its discharge into the public sewage system. The treatment of industrial wastewater involves the same processes as those used in the treatment of civil water. However, because of specific compositions, the systems tend to vary. The chemo-physical type processes are especially important for the removal of inorganic matter. The basic processes used are;

- neutralization

- the reduction and oxidation of inorganic compounds (such as chromic salts to chromates or cyanides to cyanates) and also of organics, with ion or radical substitutents;

- the precipitation of cations and anions in the form of insoluble compounds, such as the precipitation of metals, as hydroxides, and chromates (for example barium chromate) and cyanides (such as ferrocyanide).

The simplest plant system for neutralization is that in which the wastewater comes into contact with a considerable amount of a neutralizing reagent. All that remains is to determine the length of time that the wastewater is detained in the tank, where falling sludge is collected on the hopper bottom. Lime in the form of milk of lime is the chief agent used in the neutralization process. In some cases it is better to use carbonate or sodium hydroxide to prevent the precipitation of calcium sulfate. When treating corrosive waste it is advisable to add a neutralizing reactant during the first stage, so reducing the quantity of non-corrosive apparatus and tubing required. The efficiency of urban wastewater treatment can be adversely affected by highly acid or basic waste containing toxic compounds with an elevated solid, fat or emulsion content, inflammable material, clay sand or abrasive particles, not treated previously. In some industries the treatment of waste is limited to the primary stages of screening, grit removal, flotation, degassing, sedimentation and neutralization in order to reach the standards necessary for discharge into an urban sewer system. Treatment of industrial wastewater which by nature is substantially organic can be carried out according to the treatment systems generally used for the purification of domestic sewage in appropriately designed plants.

2.2.5. Industrial Acidic Waste Management Strategies and Challenges

Metal industries use substantial quantities of water in processes such as metal finishing and galvanized pipe manufacturing in order to produce corrosion-resistant products. Effluent wastewaters from such processes contain toxic substances, metal acids, alkalis, and other substances. High concentrations of metals in the effluents may cause interference with biological treatment processes at sewage treatment. The pickling solutions that are used in the treatment of metal oxides or corrosion products are acids (HCl, H_2SO_4, HF, H_3PO_4, HNO_3) or mixtures of acids. Adsorption of soluble metallic species by clays, oxides and other colloidal matter appears to be an important means of controlling the trace soluble metal concentration in heterogeneous systems (Krauskopf, 1956; Huang and Ghadrian, 1974). In the last few years, adsorption has been shown to be a cost effective technique for the removal of trace metals from wastewater and water supplies (Matsumoto et al., 1994; Allen and Brown, 1995). Bentonite as an adsorbent for the removal of malathion (Pradas et al., 1993), and Cd(II) and Pb(II) under estuarine and sea water conditions (Kozar et al., 1992).

There are a lot of wastes generated by metallurgical industries, such as flue dust from electric arc furnace and smelting operations, zinc ash, dross, flux skimming and blowing secondaries formed during hot dip galvanizing, or neutralizing zinc waste galvanic sludges, etc. In such wastes zinc is usually present in the form of metal, oxides or more complicated compounds.

Galvanizing is a metallurgical process consisting of covering the surface of iron or steel pieces with a reactive zinc layer that forms a very resistant covering. The most frequent process is hot-dip galvanizing due to its industry's development being very advanced. Hotdip galvanizing processes consist of stages such as washing, pickling or galvanizing itself that generate wastewaters containing, among other substances, high concentrations of Zn, Fe and HCl, which gives rise to an environmental problem that has to be solved due to the hazardous nature of the effluents.

Heavy metals discharged in wastewaters can be toxic to aquatic life and cause natural waters to be unsuitable as potable water sources. The toxicity of heavy metal s even in trace quantities and their tendency for bioaccumulation in food chain make it necessary to develop processes for the removal of heavy metals from wastewaters (Bayat, 2002).

CHAPTER 3

PHYSICOCHEMICAL CHARACTERIZATION OF FLY ASH AS THE BASIS FOR ACIDIC WASTE TREATMENT

3.1. Characterization of Fly Ash

Various methods are applied for the characterization of the phase, mineral and chemical composition of fly ashes. These methods include macroscopic observations, ashing procedures (high-temperature and low-temperature), physical separations (density, magnetic, particle size, froth flotation, and electrostatic), chemical leaching, sequential physical and chemical treatments, as well as optical microscopy, scanning electron microscopy, X-ray diffractometry, differential thermal and thermogravimetric analyses, infrared spectroscopy, and different chemical analyses.

Zwozdziak et al. (1989) determined the size, shape, structure and mineralogical composition of fly ash using transition electron microscopy, electron diffraction and XRD. Miwa et al. (1991) used a secondary ion mass spectrometer, X-ray microanalyser and SEM to investigate the surface characteristics and depth profile of a coal fly ash. The results of ion microprobe depth profiles and X-ray imaging of elements on spattered surfaces of fly ash particles showed fairly good agreement. Small and Zoller (1977) used the SEM technique to provide information on particle shape and origin, sample homogeneity and elemental composition which was not available from bulk analysis. SEM studies of Kawfherr and Lichtman (1984) indicated similarities in submicron and micron sized particles of fly ash; both were spherical and contained Si, Al, K, Te, Ti, and S as the main components. Sun et al. (1982) investigated the morphology of pulverised fly ash through SEM and observed three kinds of particles: spherical, irregularfused and porous carbon. The spherical and irregular fused fly ashes were at good quality and suitable for cementitious building materials.

The principle constituents of fly ashes from pulverized coal combustion were shown in Table 3.1.

Table 3.1. The primary constituents of fly ash (Hall and Livingston, 2001)

Alumino-silicates	-solid spheres
	-solid with internal pores
	-thick and thin walled spheres
	-spheres willed with spheres
Pyrite residues	-magnetite spheres
Quartz grains	-non-spherical
Non-spherical particles	-kaolinite residues
	-detached deposit material
Char residues	-honeycomb structure

3.1.1. Size Distribution Analysis of Fly Ash

Particle size analysis of coal ash is very important for estimation of the combustor efficiency and for assessing the utilization potential of the ash produced. Combustion efficiency and fly ash characteristics show close inter-relationship. A critical examination of the coal particle combustion mechanism and mineral-matter transformation of fly ash particles supports this view. According to the accepted mechanism of mineral matter transformation in coal, the first step is conversion of coal (with intrinsic and extrinsic mineral matters) to char. Subsequently, these charred particles burn out at much higher temperature. The fine inherent minerals (< 0.1 μm), within the char particles transform, and are gradually released during the char fragmentation. Decomposition of the minerals takes place at this juncture and subsequently the decomposed minerals are converted to gases (1100–1200 ºC). In the gaseous phase several homogeneous chemical reactions with subsequent heterogeneous or homogeneous condensation take place. While fly ash of particle size range 0.02–0.2 μm results from the homogeneous condensation, the fragmentation of the inherent mineral matter results in the formation of ash particles of medium size range (0.2–10 μm). Extrinsic mineral matters present in coal undergo a series of complex transformations (Figure 3.1) to form ash particles of larger size (10–90 μm).
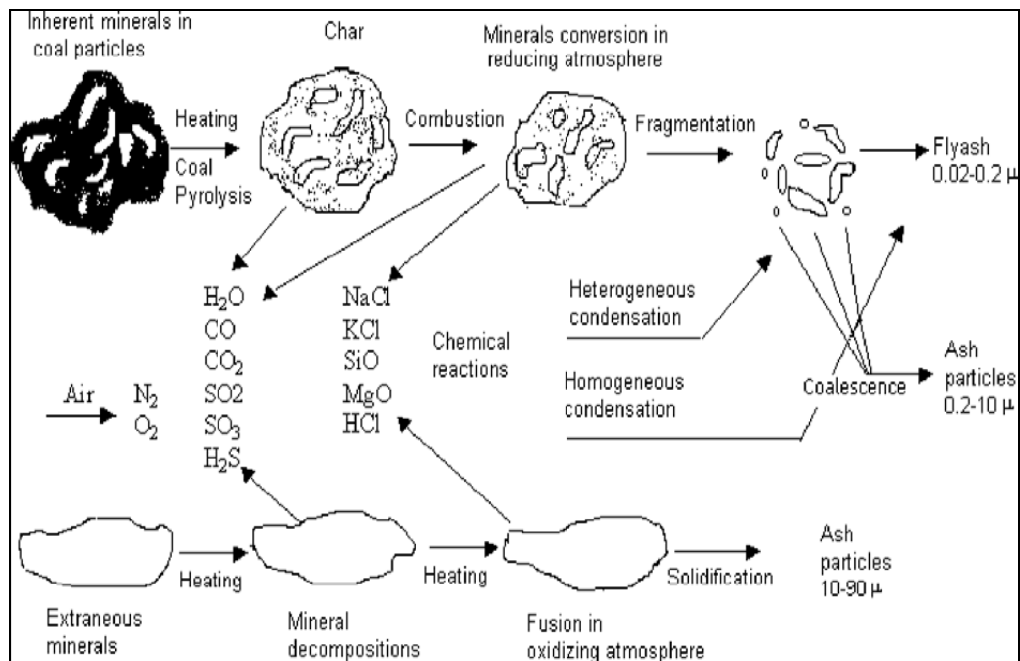
Figure 3.1. Mineral matter transformation mechanism

(Source: Flyash 2010)

3.1.2. X-Ray Diffraction Studies of Fly Ash

X-ray diffractometry (XRD) is a very useful technique, and it is one of the most common and widely used methods (together with SEM) for the identification and characterization of minerals. The advantage of this powerful technique is the detection of occurrence and degree of crystallinity of forming, major, and some minor crystalline phases (quartz, mullite, magnetite, hematite, feldspars, anhydrite, clay minerals, calcite, cristobalite, and others) independent from their size. This is a big advantage for the finely dispersed fly ashes. Individual mineral grains separated from fly ashes can be analyzed. The XRD investigation on the phase transformations in fly ash using a high-temperature chamber is also possible (Cullity, 1978).

The fly ashes from high sulphur coals have higher amounts of iron-bearing minerals compared to the fly ash from low sulphur coals. Formation of iron oxides is partially due to the decomposition of pyrite, which increases the SOx content of the system and provides the basic cation for nucleation of hematite/magnetite, which then leads to the formation of magnetite microspheres. The ash samples contain hematite,

especially in cases where bituminous coal is used. This type of coal has higher percentages of ferric oxide in comparison with lignite and the wood chips used. Hematite was frequently accompanied by anhydrite, which probably forms from reactions between pyrite sulphur and calcite. The presence of hematite in combination with the presence of periclase leads to the formation of magnesioferrite ($MgFe_2O_4$). Lime forms due to the decomposition of calcite or from dolomite through calcite. Gehlenite originates from carbonate–silicate-spinel reactions (Koukuozas et al., 2007).

Lima et al. characterized four different fly ashes. Minerals were found in differing availability. Main minerals detected by XRD were corundum (Al_2O_3), anhydrite ($CaSO_4$), calcite ($CaCO_3$), hematite (Fe_2O_3), sylvite (KCl), arcanite (K_2SO_4), magnesite ($MgCO_3$), forsterite (Mg_2SiO_4), halite (NaCl), quartz (SiO_2) (Lima et al.,2008).

Another XRD investigation of mineral composition of fly ash showed the presences of quartz, mullite, iron oxide, hematite, sulfur oxide, and CaO. The fly ash was modified with HCl and the HCl modified ash showed a similar XRD pattern to the FA, but the peaks of CaO and sulfur oxide were not clearly observed (Pengthamkeerati et al., 2008).

Bada and Vermaak (2008) found that the South African fly ash consisted of crystalline minerals mullite, quartz, hematite and small amounts of calcium oxide with large characteristic peaks of quartz (SiO_2). This result is similar to that reported for a fly ash investigated by (Sarkar, 2006). The intensity of quartz is very strong, with mullite forming a chemically stable and dense glassy surface layer.

The proportion of amorphous or glassy material in a series of fly ashes has been evaluated by X-ray powder diffraction (XRD) (Ward et al., 2006).

McCarthy et al. (1984) used XRD while identifying the crystalline phases; quartz, periclase, ferrite spinel, anhydrite and lime in fresh ash as well as in ash buried 12 years before. White and Case (1990) claimed that mullite and silica as the major crystalline phases in fly ash by using XRD technique. McCarthy et al. (1984) applied a protocol for semi-quantitative XRD analysis of fly ash in studies of the typical mineralogy of high- and low-calcium samples, the consistency of sample mineralogy from a typical power station, the partitioning of chemical constituents into crystalline phases, and crystalline phases relevant to the use of fly ash in concrete.

As for the Soma fly ash, the literature data (Karayigit et al., 2000; Bulut et al., 2002) shows that the mineral composition (in decreasing order of significance) includes

calcite, kaolinite/chlorite, quartz, pyrite, illite, smectite, gypsum, dolomite, feldspar, and siderite. Vassilev et al. (2004) confirmed the occurrence of the above minerals plus some additional minerals identified. The mean mineral composition (in decreasing order of significance) of fly ashes includes calcite, quartz, kaolinite, chlorite, plagioclase, gypsum, pyrite, montmorillonite, K-feldspar, dolomite, siderite, ankerite, opal, and volcanic glass. They claimed that additional accessory minerals may also occur in fly ashes, but they are not under consideration due to their complicated identification and quantification. For example, Cu–Zn and Cu–Zn– Pb sulphides, barite enriched in Sr, Cr oxide, halite, and Cu–Zn chloride were identified in the Soma fly ashes (Karayigit et al., 2000).

3.1.3. Scanning Electron Microscope Observations of Fly Ash

SEM is the most widely used technique with the X-ray diffractometry for the identification and characterization of phases in fly ash. The sample preparation technique is relatively simple and rapid. This includes the use of polished or unpolished blocks, pellets, and sections of powder or grains mounted in different binders (epoxy resin, duracryl, double-adhesive carbon tape, carnauba wax, nail polish, and others), depending on the samples and holders. The specimens may be coated evaporatively with carbon or gold, to reduce the charging effect. The high image quality in secondary and backscattered electrons at relatively high magnifications (up to 10-20 kx) is favorable. The possibility of using microprobe elemental analyses of small areas (up to a few square micrometers) to detect mineral and phase species is also a big advantage for finely dispersed fly ash. An SEM system that has been equipped with an energy dispersive X-ray (EDX) analyzer or a wavelength dispersive X-ray (WDX) analyzer can determine elements with atomic numbers. Mineral grains with a typical diameter of >0.5-1 μm can be observed, analyzed, and photographed. This method is an irreplaceable tool for identification, characterization, microtextural, and/or microstructural observations in situ of the minerals and phases present in fly ash. For example, many species from mineral classes such as oxides (magnetite, hematite, ilmenite, spinel, iron spinel, magnesioferrite, jacobcite, hercynite, ulvospinel, chromite, chromspinel, lime, periclase, corundum, rutile, pyrolusite, baddeleyete), silicates (quartz, mullite, clay minerals, feldspars, wollastonite, larnite, melilite, zircon), sulfates

(gypsum, anhydrite, barite, anglesite), phosphates (apatite, monazite), carbonates (calcite), as well as various glass types (Si-Al, Si-Al-Fe, Si-Al-Ca, Si-Al-Ca-Fe, Si-Al-Fe-Ca) and char types (massive, porous, vesicular, spongy, cenosphere, others) in fly ashes were identified and characterized mostly using SEM (Vassilev et al., 2004).

3.1.4. Thermal Behavior

The differential thermal analysis (DTA), thermogravimetric analysis (TGA), and other thermal analyses in air, inert, or reducing atmosphere for fly ash characterization can be used. The DTA-TGA profiles of fly ashes can be used to distinguish several features; loss of adsorbed water up to 150 °C (endothermic effect); sorption of some moisture by lime and subsequent hydroxylation to portlandite up to 600 °C (exothermic reaction), accompanied by increasing of mass; char combustion at 440-550 °C (exothermic effect), accompanied by mass loss; portlandite dehydroxylation at 500-650 °C (endothermic reaction) associated with mass loss; calcite decomposition at 650-750 °C (endothermic effect), accompanied by mass loss; anhydrite decomposition at 1150-1250 °C (endothermic reaction) associated with mass loss; and fluid ash-fusion observed above 1250 °C (endothermic effect), accompanied by mass loss (Brown, 2001).

3.1.5. Infrared Spectroscopy Method

The infrared data are useful for the identification of mineral classes or groups of minerals (Si-O-Si, O-Si-O, Al-O-Si, Si-O-Na, S-O, C-O, and others). In the literature, the infrared spectra of fly ash have been reported by many scientists. Mollah et.al. (1999) assigned the bands in their spectra. They were observed that the fly ash showed FTIR bands at 1080, 792 and 481 cm^{-1} with shoulders at 1135, 700 and 565 cm^{-1}. The band at 1080 cm^{-1} was assigned to the antisymmetric stretching vibration of Si-O-Si and the band at 792 cm^{-1} to the corresponding symmetric vibration. The band at 1135 cm^{-1} was assigned to the antisymmetric stretching vibration of Si-O-Al stretching vibration and the band at 700 cm^{-1} to the symmetric Si-O-Al stretching vibration. The band at 481 cm^{-1} was assigned to the O-Si-O bending vibration. The shoulder at 950 cm^{-1} was assigned to a non-bridging oxygen band Si-O-Na. The bands at 800 and 481 cm^{-1} were

assigned to the cristobalite, and the band at 700 cm^{-1} to the presence of mullite (Landman, 2003).

Mollah et al. (1999) claimed that the silicate bands were broad and diffuse because of the overlapping of different types of silicate molecular vibration resulting from various silicate minerals.

Lee and Deventer (2002) explained the very broad band (950-1200 cm^{-1}) at the T-O-Si (T=Al and Si) stretching vibration region as the multi-phase nature of the analyzed fly ash. The strong bands at 1165, 1080 cm^{-1} and the medium band at 798 cm^{-1} were attributed to quartz. The strong band at 561 cm^{-1} and the shoulders at 1138 and 620 cm^{-1} were the indication of mullite. Amorphous aluminosilicate phase was likely to cause vibration at around 1070-1080 cm^{-1} and similar band position can be observed for natural and glassy aluminosilicate materials. Thus, the 1074 cm^{-1} band was assigned to the amorphous aluminosilicate phases. The broad band located at 500-650 cm^{-1} also showed the silicate and aluminosilicate glasses, which indicated the long-range structural order in the form of rings of tetrahedra or octahedra (Lee and Deventer, 2002).

Jaarsveld et al. (2003) obtained a slight difference in the main Si-O and Al–O asymmetric stretching bands around 1025 and 1027 cm^{-1} for two different types of fly ashes. The band at 550 cm^{-1} and 557 cm^{-1} for both fly ashes were attributed to the bending of Si-O-Al bonds, where Al was in octahedral coordination. They were suggested that the other differences could be the result of varying furnace temperatures or changes in the feed coal composition.

According to Nathan et al. (1999), FTIR results, showed an amorphous phase rich in silicon with some aluminum and iron occured in both ashes. There was more than one calcium-aluminum silicate amorphous phase in the ash and the amorphous silicate phases and mullite in the ash almost always contained some iron.

The literature also contained FTIR studies performed to composites of fly ash and modified fly ash (Puertas and Fernandez-Jimenez, 2003; Murugendrappa et al., 2005).

3.1.6. Chemical Analysis of Fly Ash

The methods for bulk or local chemical investigations of fly ash include mainly atomic absorption spectroscopy (AAS) inductively coupled plasma-mass spectroscopy (ICP-MS) and atomic emission spectroscopy (AES). In comparison to ICP-MS, ICP-AES is more widely used because it has several advantages, such as low initial cost and easy maintenance; however, its detection limits are usually inferior to those of ICP-MS.

When fly ash samples are subjected to atomic spectrometries, the analytes need to be transferred from a solid phase to solution in order to conform to the sample introduction systems of the spectrometers. In recent years, the acid digestion assisted by microwave processing has been popularly utilized for such a pretreatment of the solid samples. A combination of HNO_3 and HF is conventionally employed in the microwave-assisted acid digestion (MWAD) of coal because coal contains an appreciable amount of inorganic matters, which mainly consist of aluminosilicate matrix. However, some recent studies have reported that good recoveries of many elements can be achieved by MWAD without HF addition (HF-free digestion). In a different study, the fly ash was melted with a mixture of boric acid and lithium carbonate at 950°C. Then, the fused mixture was treated with deionised water and concentrated nitric acid to obtain the sample solution (Ayala et al., 1998). Another analytical technique used for determination of elements is fusion with lithium tetraborate at 1100 °C followed by dissolution in 10% HCl solution (Polat et al., 2002a).

3.2. Characterization of the Waste

A waste characterization begins with an understanding of the industrial processes that generate a waste. Enough information must be obtained about the process to enable proper characterization of the waste, for example, by reviewing process flow diagrams or plans and determining all inputs and outputs. You should also be familiar with other waste characteristics such as the physical state of the waste, the volume of waste produced, and the general composition of the waste. If the total concentration of all the constituents in a waste has been estimated using process knowledge (which could include previous testing data on wastes known to be very similar), estimates of the

maximum possible concentration of these constituents in leachate can be made using the dilution ratio of the leachate test to be performed.

3.3. Fixation and Stabilization of Metals in Aggregate Structure

Fly ash contains many metals such as calcium, aluminium, silicium, cadmium, nickel and zinc in its structure in appreciable amounts. Some of these elements may be toxic or harmfull for the organisms and can be leach out into surface and ground water. Acidic process waste waters also contain many toxic elements and carry the same risk for the environment. The utilization of these wastes together in product bodies which is called "aggregate" and encapsulation of the metals in this structure for the purpose of waste elimination is a challanging approach (Koseoglu et al., 2010).

3.3.1. Neutralization Studies of Fly Ash

Neutralization of industrial wastes and removal of toxic metal ions by low cost adsorbents such as fly ash have been receiving increasing attention owing to being an unavoidable side-product of electricity production and their unique properties (Theis et al., 1977; Talbot et al., 1978, Wang and Viraraghavan 1997; Jackson et al., 1999; Gupta, 2000; Cohen et al., 2001; Lin et al., 2001; Ricou et al., 2001; Lin and Chang, 2002; Bayat, 2002).

Polat et al. treated various strongly acidic and heavy metal-laden waste waters (acid mine drainage (AMD), engine oil refinery waste, potash industry waste, etc) using several fly ashes from South Africa, Colombia and Turkey. They mixed fly ashes and different acidic wastes in different ratios and dried the resulting mud to prepare an aggregate product. Neutralization studies with Soma fly ash showed that 1kg Soma fly ash could theoretically neutralize 478 kg AMD. This calculation was done by assuming that all Ca and Mg are in oxide form and could be accessed by the AMD (Figure 3.2). It can be seen that the amounts of AMD required neutralizing 1 kg of Soma ash sample is around 150 kg. This shows that these ashes had significant neutralization potential for the AMD, given enough contact time. The fact that these amounts were much smaller than the theoretical values suggests that a large fraction of the Ca and Mg is not available for leaching (Polat et al., 2002a).
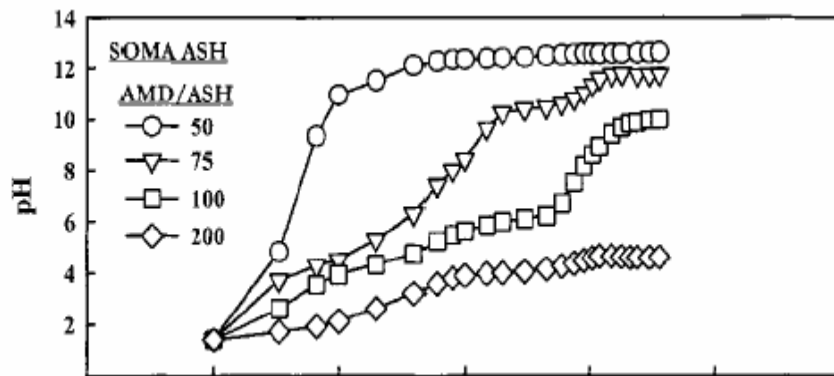
Figure 3.2. Titration behavior of Soma fly ash samples with AMD

It was observed that there was a notable leaching of Cr and Cu when only ash and AMD were mixed, in these studies the concentrations in aggregate-water solutions dropped to practically zero when motor-oil was used as an additive. This similar behavior for Cr and Cu elements can be seen in Figure 3.3 and Figure 3.4.

The leaching experiments with the aggregates showed that the pH of the aggregate-distilled water solution could be finely adjusted by varying the fly ash/acidic waste ratios and that the heavy metal concentration in the solution was below detection limits for the majority of the heavy metals. Their results showed that metals started to adsorb onto fly ash starting from at low pH values (around 3-4) and most of the metal removal was completed before the pH of hydrolysis. They suggested that fly ash fixes the metals in its structure by coordinative bonding of the surface MeOH sites with the metal cations rather than simple precipitation.
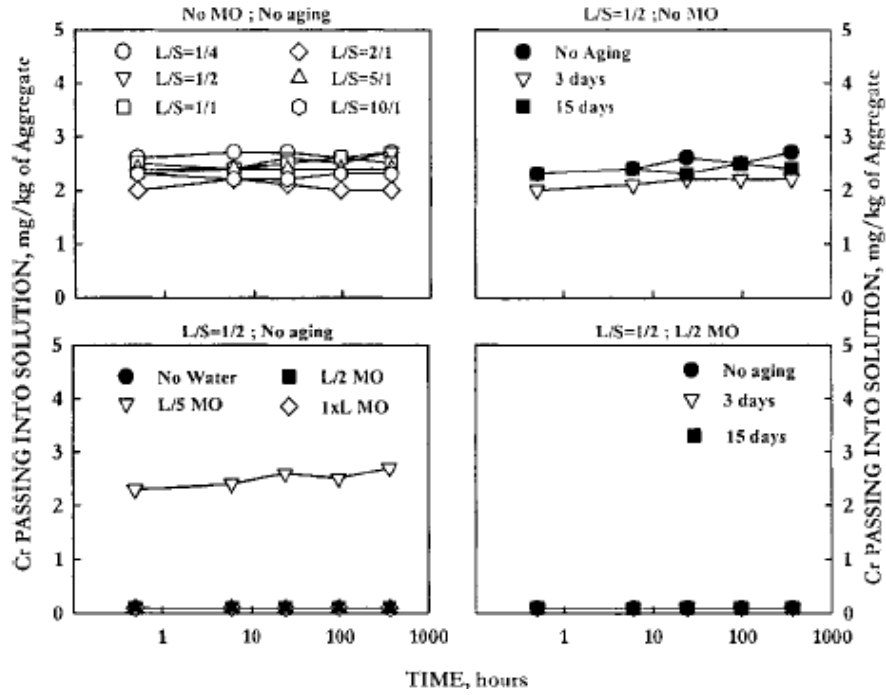
Figure 3.3. Effect of different parameters on the leaching of Cr from the aggregate for Soma ash for A/W ratio of 1/10 (Cr conc. 64 ppm in ash, 0.1 ppm in AMD and 0.2 ppm in MO)
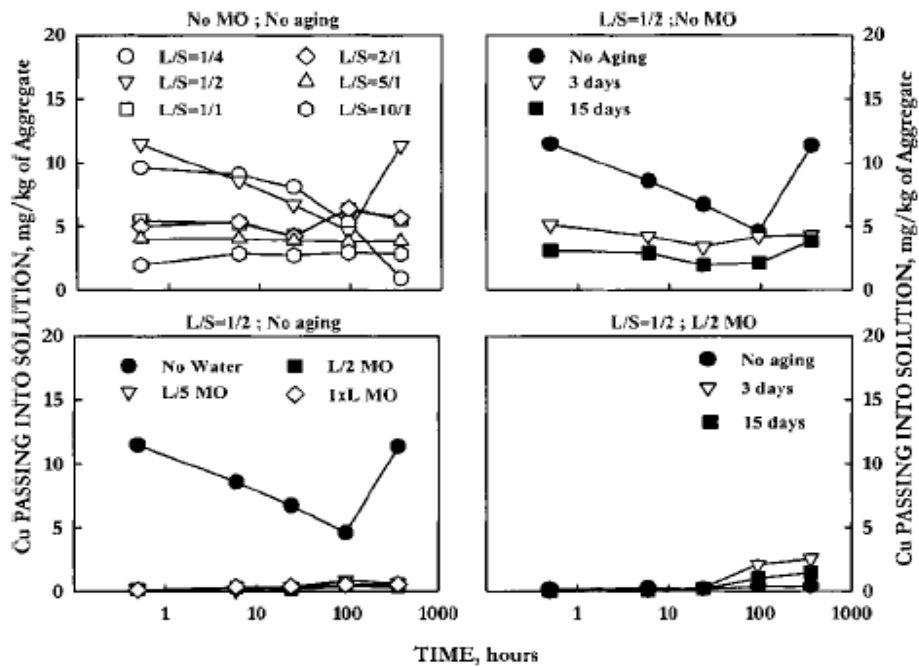
Figure 3.4. Effect of different parameters on the leaching of Cu from the aggregate for Soma ash for A/W ratio of 1/10 (Cu conc. 172 ppm in ash, 55 ppm in AMD and 0.1 ppm in MO)

Metal removal, if it is due to simple precipitation, has nothing to do with the adsorbing properties of the fly ash and should not be called 'fixation'. Metals removed from the solution by simple precipitation will leach back into solution when the pH of the solution is lowered below the pH of the formation of metal hydroxides. The term 'fixation' should be reserved for adsorption of metallic ions onto the fly ash (Üzelyalçın and Polat, 2004) or production of more stable spheres by chemical reactions. Both mechanisms are less sensitive to pH variations compared to simple precipitation and are more preferable since they may result in lower leachability of the metals over a wide pH range, especially at lower pH values. Hence, a quantitative assesment of the contributions of these mechanisms is extremely important to assess the potential of the fly ash for fixation of trace elements.

3.3.2. Production of Aggregates from Fly Ash and Acidic Waste Mixtures

The use of fly ash mixtures for hazardous waste stabilization and solidification accounted for the reuse of approximately 1.93% (11.9% of total reuse) of fly ash in 1996. The process of stabilizing a waste consists of encasing the waste in a solid block, whereas solidification transforms a semi-liquid waste to a solid. Stabilization limits the solubility or mobility of hazardous contaminants by sealing material in an impermeable monolith, adjusts the pH of a waste to a range where amphoteric metals are less leachable. Adjusting the pH can reduce the permeability of the waste, providing a decrease in metal precipitation/Ieachability at both high and low pH values. By the application of solidification process, a strong, durable solid structure waste block is produced with hydration properties similar to those of Portland cement. Solidification increases material strength to improve handling characteristics (Scheetz and Earle, 1998).

3.4. Metal Ions in Aqueous Solution

In a broad classification of chemical reactions, we distinguish between two general groups of reactions by which atoms achieve such stabilization; 1) redox processes, in which the oxidation states of the participating atoms change, and 2) reactions in which the coordinative relationships change. The coordinative relations

change if the coordinative partner changes or if the coordination number of the participating atoms is changed. The following examples can be given to illustrate the mechanism;

If an acid is introduced into water,

$$HClO + H_2O = H_3O^+ + ClO^- \tag{3.1}$$

The coordinative partner of the hydrogen ion (which has a coordination nu mberis changed from ClO^- to H_2O.

2) The precipitation that frequently occurs in the reaction of a metal ion with a base,

$$Mg^{2+} (aq) + 2OH^- = Mg(OH)_2 (s) \tag{3.2}$$
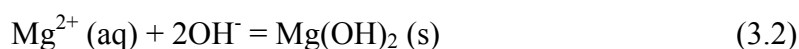
can be interpreted in terms of a reaction in which the coordinative relations are changed, in the sense that a three dimensional lattice is formed in which the metal ion is surrounded by and coordinatively saturated by the appropriate number of bases.

3) Metal ions can also react with bases without formation of precipitates in reactions such as;

$$Cu^{2+} (aq) + 4NH_3 = [Cu(NH_3)_4]^{2+} \tag{3.3}$$
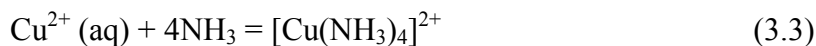
In this simple classifiction of reactions, no distinction needs to be made between acid-base, precipitation, and complex formation reactions, they are all coordinative reactions (Stumm et al., 1996).

Stability constants or equilibrium constants for metal complex formation, have long been employed as an effective measure of the affinity of a ligand for a metal ion in solution (Martell and Motekaitis, 1988).

3.4.1. Concentrations of Heavy Metals in Natural Waters

Any combination of cations with molecules or anions containing free pairs of electrons (bases) is called coordination (or complex formation) and can be electrostatic, covalent, or a mixture of both. The metal cation will be called the *central atom*, and the anions or molecules with which it forms a coordination compound will be referred to as *ligands*.

Two types of complex species can be distinguished; ion pairs and complexes.

1. *Ion pairs.* Ions of opposite charge that approach within a critical distance effectively form an ion pair and are no longer electrostatically effective. The metal ion or the ligand or both retain the coordinative water when the complex compound is formed; that is the metal ion and the base are separated by one or more water molecules.

2. *Complexes.* Most stable entities that result from the formation of largely covalent bonds between a metal ion and an electron-donating ligand-the interacting ligand is immediately adjacent to the metal cation-are called complexes.

3.4.2. Chemical Speciation

The term species refers to the actual from in which a molecule or ion is present in solution. For example, iodine in aqueous solution may conceivably exist as one or more of the species I_2, I^-, I_3^-, HIO, IO^-, IO_3^-, or as an ion pair or complex, or in the form of iodo compounds (Stumm and Morgan, 1996).

In all solutions the bare metal ions are in continuous search of a partner. All metal cations in water are hydrated and they form aquo complexes. The coordination reactions in which metal cations participate in aqueous solutions are exchange reactions with the coordinated water molecules exchanged for some preferred ligands.

Hydroxides and sulphides of metals often occur in amorphous and several crystalline modifications (Stumm and Morgan, 1996). The solubility of amorphous Fe $(OH)_3$, and ZnO with pH is shown in Figure 3.5. It can be seen that there is a pH value at which the solubility is minimum. In highly alkaline or highly acidic regions, the solubility becomes larger. In natural water systems, the concentration of metal ions is controlled by the solubility of the metal carbonates. Theis and Wirth (1977) have studied the sorptive behavior of trace metals on fly ash in aqueous systems. Weng and Huang (1994) have studied the treatment of industrial waste water containing heavy metals by fly ash and cement fixation. The fly ash has been demonstrated to be a potential heavy metal adsorption medium for industrial waste water (Pandian, 2004). Thus it can be seen that the release of metal ions from fly ash depends on its own characteristics (chemical composition, surface area, and cation exchange capacity), solution (permeant) characteristics (pH of the solution, valency and concentration of the ion), and other factors like duration of reaction of time, temperature, etc. The leaching

characteristics of fly ash mainly depend on the amount of free lime present in it. The desorption of metal ions from fly ash also depends on the pH of the leachate.
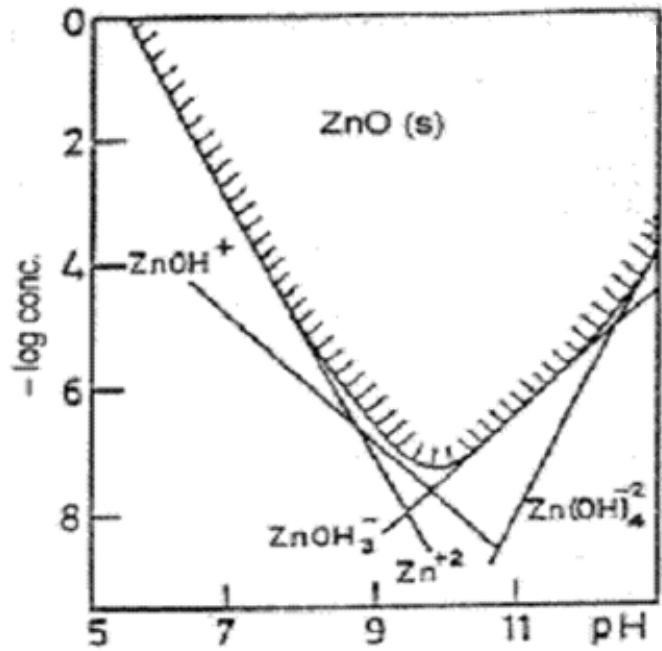
a)
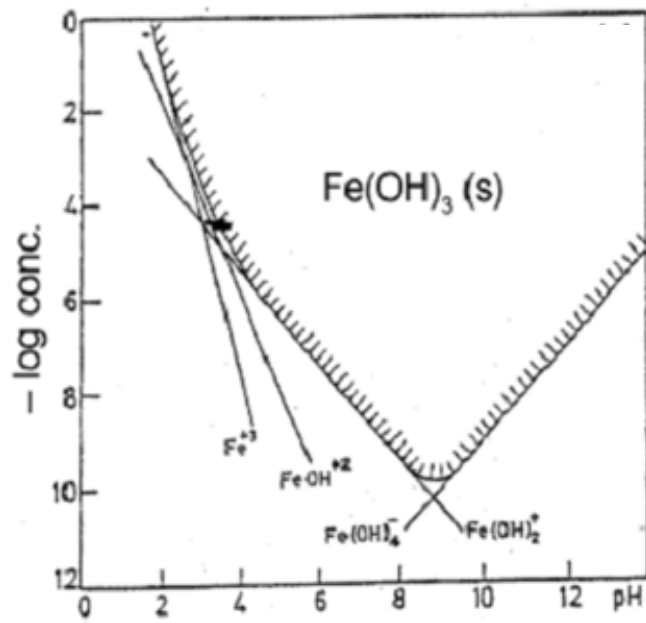
b)

Figure 3.5. The solubility of zinc and iron oxides

(Source: Pandian, 2004)

CHAPTER 4

MATERIALS AND EXPERIMENTAL METHODS

4.1. Soma Fly Ash (SFA)

In this study, a fly ash from Soma Thermal Power Plant located in Manisa, Turkey was used. The Soma basin is one of the most productive coal basins of western Anatolia-Turkey. Soma Thermal Power Plant generates electricity by combustion of the lignite coals and it is the region's largest electricity producer. The amount of fly ash which has to be disposed off every single day is 12 thousand tons. In Table 4.1, the production-capacity values of the Soma Power Plant were given.

Table 4.1. Production capacities of Soma Power Plant

Lignite reserve	Coal (tons/day)	Ash (tons/day)	Units	Capacity MW/unit
Soma basin	30000	12000	8	1034

The solid waste is transported to the disposal site by the use of conveyor belts, nearly 10 km in length. The solid waste is damped using nozzle on the conveyer belts to prevent spreading of ash by wind. Furthermore, the waste is mixed with water at the disposal site creating a slurry pond. Generally, water requirements for sluicing coal ashes in the Soma thermal power plant are 7 L of water per kg of fly ash. Due to high area requirements and water quality deterioration of sluicing waters, ponds are not frequently used in Turkey. However, the Soma thermal power plant has a rather large ash pond and used as the ultimate waste disposal site. The collected water in waste pond is used for various purposes such as moistening ash in the plant without any treatment (Baba and Kaya, 2004).

This basin has a coal potential of 626 Mt, and producing run-of-mine coals of about 11 Mt per year are consumed for domestic heating due to relatively low-sulphur

content and high calorific value, and as feed coals in the coal-fired Soma. The geology of the Soma coal basin has been described and illustrated in detail earlier (Karayigit and Whateley, 1997; Karayigit, 1998; Inci, 2002). Briefly, this basin contains two mineable coal seams, lower (k1) and upper (k3), which are currently exploited in underground and mainly open-cast mines. The lower seam is located in the Soma Formation of Early Middle Miocene age and the upper seam in the Denis Formation of Late Miocene age. The Soma and Denis Formations, which are characterized by non-marine, laterally extensive limestone–marl–claystone dominated units, form the sedimentary sequence of the basin. Pyroclastic materials are more common in the Denis Formation. Preliminary results relating to the characterization of feed coals, bottom ashes, and fly ashes from the Soma (Turkey) have been reported by Bulut et al. (2002). Additional studies on the variations in composition for individual fly ash samples from two power units in the Soma Thermal Power Plants have been also performed (Karayigit et al., 2005).

4.1.1. Sampling of SFA

The fly ash used was obtained directly from a coal combusting power generating plant in western part of Turkey; Soma and were mixed in laboratory conditions by applying "coning and quartering method" to get homogenous samples. The mixed fly ashes are kept in tightly locked PVC buckets to prevent ingress of CO_2 which leads to loss of alkalinity (Gitari et al., 2010). The fly ash samples were collected from the precipitators.

4.1.2. Chemical, Mineralogical and Micro-Structural Analysis

Element concentrations of fly ash were detected using Inductively Coupled Plasma Mass Spectrometry (ICP-MS, Agilent 7500ce) and Inductively Coupled Plasma Atomic Emission Spectrometry (ICP-AES, Varian Liberty Series II, Axial). The instrument operating conditions of ICP-AES and ICP-MS are described in Table 4.2. The digestion of samples was performed by both tetraborate fusion and microwave digestion (CEM MARS 5) for ensuring reproducible analysis. Element concentrations were also checked by X Ray Fluorescence Spectroscopy (XRF, Spectro IQ, II) and Energy-Dispersive X-Ray analysing system (SEM-EDX, Phillips).

Table 4.2. ICP-AES and ICP-MS Operating Conditions

ICP-AES Operating Conditions		ICP-MS Operating Conditions	
Argon gas flow	15 L/min	RF power	1550 W
Argon auxiliary flow	1.50 L/min	Reaction system	Octopole
PMT voltage	650 V	He integration time/ He gas flow	0.1 sec / 4 mL/min
Sample uptake	30 sec	Dwell time	48.44 sec
Rinse time	10 sec	Carrier gas flow	0.9 L/min
Spray chamber	Glass Cyclonic	Make-up gas flow	0.15 L/min
Nebulizer	Glass nebulizer	Nebulizer/ Nebulizer pump	Concentric/ 0.11 ramp/sec

Major elements were detected by ICP-AES after tetraborate digestion procedure. The aliquots were prepared by the ASTM fusion method and the dissolution procedure was shown below;

- Soma fly ash sample was taken and dried at 110 ºC for 1-2 h.
- 0.1 g of fly ash sample was fused with 1 g of 1/1 mixture of lithium tetraborate and lithium metaborate in platinum crucible at 1000 ºC.
- The fly ash was fused 15 min; the melt was then permitted to cool.
- Fused sample was dissolved in 10% HNO_3.
- Upon complete dissolution, the solution sample was completed to 500 mL.

Trace elements quantification by ICP-MS requires an adequate digestion technique to extract all the minor elements into liquid solutions. To select the best sample treatment of fly ash samples, two microwave assisted digestion methods were evaluated (Hassan et al., 2007) and applied to the JR-3 Japanese Reference Rock Standard. Based on this evaluation, following procedure which utilizes Model CEM MARS 5 microwave was selected. The parameters of this procedure are listed in Table 4.3.

Table 4.3. Operating parameters, temperature programme and digestion reagents for Mars 5 microwave system

Parameters	MARS 5 Microwave
Power (W)	0-1,200
Vessel volume (mL)	120
Number of vessels	12
Micro-vessels volume (mL)	7.0
Sensors control	P and T
Ramp time (min)	5.5
Hold time (min)	10
Hold temperature (ºC)	175
Mass (mg)	10, 30 and 100
HNO_3 digestion solution (mL)	3.0 conc. HNO_3
HNO_3/HCl digestion mixture (mL)	3.0 mL of 5.6% HNO_3 and 16.7% HCl (v/v)

High-purity deionized distilled water (DDW) 18 MΩ cm^{-1} (Milli-Q Element, Bedford, MA) was used in all experiments. pH measurements were done using Orion 5 star pH meter.

Major elements were determined also by X-ray flourescence (Spectro IQ II). Approximately 1.0 g of powdered fly ash sample was weighed in a porcelain crucible and heated at 1000°C in a muffle furnace for 2 hs. After cooling to room temperature in a dessicator for 1 h, the sample (with the crucible) was re-weighed and the weight difference was calculated as the loss on ignition (LOI).

4.1.3. Physical and Geotechnical Characterization

Fly ash particles were dried in an oven at 110 °C. Particle diameter and size distribution were measured by laser light diffractometry equipment (Mastersizer 2000, Malvern Instrument, UK). The average particle size was expressed as the volume mean diameters in micrometers. Wet sieve analysis was done using Retsch series of screens with 75, 53, 38 and 25 μm apertures.

The mineralogy of the samples was determined by X-ray diffraction (XRD) (Phillips X'Pert Pro) and Fourier transform infra-red (FTIR) spectrometry (Shimadzu, 8201). A Phillips XL-30S FEG model SEM was used to study the morphology, texture and chemistry of the samples. Perkin Elmer Diomand TG/DTA was used to measure the changes in weight of a sample with increasing temperature. Surface measurements were performed with BET by Micromeritics Gemini V.

Figure 4.1 summarizes the complete procedure employed in characterizing the Soma fly ash sample as a flowsheet;
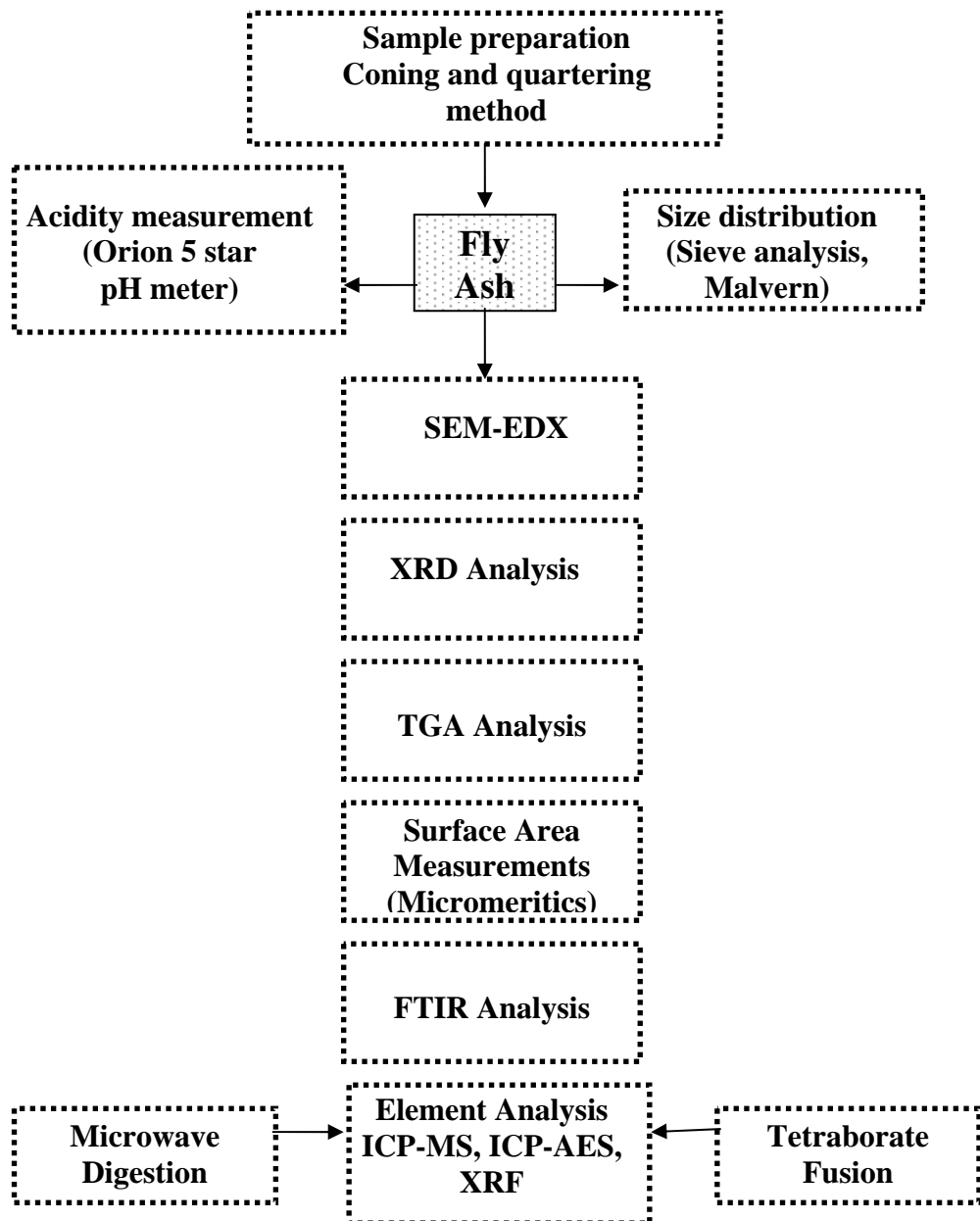
Figure 4.1. Experimental procedure for the characterization of fly ash.

4.1.4. Toxicity Characteristics Leaching Procedure for Fly Ash

In this study, fly ash sample obtained from Soma Thermal Power Plant was subjected to toxicity test such as European Committee for standardization (CEN). This method has been developed by the European Committee for Standardization in order to predict the leaching behavior of trace elements over the long term using demineralized water for the leaching test.

CEN test procedure involves the following steps; first 100 g of dry ash was weighted and put in a bottle. 1 L of distilled water was added and the capped bottle was placed in an agitation device for 24 hr at room temperature. All samples were filtered through 0.45 μm membranes (Baba and Kaya, 2004a).Leaching tests were carried out by dublicate. The contents of major and trace elements in the laboratory were determined by means of Inductively Coupled Plasma Mass Spectrometry (ICP-MS) and Inductively Coupled Plasma Atomic Emission Spectrometry (ICP-AES).

4.2. Acidic Waste (AW) Tests

4.2.1. Sampling of AW

Acidic waste was scoped from from a company which is located in Atatürk Organized Industrial Zone (AOIZ) at Çiğli-İzmir. It manufactures light metal constructions and hot-dip galvanized cable trays and produces significant amount of hydrochloric acid containing dissolved heavy metals from the acid-washing process. It was reported that the yearly output of this waste is around 50,000 L. The waste was scoped from a waste tank by use of 5 L high density polyethylene containers which were initially rinsed with 2% nitric acid solution. The containers were rinsed thoroughly with the acidic waste before sampling. Samples were cooled at 4 $^{\circ}$C in the refrigerator in the laboratory.

4.2.2. Characterization Tests with the AW

The industrial acidic wastewater was collected into plastic containers in the factory and filtered from blue ribbon filter paper immediately after coming to the laboratory. Density measurements of the filtered solutions were done by a picnometer. The pH measurements and neutralization tests were carried out using an Orion 5 Star pH meter. The element determinations were performed after filtering, diluting and lastly acidifying the final solution by nitric acid (HNO_3, Merck, 65% concentrated) up to 1% acidity. Neutralization tests of the acidic waste were performed on solutions containing different amounts of fly ash shaking in an orbital shaker at room temperature at 120 rpm (Thermoshake, Gerhardt). The cation analyses were performed by ICP-MS (Agilent 7500) for minor and ICP-AES (Varian Liberty Series II, Axial) for major elements. The anions were measured by Ion Chromatography (IC, Dionex GP50). IonPac AS-HC (4*250 mm) anion exchanger column (elution rate; 0.1 mL/min) and ED50 chemical detector was used. The IonPac AS9-HC column provides improved separation of the common inorganic anions and the oxyhalides over the AS9-SC. Increased retention time on the AS9-HC (approximately 22 minutes) is due to the high capacity (190 μeq for 4 x 250 mm) of the column. High capacity allows for the determination of trace bromate in drinking water using a large loop injection and an isocratic carbonate eluent. The AS9-HC also provides improved separation of bromate/chloride, chloride/nitrite, and chlorate/nitrate analyte pairs. The AS9- HC column is specified in validated methods such as U.S. EPA Method 300.1.

A simple diagram of the characterization steps for industrial acidic waste is prepared in Figure 4.2.
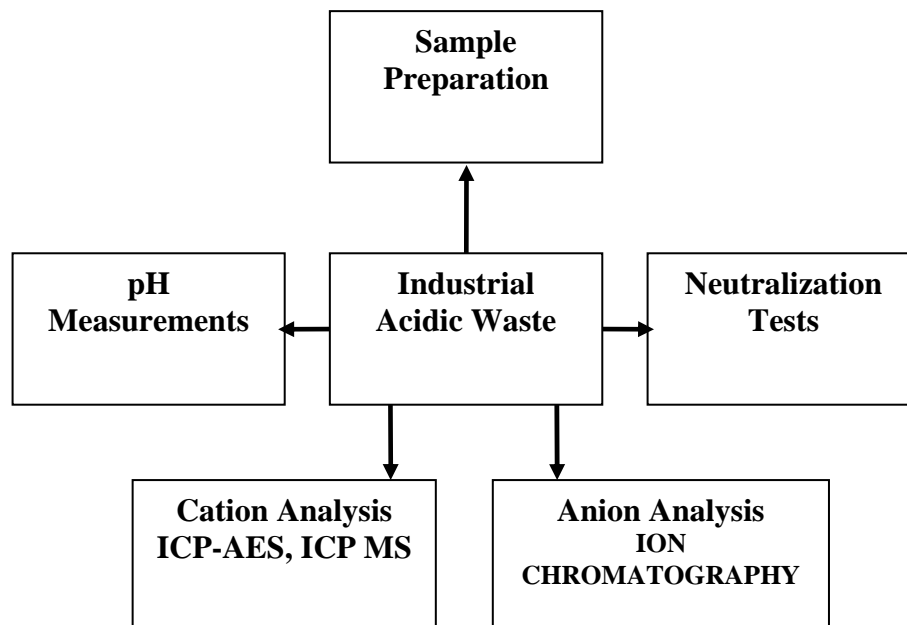
Figure 4.2. Experimental procedure for the characterization of industrial acidic waste.

4.3. Aggregate (AG) Tests

4.3.1. Neutralization Studies

Soma fly ash was titrated separately with hydrochloric acid (HCl) and industrial acidic waste to determine its theoretical and actual neutralization capacity. The titration experiments were performed in polypropylene erlenmeyer flasks with caps and shaked at 120 rpm (Thermoshaker, Gerhardt) until the slurry comes to a stable pH. The measured amount of fly ash samples were given in the flask and diluted. The mathematical results of the titration were calculated multiplying with dilution factors of the measured amounts. Soma fly ash-water slurries were prepared at incremental solid weight percentages of 2%, 5%, 10%, 25% and 50%. This corresponds to respective fly ash amounts of 1 g, 2.5 g, 5 g, 12.5 g and 25 g in a water slurry amount of 50 grams. The titration procedure was repeated in two parallel sets of experiment. Titration studies were carried out with 1 N HCl which was obtained by completing 82.89 mL of 37% concentrated HCL (Merck) into 1 L volumetric flask with ultra pure water. The initial pH of 1 N HCl was 0.26. The acid was added into the fly ash-water mixtures at long time intervals (24 hours) which were required to reach a stable pH value for the

slurry. The titration was started with an Erlenmayer flask containing a precise volume of the diluted solutions placed underneath an automatic burette containing the acid. No indicator was used for titration. By controlling the added amount of acid into the basic fly ash solutions, the consumed amounts were recorded. A typical titration curve was obtained for each acid-base titration.

In the second part of the study, the neutralization potential of the fly ash sample was measured using the actual acidic waste with the same procedure outlined in the previous paragraph for different amounts of fly ash in the slurry. The incremental amounts of fly ash were again 2.5 g, 12.5 g, 25 g and 50 g. No water was used in these tests.

4.3.2. Aggregate Production

The fly ash was mixed with acidic waste at pre-determined solid/liquid ratios (estimated from the neutralization potential work) for 20 minutes using a semi-automatic stand mixer (KitchenAid Bowl Lift Stand Mixer, Model Professional 5 Plus) to obtain an aggregate mixture. Effective and uniform mixing of fly ash with water and waste is an important condition for producing good quality fly ash aggregates. Initially a mechanical overhead stirrer (Heidolph-RZR 2102 Control Z) was used with standard shaft. However, it was discovered that the quality of mixing by overhead stirrer was poor and inconsistent due to high viscosity of the mixing sludge. Therefore, a semi-automatic stand mixer (a dough maker) was purchased and used with much better mixing with consistent results. The solid amounts were kept constant in each experiment so that 150 grams of fly ash were added into the mixture. Then the 5 grams of mixture was pressed in twelve ton, manual hydraulic press by applying 1 ton of force (Carver Standard Press, 3851 Model C) to produce aggregate pellets in 2 cm diameter. For each set of experiment; 3 samples were produced for pH measurements (for 2, 4 and 16 days drying). The samples were immersed in water in separate plastic containers to achieve a product/water ratio of 1/10. Then, pH measurements were done at time intervals of 0, 30 min, 7h, 2 days, 4 days, 16 days and 90 days on these samples (Figure 4.3).
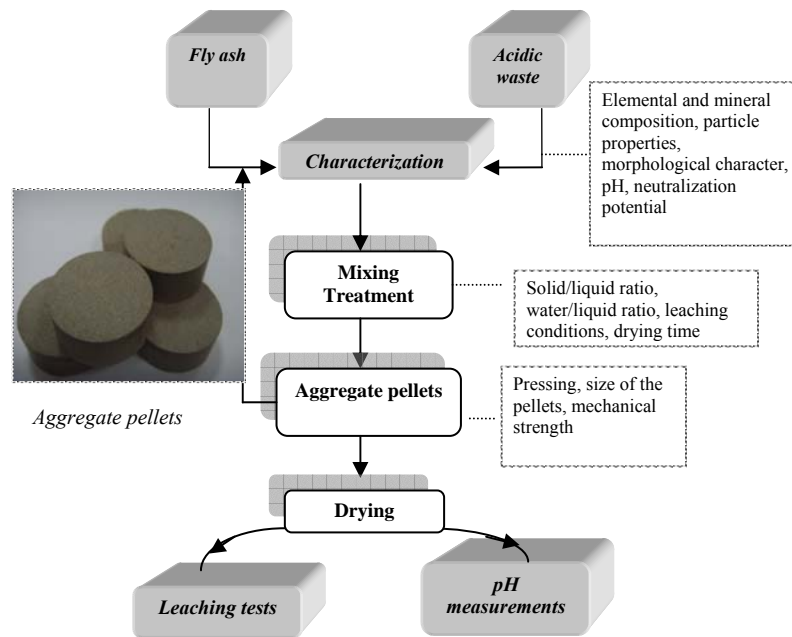
Figure 4.3. General flowsheet of the experimental procedure.

4.3.3. Leaching Tests

Leaching studies were carried out on the aggregate pellets to determine the amount of metals leaching into solution. The aggregates were dried for 2 days, 4 days and 16 days before these tests. The reason for drying was essentially to allow enough time for the reactions which may be taking place between the fly ash particles and acidic waste in the aggregate. 21 samples were produced for leaching measurements (7 samples for 2 days drying, 7 samples for 4 days drying, 7 samples for 16 days drying; each of the 7 sample was for obtaining a single leach-time sample) and immersed in deionized water at a ratio of 1/10. The containers were shaken two times a day to provide mixing and ensure water-aggregate contact. Solution samples were filtered from Whatman, Grade 589 Blue Ribbon quantitative filter paper, diluted with deionized water and acidified with concentrated nitric acid (65%) prior to the elemental analysis to determine the extent of leaching of various species into solution from the aggregates.

4.3.4. Aggregate Characterization Tests

Aggregates were tested according to the procedure given in Figure 4.4. The samples subjected to the 16 days aging at room temperature (AG16) and the samples

subjected to the 16 days leaching after 16 days aging period (LAG16) were tested and compared with each other and the fly ash properties. The aggregates were produced at S/L=4 ratio.
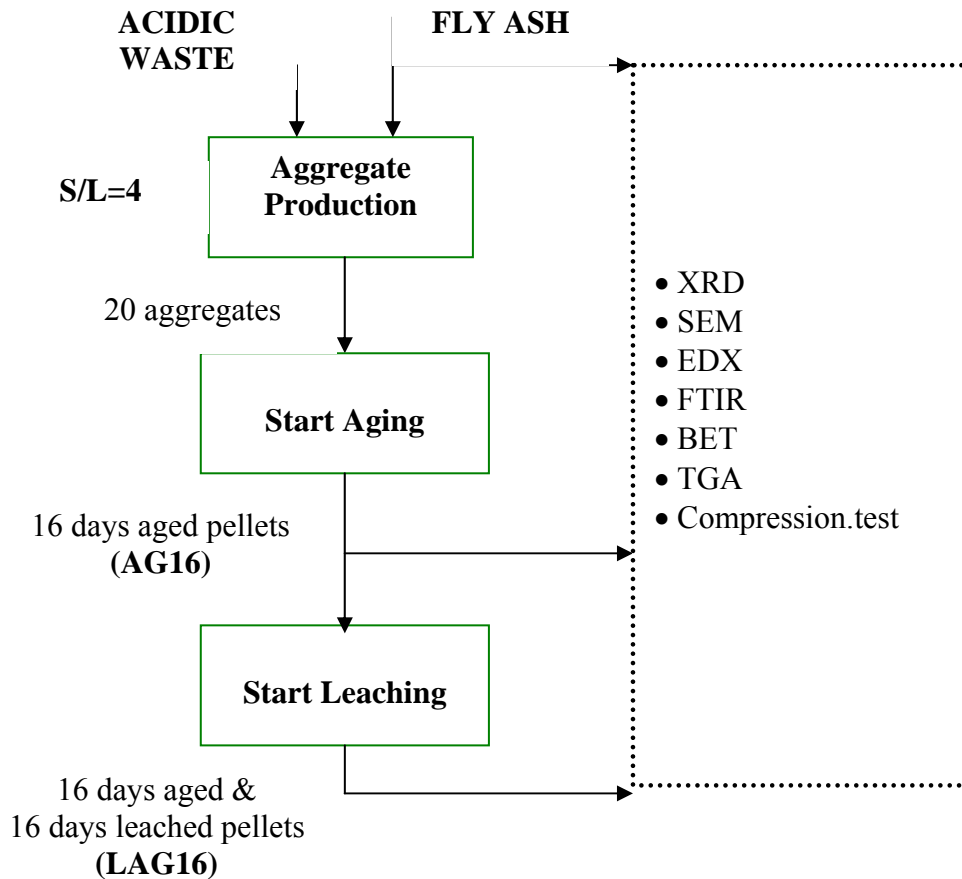
Figure 4.4. Aggregate characterization tests

The X-ray diffraction (XRD) tests were performed using a Phillips X'Pert Pro X-ray diffractometer. XRD spectra of the powder mounts of the fresh fly ash and aggregates were obtained by step-scanning at intervals of 0.03° 2θ from 5 to 80 and counted 0.6 s per step. Phillips X'Pert Pro was used. Aggregates were cut into two parts horizontally to observe the cross section and the surface and directly given to the equipment.

A Phillips XL-30S FEG model SEM was used to study the morphology, texture and chemistry of the samples. Analysis by SEM-EDX of the aggregates (cross-section and surface) and unreacted fly ash was done to qualitatively identify probable mineral phases that formed in the process and eluded detection by XRD.

The Spectro IQ II simultaneous XRF spectrometer was used to determine the elemental composition of the aggregates. The powdered form of aggregates were digested with lithium tetraborate before the analysis.

The BET surface area of the aggregates was determined by N_2 adsorption. Aggregate pellets were rasped with a mini-handsaw and a small fragment approximately 5 mm*5 mm in size were taken for the analysis (A piece which does not to contact with O_2 in air). Degassing was applied at 60 ^{o}C.

The pressed aggregates were also subjected to mechanical tests to find compressive strength and X-ray diffraction tests to determine the micro-structural development. Mechanical tests were performed using compression test equipment (Autograph AG-I 250 kN, Schimadzu). Aggregates were loaded at a constant axial strain of 0.0282 in/min. A dial gauge was used to measure the vertical deformation, and a load ring to measure the load.

XRD, SEM, FTIR, SEM-EDX, BET, XRF and the unconfined compressive strength tests were performed on each aggregate which were stabilized by drying 16 days and drying 16 days and waited 16 days to see the leaching effect at room temperataure.

4.3.4.1. Mechanical Tests of Aggregates

Compressive strength is the capacity of a material to withstand axially directed pushing forces. When the limit of compressive strength is reached, materials are crushed. Concrete can be made to have high compressive strength, e.g. many concrete structures have compressive strengths in excess of 50 MPa, whereas a material such as soft sandstone may have a compressive strength as low as 5 or 10 MPa.

By definition, the compressive strength of a material is that value of uniaxial compressive stress reached when the material fails completely. The compressive strength is usually obtained experimentally by means of a compressive test. The apparatus used for this experiment is the same as that used in a tensile test. However, rather than applying a uniaxial tensile load, a uniaxial compressive load is applied. As can be imagined, the specimen (Usually cylindrical) is shortened as well as spread laterally. A Stress–strain curve is plotted by the instrument and would look similar to the following (Figure 4.5);

Figure 4.5. A typical stress-strain curve

The compressive strength of the material would correspond to the stress at the red point shown on the curve. Even in a compression test, there is a linear region where the material follows Hooke's Law. Hence for this region $\boldsymbol{\sigma = E\varepsilon}$ where this time E refers to the Young's Modulus for compression.

This linear region terminates at what is known as the yield point. Above this point the material behaves plastically and will not return to its original length once the load is removed.

There is a difference between the engineering stress and the true stress. By its basic definition the uniaxial stress is given by:

$$\sigma = \frac{F}{A}$$

(4.1)

where, F = Load applied [N], A = Area [m^2]

As we said, the area of the specimen varies on compression. In reality therefore the area is some function of the applied load i.e. $A = f(F)$. Indeed, we can however say that the stress is defined as the force divided by the area at the start of the experiment. This is known as the engineering stress and is defined by,

$$\sigma_e = \frac{F}{A_0}$$

(4.2)

A_0=Original specimen area [m^2]

Correspondingly, the engineering strain would be defined by:

$$\epsilon_e = \frac{l - l_0}{l_0}$$

(4.3)

where l = current specimen length [m] and l_0 = original specimen length [m]

The compressive stress would therefore correspond to the point on the engineering stress strain curve $\left(\epsilon_e^*, \sigma_e^* \right)$ defined by

$$\sigma_e^* = \frac{F^*}{A_0}$$

(4.4)

$$\epsilon_e^* = \frac{l^* - l_0}{l_0}$$

(4.5)

where F^* = load applied just before crushing and l^* = specimen length just before crushing.

The *strength* of a metal is its ability to withstand the action of external forces without fracture. *Tensile strength*, also called *ultimate stress* (σ_u), is the maximum stress that can be applied to a specimen. It is the highest point on the stress-strain curve.

Modulus of elasticity, or *Young's modulus* (E), is the slope of the stress-strain curve in the elastic region. The elastic region is the linear portion at the beginning of the curve. As long as the material is loaded within the elastic region, the strains are totally recoverable and the specimen will return to its original dimensions as the load is relaxed to zero (Smith, 1993).

In this study, a computer controlled compression test machine (Schimadzu AG-I 250 kN) was used to determine the mechanical properties of aggregates. The test method was set by the operator using *Trapezium2* software program (v.2.15).

4.4. Calculation of Saturation States

MINTEQ-Visual was used to determine the equilibrium concentrations in the leaching solution as a function of pH. MINTEQ-Visual is a geochemical model capable of calculating equilibrium aqueous speciation, adsorption, gas phase partitioning, solid phase saturation states, and precipitation-dissolution of metals.

4.5. Statistical Evaluation of the Experimental Results

MINITAB Release 14 was used to evaluate the experimental results of leaching amount of elements at maximum leaching time (90 days). For each element, 2 way analysis of variance (ANOVA) was performed using 12 experiments as the response factor. S/L ratios and aging time factors were evaluated based on the results from the ANOVA. Analysis was performed using the statistically significant factors at the $\alpha=0.05$ level.

CHAPTER 5

RESULTS AND DISCUSSIONS

5.1. Results of Characterization of Soma Fly Ash (SFA)

This part of the thesis deals with the treatment of the coal fly ash from Soma Thermal Power Plant in Manisa-Turkey to see if it had suitable engineering and environmental properties needed for use in industrial acidic waste management and it could be used as a low-strength building material. For this purpose, a detailed study of the physical and chemical properties, engineering and leaching behavior was required. To achieve this, samples of Soma fly ash were collected and studied using proximate and ultimate analyses, such as X-ray powder diffractometry, Fourier transform infrared spectra, scanning electron microscopy with energy-dispersive X-ray microanalysis techniques, inductively coupled plasma-atomic emission spectrometry, inductively coupled plasma-mass spectrometry, XRF and N_2 adsorption techniques.

5.1.1. Physical Properties of SFA

The pH of the Soma fly ash solution was calculated as 12.1 in a solid/liquid ratio of 1/30 (ash samples were diluted 30 times with deionized water for pH measurement). The specific gravity of Soma fly ash was 1.97. The values are the average of three measuremets.

5.1.2. Particle Diameter and Size Distribution of SFA

Particle size distribution of fly ashes is of particular interest when the material is used as a substitute in aggregate mixtures. Potential effects influenced by particle size distribution are related to the structure of the aggregate mixture, permeability of the dried aggregate and mechanical strength. Particle characterization of fly ashes is also

important for the leachability of the smallest particles is easier as they have more reactive surfaces which also lead concentration of trace elements in the finest particles.

Particle size distribution of Soma fly ash was determined using 38, 53 and 75 µm sieves and the cumulative percentage of each size was shown in Figure 5.1.
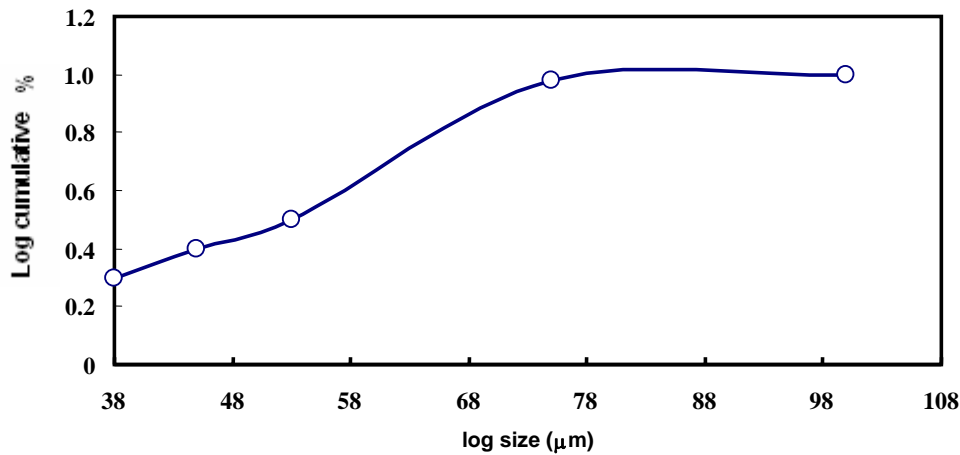
Figure 5.1. Cumulative size distribution of Soma fly ash.

In order to see the size distribution of the ash at sizes below 38 µm, size distribution of the raw fly ash was also measured using a laser light diffractometry equipment (Mastersizer 2000, Malvern Instrument, UK) using the wet dispersion method in water. The ash sample was dispersed in distilled water solution using the on-line dispersed system of the analyzer. The measurement represents an average of three nearly identical readings from Malvern. The grain size distribution of Soma fly ash can be classified as Normal-Gaussian particle size distribution with d(0.1), d(0.5) and d(0.9) values of 8.202 µm, 56.008 µm and 210.187 µm respectively. The results of the volume distribution are given in Figure 5.2.
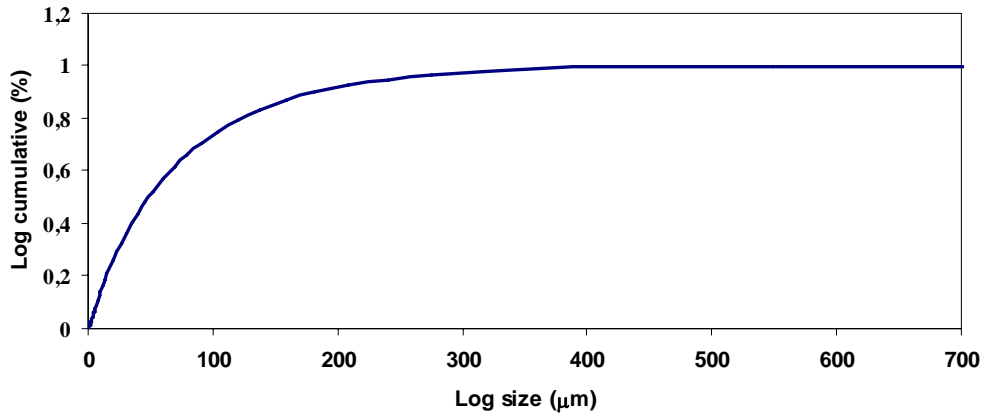
Figure 5.2. Volume size distribution graph of Soma fly ash.

If the ash particles can be assumed solid, spherical particles, one can determine an approximate surface area of the sample from the size distribution data. In order to achieve this, the volume distribution given in Figure 5.2 must be transformed into a number distribution. The number size distribution can easily be calculated from the volume distribution using the size intervals and frequencies assuming solid spherical particles. The number size distribution calculated is given in Figure 5.3. It can be seen that d(0.5) value of the distribution shifted to less than 1 μm (Figure 5.4).

The surface area of the sample calculated from the number distribution is around 0.4 m^2/g. This is rather low most probably due to the "solid particles" assumption since fly ash is known to contain hollow cenospheres which would certainly increase surface area. However, the value 0.4 m^2/g can be assumed to be the "lowest" possible surface area for the Soma ash sample.
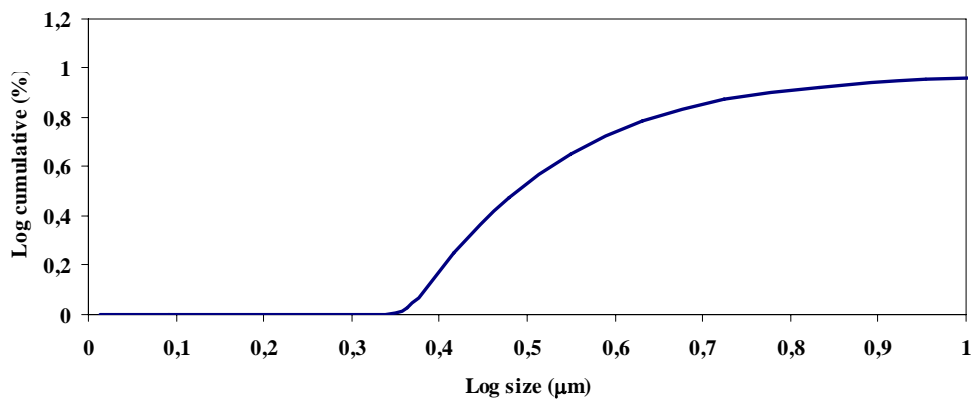
Figure 5.3. Number distribution graph of Soma fly ash.
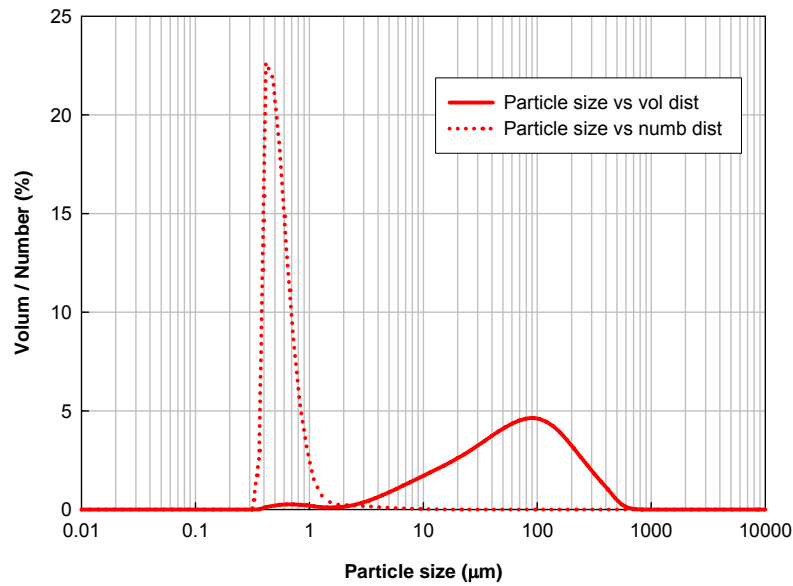
Figure 5.4. Volume versus number distribution graphs of Soma fly ash.

Actually, the specific surface area of the ash sample has also been determined by the BET sorption method. Specific surface area of Soma fly ash sample as measured as by the BET method is 7.26 m^2/g (Micromeritics Gemini V). In the determination of BET surface area by gas adsorption, inert gas nitrogen is adsorbed onto the surface of a solid material. This occurs on the outer surface and in case of of porous materials, also on the surface of pores. The calculation of higher specific surface area by BET confirms the fly ash particles which appear to be mainly solid spheres under the microscope contain large pores. The SEM photographs (Figure 5.7; a, b, c, d) show the indications of such a porous structure. Also note that the ash particles, especially at very fine sizes, show agglomeration, which might not have been dispersed during the Malvern size measurement. These agglomerates might have resulted in a larger than actual mean size, hence a very low specific area of 0.4 m^2/g.

5.1.3. The Mineralogy of SFA by XRD

X ray diffraction data were recorded by a powder diffractometer using CuKα radiation. Figure shows the XRD results of raw Soma fly ash sample. The main chemical compositions of the Soma fly ash identified through XRD and chemical analysis are quartz (SiO_2), anhydrite ($CaSO_4$), mullite ($3Al_2O_32SiO_2$), feldspar ($KAlSi_3O_8$ or $NaAlSi_3O$ or $CaAl_2Si_2O_8$), lime (CaO), hematite (Fe_2O_3) and gehlenite ($Ca_2Al[AlSiO_7]$) (Figure 5.5). This composition is in aggreement with the ash composition for Soma fly ash given in the section 3.1.2 (Karayigit et al., 2000; Bulut et al., 2002, Vassilev et al., 2005).
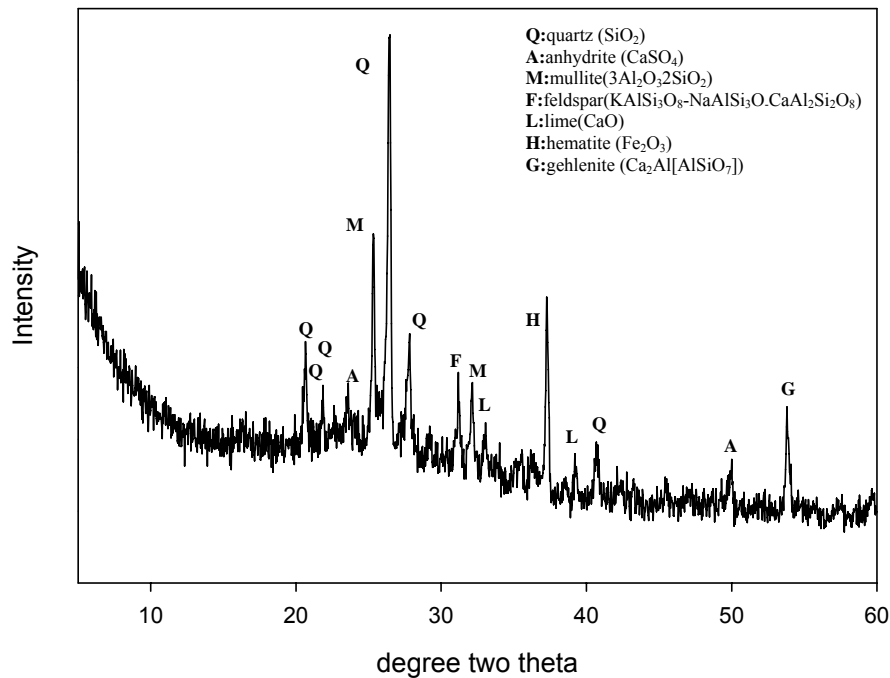
Figure 5.5. X-Ray diffractogram of Soma fly ash.

5.1.4. Infrared Spectra of SFA by FTIR

In this study, Fourier transform infrared spectra were acquired using a Shimadzu, 8201 FTIR Spectrometer. This structure implies that fly ash consists of mainly Si-O-Si and Si-O-Al bands, -H_2O and -OH groups, SO_4^{2-} and CO_3^{2-} bands.

The band at 3363 cm^{-1} for Soma fly ash has been attributed to the stretching vibration of (-OH and H_2O) band and the bending vibration (HOH) at 1650 cm^{-1}. The

asymmetric stretching of Si-O-Si and Si-O-Al groups is assigned at between 947 and 1077 cm^{-1} and symmetric stretching of Si-O-Si and Al-O-Si are assigned at 463 and 947 cm^{-1}. Mollah et al. (1999) defined the Si-O-Si and Al-O-Si bands in close regions. The band at 1080 cm^{-1} was assigned to the antisymmetric stretching vibration of Si-O-Si and the band at 792 cm^{-1} to the corresponding symmetric vibration. The band at 1135 cm^{-1} was assigned to the antisymmetric stretching vibration of Si-O-Al stretching vibration and the band at 700 cm^{-1} to the symmetric Si-O-Al stretching vibration. They claimed that the silicate bands were broad and diffuse because of the overlapping of different types of silicate molecular vibration resulting from various silicate minerals. Lee and Deventer (2002), Jaarsveld et al. (2003) and Nathan et al. (1999) were also reported very broad bands in IR spectra.

Generally, sulfate and carbonate bands are also obtained in their spectra. One of the bands at 590-670 cm^{-1} is attributed to SO$_4^{2-}$ and the ionic sulfate is at 1100 cm^{-1} band. The band at 1417 cm^{-1} is assigned to CO$_3^{2-}$ and the symmetric band of carbonate is at 860 and 880 cm^{-1} region (Figure 5.6).
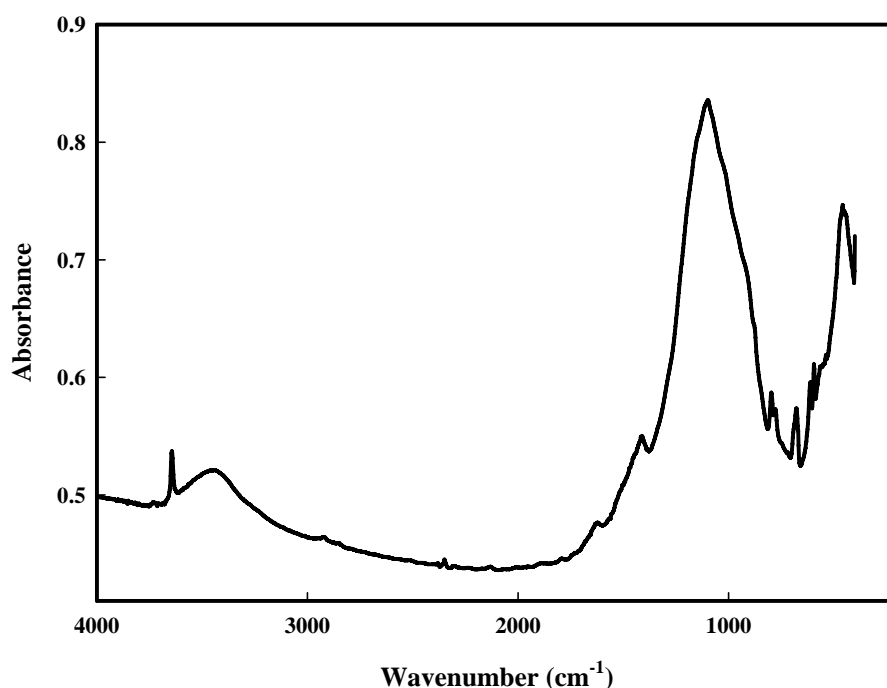
Figure 5.6. FTIR graphics of Soma fly ash.

5.1.5. The Morphology of SFA by SEM

The morphology of a fly ash particle is controlled by combustion temperature and cooling rate. The sizes of the particles observed in this study ranged from sub-micron to greater than 100 μm. However, it can be seen from Figure 6.1 that 90 % of particles (passing size) are below 100 μm. Different sized hollow cenospheres (illustrated with blue arrows) and irregularly shaped unburned carbon particles can easily be noticed. Minerals and mineral aggregates, such as quartz, often showed surface melting. Agglomerated particles and irregularly shaped amorphous particles may have been due to inter-particle contact or rapid cooling (Figure 5.7).

a)   b)

c)   d)
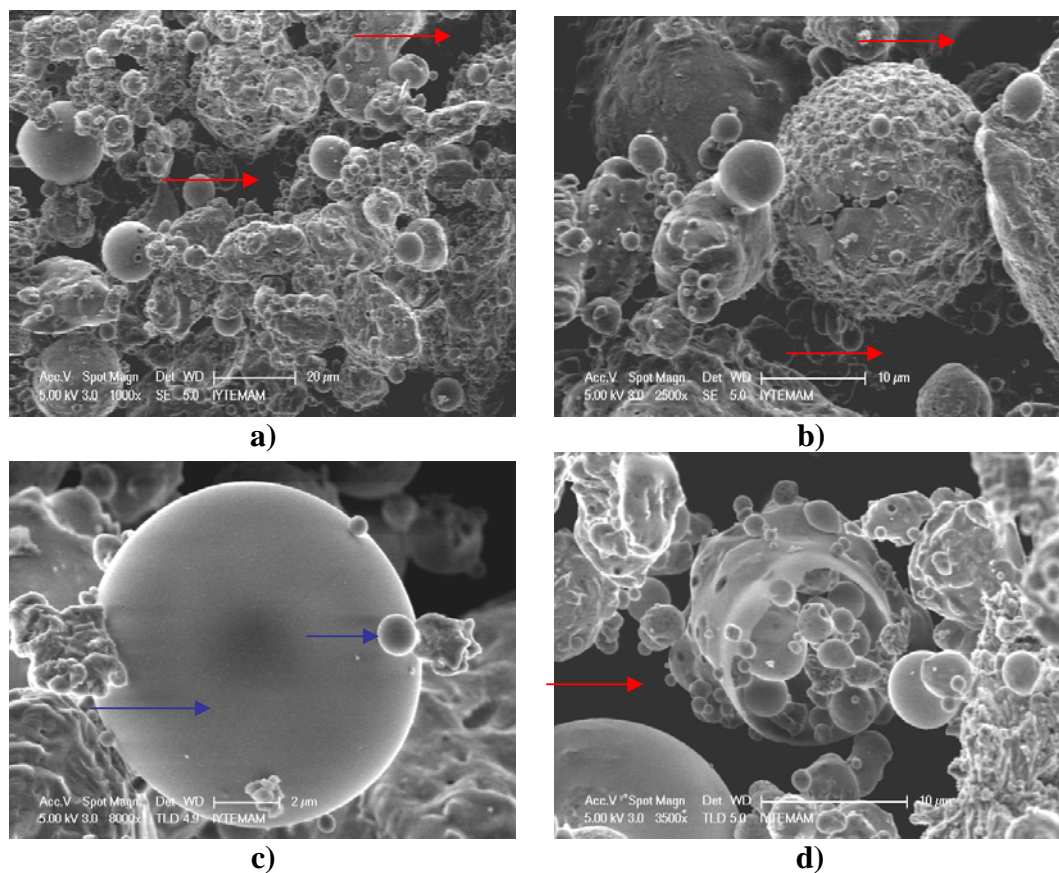
Figure 5.7. SEM images of typical Soma fly ash spheres; a, b, c, d.

5.1.6. Thermal Analysis of SFA by TGA

TGA thermogram of fly ash is shown in Figure 5.8. It can be clearly seen in this curve that there are three steps of mass loss. The first is upto 150 ^{o}C which corresponds to loss of adsorbed water. The loss of ignition value of fly ash was very low (2.1 %), so the amount of loss of water was very low that it was detected also by TGA. Second mass loss step was at 545.99 ^{o}C which corresponds to 2.833 % mass loss. Brown, 2001 suggested portlandite dehydroxylation at 500-650 °C (endothermic reaction) associated with mass loss. The loss of mass at 683.26 ^{o}C was related to calcite decomposition at 650-750 °C (endothermic effect), accompanied by mass loss (Brown, 2001).
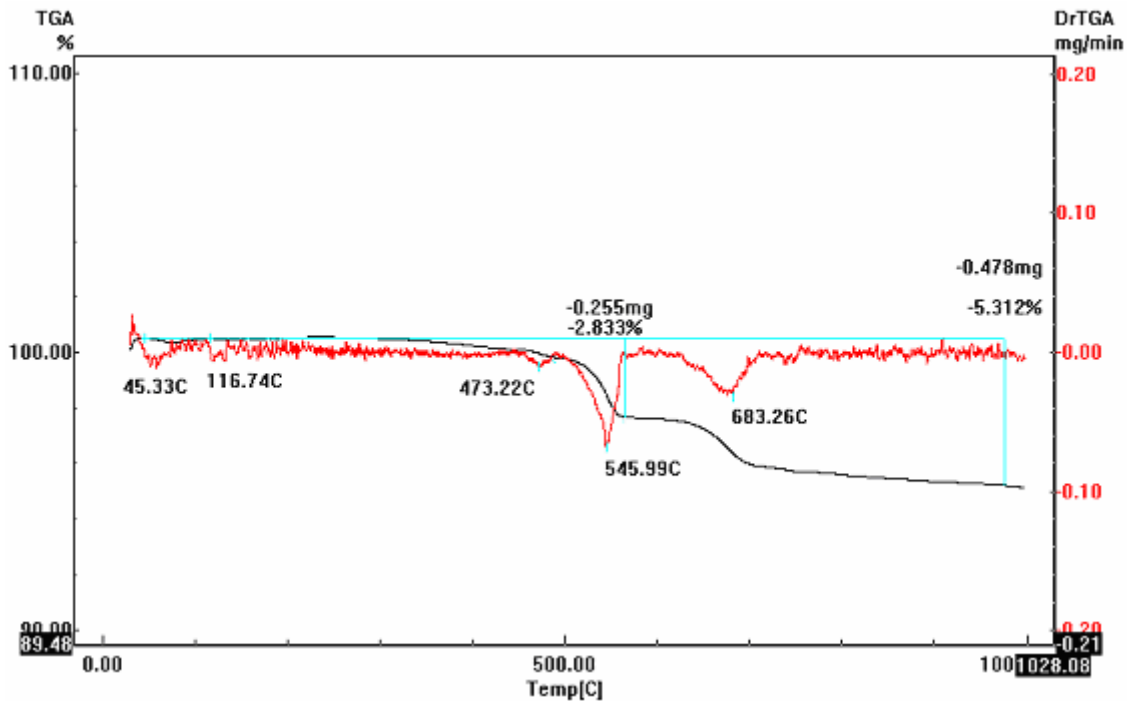
Figure 5.8. TGA and first derivative TGA curve of Soma fly ash.

5.1.7. The Chemical Composition of SFA

The chemical composition of the Soma fly ash was determined by following the steps given below;

- Determination of the major element composition by ICP-AES after lithium tetraborate fusion by direct calibration method.

- Comparison of the major compounds detected by ICP-AES method with XRF and EDX results.

- Determination of the major and minor element compositions of fly ash and the reference (JR-3, Japanese Rock Standard) by ICP-MS after microwave digestion of samples using two different acid digestion solutions.

- Comparison of the two acid digestion methods in microwave technique.

The major components of Soma fly ash was measured with ICP-AES after lithium tetraborate digestion and the measurements were compared with the results of XRF and EDX techniques. There appeared no significant difference among the readings of   ICP-MS and XRF for Al_2O_3, SiO_2, CaO, Fe_2O_3 and BaO, while there were small differences between Na_2O, MgO and K_2O percentages. Although EDX was not a good way to understand the chemical composition of a material quantitatively, there was an acceptable agreement with the results of ICP-AES and XRF (Table 5.1).

Table 5.1. Analysis of Soma fly ash by direct calibration method.

Major components	ICP-AES (borate fusion) (w/w)%	XRF (w/w)%	EDX (w/w)%
Na_2O	0.1	0.2	1.5
MgO	1.9	2.7	2.1
Al_2O_3	24.0	24.3	22.8
SiO_2	45.5	48.5	37.7
K_2O	2.0	1.2	1.8
CaO	21.3	18.2	26.3
Fe_2O_3	5.1	4.8	5.8
BaO	0.1	0.1	2.1

The detection of the minor elements existing in Soma fly ash was performed by microwave assisted ICP-MS technique. A Japanese reference rock standard JR-3 was also analysed with the same techniques and the results were compared with the certified values. Two digestion procedures were applied. HF was not used for the digestion to prevent the health risks. Acid additions in two different protocols were applied. The

concentration results of the digestion using HNO_3 and HCl mixture were higher than only HNO_3 digested samples for almost all elements (Table 5.2).

Table 5.2. Element concentrations determined by microwave asisted ICP-MS technique.

Elements	Microwave digestion (HNO_3+HCl) (mg/kg)	Microwave digestion (HNO_3) (mg/kg)	Microwave digestion (HNO_3+HCl) (mg/kg)	Microwave digestion (HNO_3) (mg/kg)
	Reference-JR-3		*Soma Fly Ash*	
Li	89.5	37.3	123	91.9
Na	584	438	126	119
Mg	219	223	8044	7255
Al	16500	13325	69558	61491
Si	16383	19966	22291	1080
K	11241	7958	5807	4753
Ca	999	425	43666	44408
Cr	13.6	6.0	108	73.3
Mn	431	257	375	351
Fe	22383	13258	31325	26941
Co	7.8	3.3	16.2	13.7
Ni	49.2	29.5	198	104
Cu	60	35.64	115	71.8
Zn	193	149	248	691
Cd	10.6	2.3	5.4	9.3
Ba	265	121	1649	872
Pb	92.9	55	50.7	152

Figure 5.9 and Figure 5.10 shows the recovery of elements comparing two digestion protocols in microwave for reference material and Soma fly ash, respectively. These graphs give a better indication of the differences between the two acid addition methods.
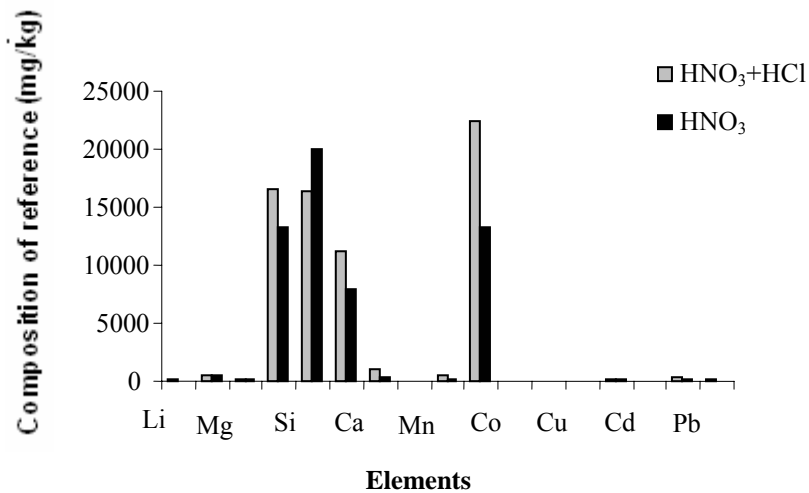
Figure 5.9. Comparison of two microwave digestion methods for reference material
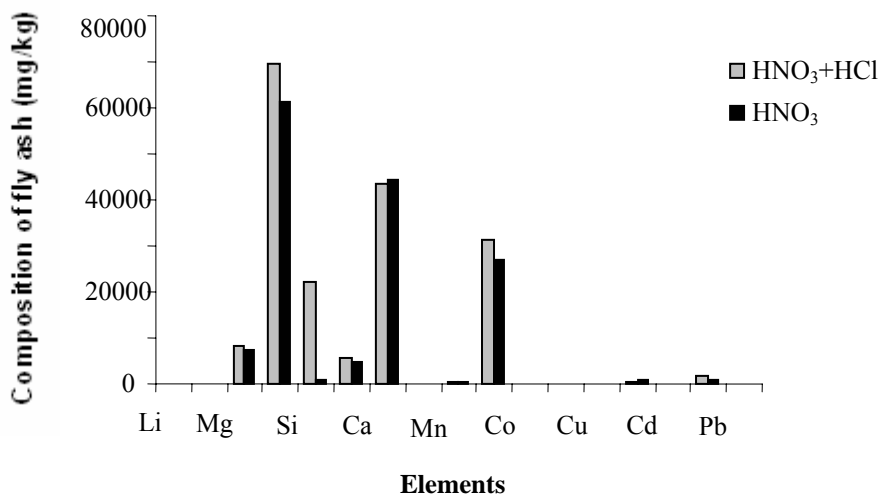
Figure 5.10. Comparison of two microwave digestion methods for Soma fly ash

The results of microwave asisted (by addition of HNO_3 and HCl mixture) ICP-MS and XRF methods were compared with the cerificate of the reference material to detect the applicability of the used microwave digestion procedures in Table 5.3. Microwave assisted ICP-MS technique with this acid mixtures was not suitable to recover all the elements into the solution especially majors. Al-Si bonds could not be broken and Si could not be taken to the solution completely, so the concentration of this element was considerably low in microwave asisted digestion technique. Therefore the

relative concentration of others such as Al_2O_3 or Fe_2O_3 was much higher in the ICP-MS. Hence, only the minor element concentrations were taken into the consideration performed by microwave assisted ICP-MS analysis.

Table 5.3. Comparison of the ICP-MS and XRF methods with the reference certificate

Major components	Certified (w/w)%	Measured ICP-MS (w/w)%	Measured XRF (w/w)%
SiO_2	72.5	24.4	72.5
Al_2O_3	12.1	21.7	12.4
Fe_2O_3	2.6	22.2	5.0
MnO	0.1	0.4	0.02
MgO	0.1	0.3	0.7
CaO	0.1	0.9	0.1
Na_2O	4.7	0.5	2.8
K_2O	4.3	9.4	3.7
Minor elements (ppm)			
Co	1.0	7.8	0
Cr	2.5	13.6	212
Cu	2.1	60.4	2800
Li	118	90	-
Ni	1.1	49.0	41
Pb	34.5	92.9	0
Zn	204	193	302

It is believed that the differences in the concentration of elements are due to leaching characteristics of the fly ashes. It is known that, the fly ash of Soma thermal power plant waste site is mixed with water and a slurry type waste forms. This procedure causes large quantities of calcium deposition and creates a very stiff and impermeable layer at the site. Existence of such impermeable layers has created a pond of which pH differs between 11 and13 (Baba and Kaya, 2002b).

As a summary, the elemental composition of Soma fly ash and the literature values for Soma fly ash composition were given for the comparison in Table 5.4. As it was concluded, Soma fly ash contains mainly SiO_2 and after that Al_2O_3 in its composition. The main minerals measured are in high correlation with literature data. Determined SO_3 content of SFA is lower than the literature values. This can be due to the coal composition that fly ash comes from. There are diversities between the trace element composition of each literature values and results of this study. This is the result of the applied digestion technique, detection limits and analytical corrections applied to equipment to determine such a low concentration.

Table 5.4. Elemental composition of Soma fly ash in literature

Eren and Acar, 2007		Baba and Kaya, 2004a		Polat et al., 2002 a		In this thesis;	
SiO_2 %	42.82	SiO_2 %	54.34	SiO_2 %	33.4	SiO_2 %	45.5
Al_2O_3 %	20.82	Al_2O_3 %	22.01	Al_2O_3 %	16.1	Al_2O_3 %	24.0
Fe_2O_3 %	4.57	Fe_2O_3 %	8.14	Fe_2O_3 %	6.0	Fe_2O_3 %	5.1
CaO %	23.45	CaO %	8.01	CaO %	33.8	CaO %	21.3
MgO %	1.74	MgO %	1.17	MgO %	6.07	MgO %	1.9
SO_3 %	1.47	SO_3 %	2.22	SO_3 %	2.8	SO_3	0.8
K_2O %	1.31	K_2O %	0.90	K_2O %	0.7	K_2O %	2.0
Na_2O %	0.32	Na_2O %	1.00	Na_2O %	1.0	Na_2O %	0.1
Cl ppm	0.01	TiO_2 %	1.01	BaO %	0.2	BaO %	0.1
BET m^2/g	5.35	As^{2+} ppm	140	Co ppm	104	Mn ppm	375
		Ba^{2+} ppm	682	Cu ppm	172	Zn ppm	248
		Cd^{2+} ppm	<1	Pb ppm	420	Ni ppm	198
		Cr^{6+} ppm	491	Cd ppm	40	Cu ppm	115
		Pb^{2+} ppm	138	Cr ppm	64	Cr ppm	108
				Mo ppm	72	Pb ppm	51
				Zn ppm	116	Cd ppm	6
				Mn ppm	404		
				Ni ppm	152		

5.1.8. Index Properties of SFA

The determination of accurate amounts of Soma fly ash composition was performed at previous sections. From all the data related to the composition it can be said that Soma fly ash consists of three major phases: SiO_2, Al_2O_3 and CaO. The American Society for Testing of Materials (ASTM) uses three phases (SiO_2, Al_2O_3,

Fe$_2$O$_3$) to classify fly ashes based on coal source. The results of the chemical analysis show that Soma fly ash contain more than 70% SiO$_2$ (%) + Al$_2$O$_3$ (%) + Fe$_2$O$_3$ (%), (average 74.6%) (Table 5.4) but CaO more than 10% (21.3%). Based on the SiO$_2$ (%) + Al$_2$O$_3$ (%) + Fe$_2$O$_3$ (%) sum, Soma fly ash can be classified as type F, but, due to the high CaO content (>10), it can be classified as type C (Baba et al., 2010). For these reasons Soma fly ash analyzed in this study, shows different index properties.

5.1.9. Toxicity Test Results of SFA

In general, the determination of the chemical composition tests results indicate that Soma fly ash is composed of mainly SiO$_2$, Al$_2$O$_3$, CaO, and Fe$_2$O$_3$. Leaching characteristics of fly ashes changes according to the location and waste site of ash.

The extract concentrations of the selected elements as a result of the CEN leaching procedure were given below (Table 5.5). While the elements which are not tabulated Mg, Si, Fe, Zn, Mn and Pb were below the detection limit which is zero or very close to zero, Ca element was above the 140 ppm. The high extracting value of calcium was high due to the solubility of calcium in water. Elementary calcium reacts with water. Calcium compounds are more or less water soluble.

Table 5.5. Composition of Soma thermal power plant ash extract

Elements	K	Na	Ba	Cr	Al	Cd	Ni	Co	Cu
Leached(ppm)	2.73	0.68	0.44	0.33	0.27	0.05	0.05	0.05	0.04
Max.allowable concentration (mg/L)	-	-	100	-	-	1	-	-	-

5.2. Results of Characterization of Acidic Waste (AW)

5.2.1. Physical Properties of AW

The density of acidic waste was found as 1.298 kg/liter. Density of HCl solution as a function of HCl concentration (in water) is given in the Figure 6.10 below for

reference purposes. It can be seen that pure HCl would have a density of 1.5 kg/liter which should be accepted as a reference value for calculations in the following sections.
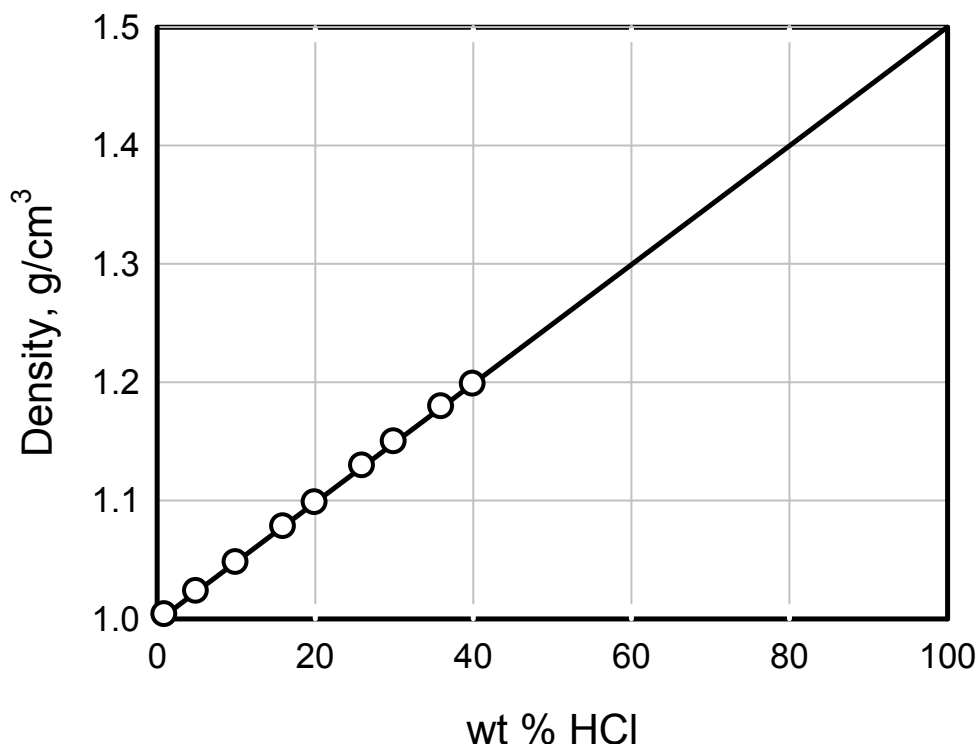
Figure 5.11. Density of HCl solution as a function of HCl concentration in aqueous solution at 25 $^{\circ}$C.

5.2.2. Determination of the [H$_3$O$^+$] Concentration and pH of Highly Acidic Industrial Waste

[H$_3$O$^+$] Concentration of highly acidic wastes was calculated bu using two different methods. The calculated and measured values were compared to determine the accurate pH of the acidic waste.

5.2.2.1. Determination of [H$_3$O$^+$] Concentration Using Direct Measurement Method

The pH of highly acidic waste was directly measured with an Orion 5 star pH meter which was calibrated by using pH 4,7,10 calibration standards. The direct measurement of the pH of highly acidic waste was made three times and pHs of the solutions were recorded during 24 h time period to be sure to reach the stability. The determined pH of the acidic waste was -0.3 which corresponds to the 1.99 M [H$_3$O$^+$].

The moles of H exist in the acidic waste sample can be calculated and highlighted below;

In 1 g acidic waste, 0.00153 mol [H₃O⁺] exists.

5.2.2.2. Calculation of the [H₃O⁺] Concentration Using NaOH Titration of Acidic Waste

Diluted acidic wastes were titrated with 0.1 N NaOH. NaOH solution was adjusted with oxalic acid and fenolftalein indicator to 0.119 N. Figure 5.12 shows the neutralization behavior of industrial acidic waste with 0.1 (0.119) N NaOH. The end points were recorded from the first turning points. Lineer calibration curve obtained from these points is in Figure 5.13.
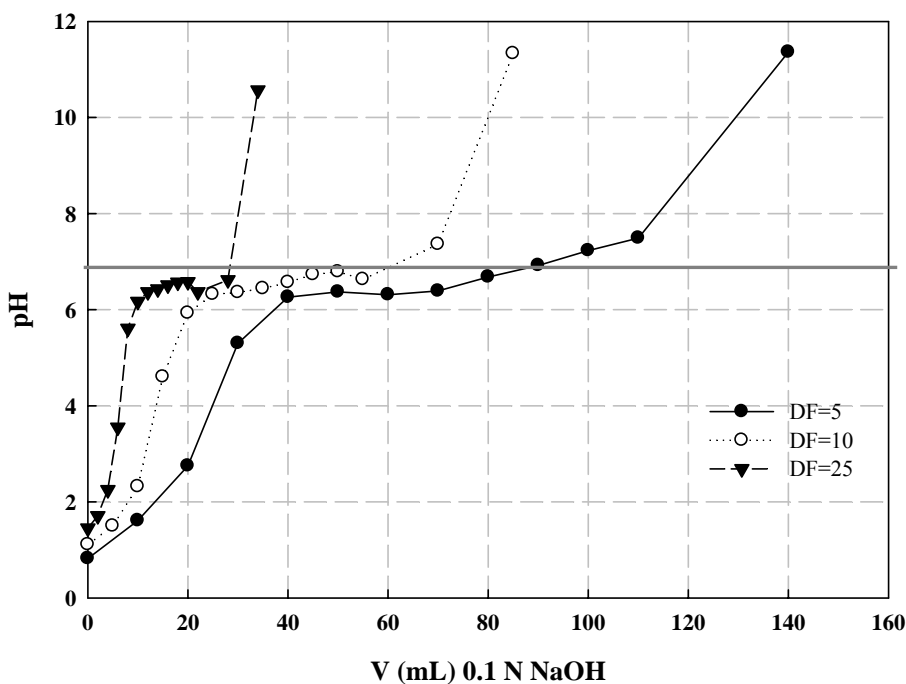
Figure 5.12. Neutralization of diluted acidic wastes

In titration, the consumed amount of NaOH with diluted acidic wastes (5, 10 and 25 times diluted) showed a lineer correlation with 0.1 (0.119) N NaOH solution as it was shown in Figure 5.15.
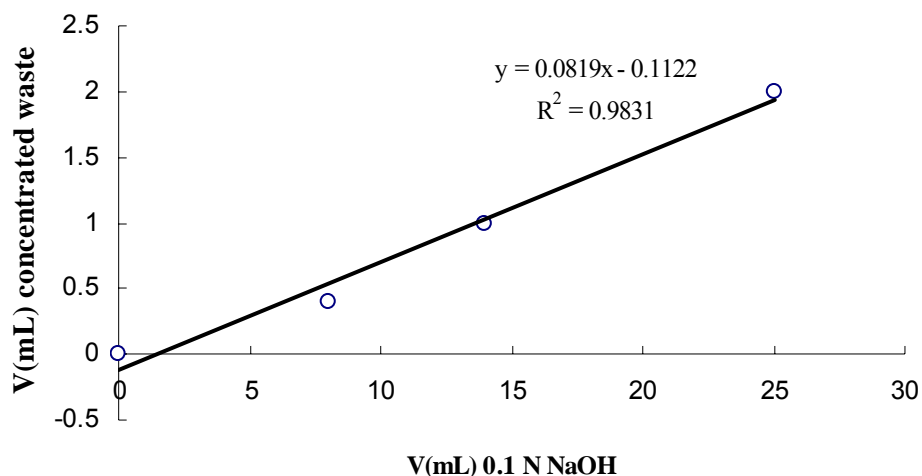
Figure 5.13. Linearization of titration curves.

Consumed amount of NaOH and acidic wastes were tabulated in Table 5.6 including the moles of H and OH values calculated form these amounts.

Table 5.6. Tabulated forms of OH^- and H_3O^+ moles

NaOH (consumed for neutralization) V(ml)	mol [OH⁻]	Acidic Waste (neutralized volume of waste) V(ml)	mol [H₃O⁺]
8	0.0008	0.4	0.000952
14	0.0140	1	0.001580
25	0.0025	2	0.004546

To show the relationship between the consumed amount of waste and moles of H_3O^+ and to find the moles of H_3O^+ corresponding to 1 gram (0.77 ml) concentrated acidic waste, Figure 5.14 was given. The graph shows linear relationship of concentrated acidic waste volume and H_3O^+ mole.
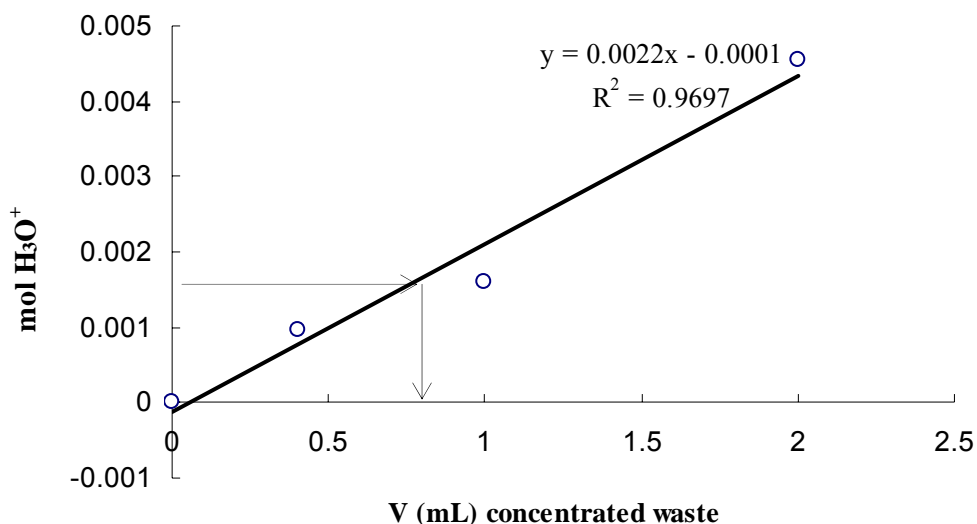
Figure 5.14. Moles of $[H_3O^+]$ corresponding to volume of concentrated acidic waste titrated with NaOH

And the moles of H_3O^+ which 1 gram of acidic waste contained is shown below as highlighted.

> **So, 1 g acidic waste contains 0.00159 mol H_3O^+.**

5.2.3. The Cation Content of the AW by ICP-AES and ICP-MS

In this part of the study, the characterization of the industrial acidic waste, in terms of major and minor elements was achieved. The company produces this waste as a result of the galvanization process; hence the main cations of acidic waste were zinc and iron. The concentrations of Zn, Fe, Mg, Ca, Pb and Na were detected by ICP-AES, while the others were determined by ICP-MS. Due to the huge amount of Fe and Zn, acidic waste was much diluted only for these two elements. The elements at low concentrations were easily detected by ICP-MS due to the low detection limits of this equipment. All element concentrations of acidic waste were illustrated in Table 5.7 in mg per kg of acidic waste.

Table 5.7. Cations of the acidic waste

Cations	Fe	Zn	Mn	Ca	Pb	Na	Mg	Al	Cr	Ni
mg/kg	88650	54460	675	400	379	281	126	65	55	50

5.2.4. The Anion Content of the AW by Ion Chromatography

The main ions of acidic waste were determined by ion-exchange column. AW was hydrochloric acid waste, so the chloride concentration was expected at very high level. As it was forseen, the chloride anion was at very high level (~25% of solution) and suppressed the other ions in the studying solution. Therefore, two different dilutions were tested to determine the chloride and the other ions. The calculated amount of anions in acidic waste was tabulated in Table 5.8 in g/L concentrated acidic waste.

Table 5.8. Anions of the acidic waste

Anions	Cl^-	F^-	SO_4^{2-}	NO_3^-
g/L	248	0.012	2.5	0.3

5.2.5. Evaluation of the Results According to Mass Balances

The accuracy of the results was checked by mass balances. In following sections, the comparisons and evaluations were performed to discuss on errors that possibly comes from the elemental compositions.

5.2.5.1. Mass Balance of Cations and Anions in AW Composition

After the determination of cations and the anions in acidic waste composition, it was determined that Cl^- is the dominant anion compared with other ions 100 times that

of SO_4 and 1000 times that of NO_3. Balancing the masses in mole bases, it was assumed that all determined cations were reacted with only chloride ion with 1% error at most. So, the presumed reactions were shown below;

$$FeCl_3 \ (aq) \longrightarrow Fe^{3+} + 3Cl^-$$
$$ZnCl_2 \ (aq) \longrightarrow Zn^{2+} + 2Cl^-$$
$$MnCl_2 \ (aq) \longrightarrow Mn^{2+} + 2Cl^-$$
$$CaCl_2 \ (aq) \longrightarrow Ca^{2+} + 2Cl^-$$
$$PbCl_2 \ (aq) \longrightarrow Pb^{2+} + 2Cl^-$$
$$NaCl \ (aq) \longrightarrow Na^+ + Cl^-$$
$$MgCl_2 \ (aq) \longrightarrow Mg^{2+} + 2Cl^-$$
$$AlCl_3 \ (aq) \longrightarrow Al^{3+} + 3Cl^-$$
$$CrCl_3 \ (aq) \longrightarrow Cr^{3+} + 3Cl^-$$
$$NiCl_2 \ (aq) \longrightarrow Ni^{2+} + 2Cl^- \qquad (5.1)$$
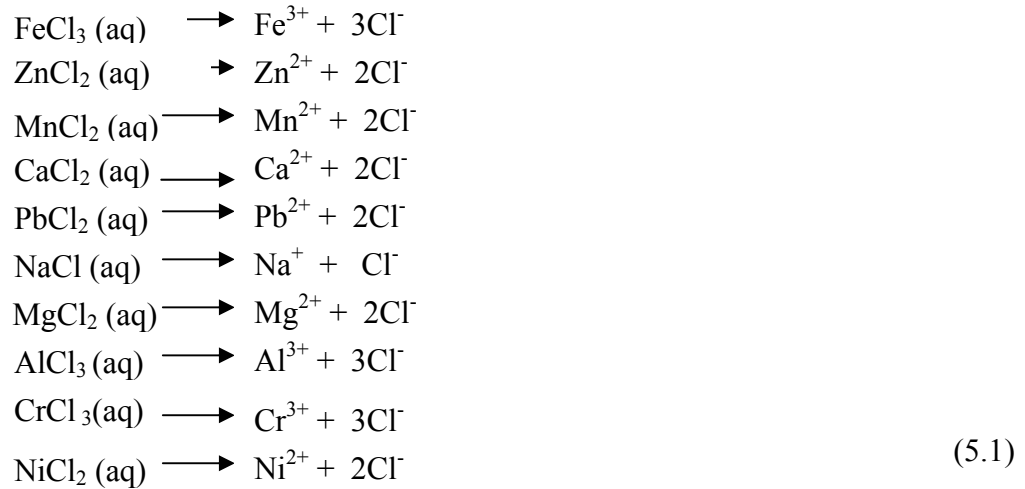
By considering the complete reactions, total moles of chloride ion required for cations were calculated by multiplying the molecular weight and the density and found 8.6 mol/L (Table 5.9).

Table 5.9. Mass balances in acidic waste composition

	Cations (g/kg)	Molecular weight (g)	(In 1 L waste) moles	(as a result of the rxn with HCL) moles of Cl	moles of total Cl/L
Fe	88.6	55.8	2.062	3.0	6.18644
Zn	54.5	65.4	1.080	2.0	2.162
Mn	0.67	54.9	0.016	2.0	0.032
Ca	0.40	40.0	0.013	2.0	0.026
Pb	0.38	207.2	0.002	2.0	0.005
Na	0.28	23.0	0.016	1.0	0.016
Mg	0.13	24.3	0.007	2.0	0.013
Al	0.65	27.0	0.031	3.0	0.094
Cr	0.55	52.0	0.014	3.0	0.041
Ni	0.50	58.7	0.011	2.0	0.022
				Total=	8.6
	Anions (g/L)				
Cl⁻	248.000	35.5	6.98592		
F⁻	0.012				
SO₄	2.5				
NO₃	0.3			Total=	7.0

On the other hand, total moles of chloride ion was nearly 7.0 mol/L which was close but lower than the calculated amount of chloride required for complete reactions with cations. This suggested that the majority of the cations came from metallic forms dissolving in HCl solutions. For example, iron in solution can be found as Fe^{2+} or Fe^{3+}, so, 2 moles can react with Cl^-. This decreases the total amount of Cl needed to react with chloride and masses are balanced. Figure 3.5 at Chapter 3 showed the speciation of iron and zinc in different pHs.

5.2.5.2. Mass Balance of Elements in Aggregate Structure

The elements of aggregates prepared at three different S/L ratios (2,3, and 4) were analyzed by using XRF. On the other hand, element concentrations of aggregates were calculated from the acidic waste and fly ash compositions. Calculated and measured amount (%) of metal oxides was compared in Figures 5.15-5.21 for 3 S/L ratios.

The results showed that the difference between the calculated amounts of SiO_2 and Al_2O_3 was very small (Figure 5.15 and 5.16). The amount of these compounds in fly ash structure is very high so that the error percent was very low. Si and Al were the major ions in fly ash and detected by ICP-AES as a result of tetraborate digestion. The digestion procedure applied before the XRF was also tetraborate digestion. So that the Al-Si composition of the matrices were separated by the same method. This could be the reason of the good accuracy.
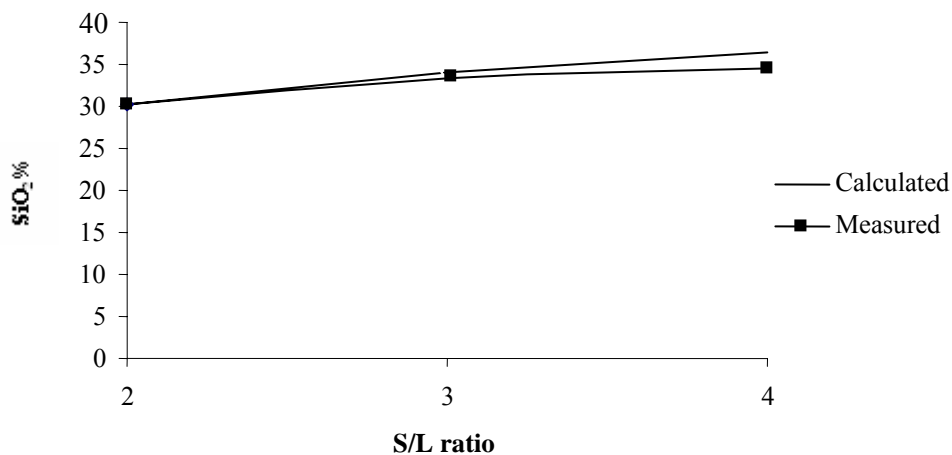
Figure 5.15. Comparison of calculated and measured SiO_2%
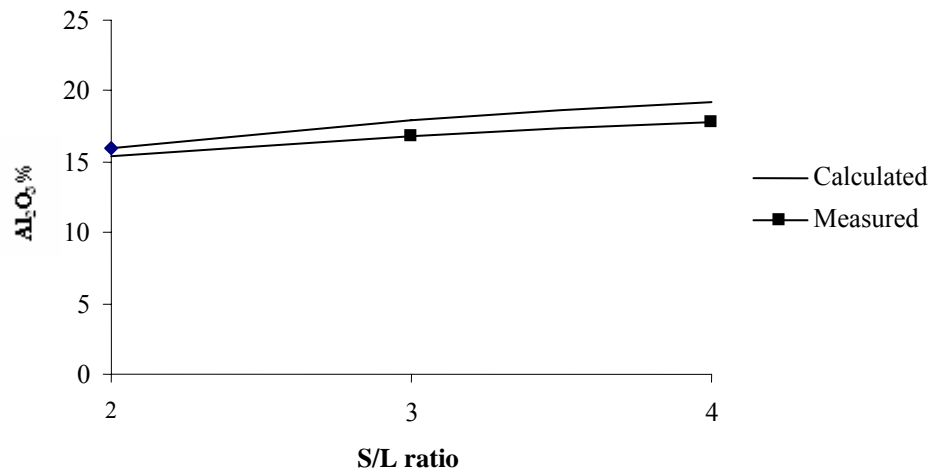
Figure 5.16. Comparison of calculated and measured $Al_2O_3\%$

Figure 5.17 and 5.18 show the comparison between the specified amount of the CaO and MgO respectively. These compounds exist both in fly ash and acidic waste structure to which different sample preparation methods were applied. So the error was higher in this case.
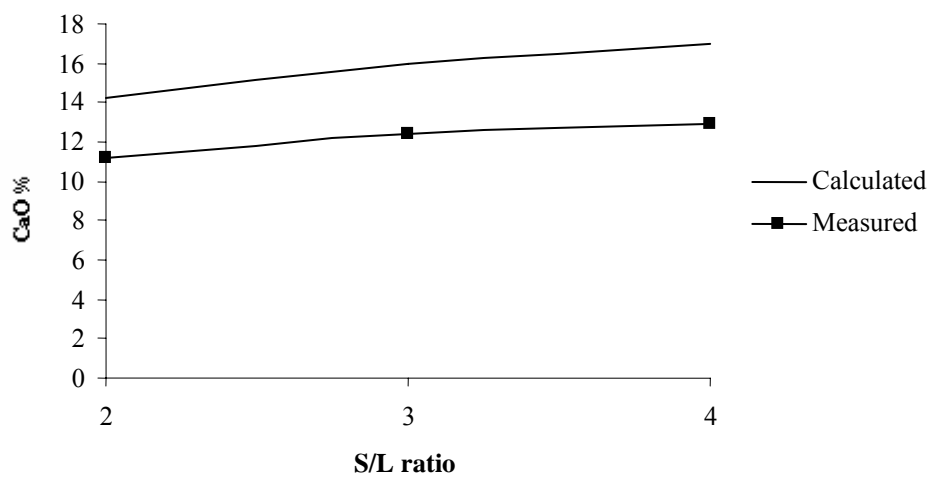
Figure 5.17. Comparison of calculated and measured CaO%
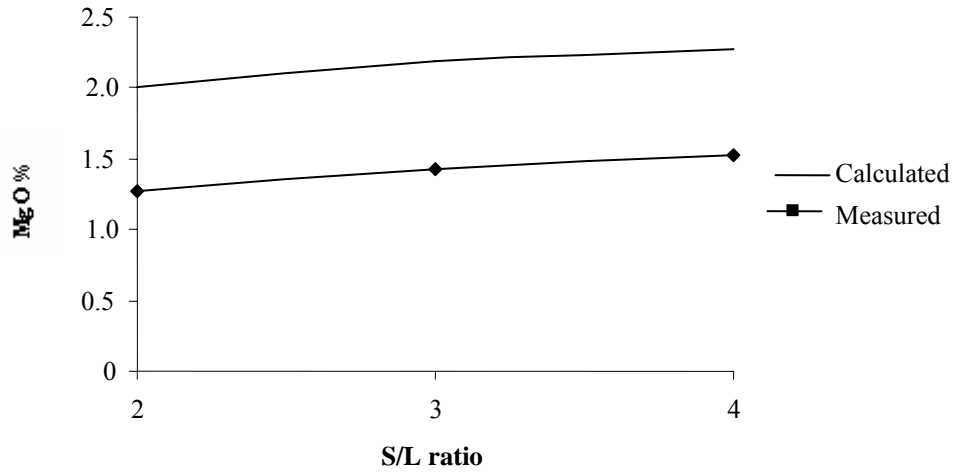
Figure 5.18. Comparison of calculated and measured MgO%

Small amount of potassium was found in fly ash structure and no potassium was detected in acidic waste. This increased the difference between the calculated and measured amounts (Figure 5.19).
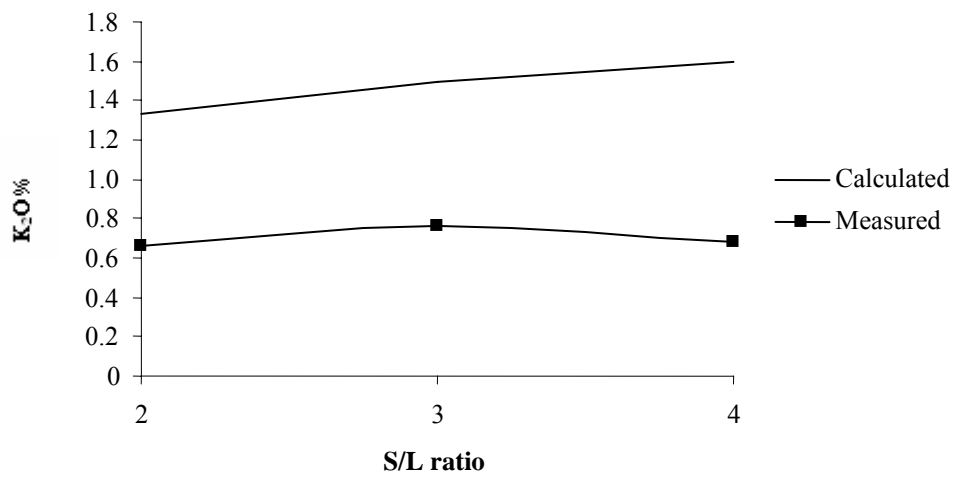
Figure 5.19. Comparison of calculated and measured K_2O%

Most iron and nearly complete amount of zinc come from acidic waste composition to aggregates. The preparation methods before the elemental analysis were the same, so the differences between calculated and measured amounts were very small (Figure 5.20 and 5.21).
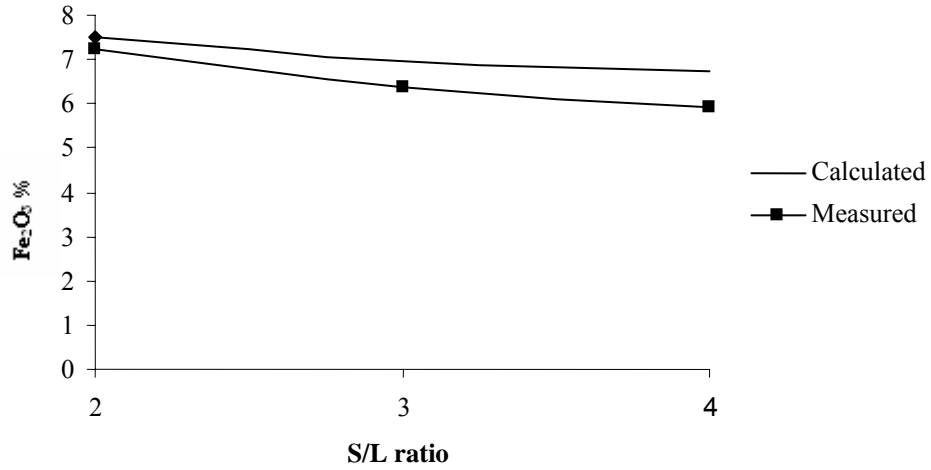
Figure 5.20. Comparison of calculated and measured Fe_2O_3%
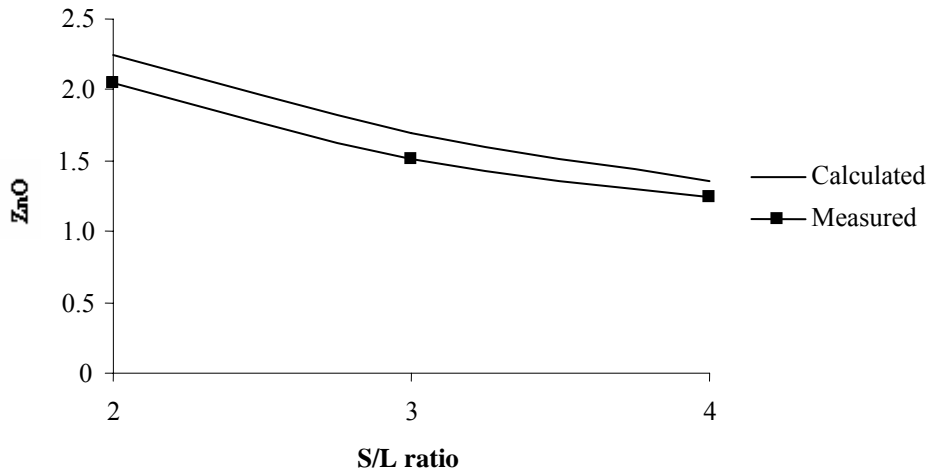
Figure 5.21. Comparison of calculated and measured ZnO%

5.3. Neutralization of Acidic Waste by Soma Fly Ash

5.3.1. The Results of Neutralization Studies

Chemical neutralization of fly ash in different conditions was studied. First, fly ash was titrated with hydrochloric acid (HCl) solution to obtain the theoretical amounts of the acid and fly ash which will be used in the forthcoming experiments. Then, the real neutralization studies were carried out with the acidic waste. The purpose here was to determine of the theoretical and experimental neutralization capacity of the acidic waste with Soma fly ash and finally to decide on the fly ash (solid)-acidic waste (liquid) and water ratios which will be used in fixation and stabilization experiments.

First, the neutralization of fly ash with HCl in different concentrations of water was carried out in two repeat experiments. The slow rate of the titration was attributed to the small formation of aluminium (III) and iron (III) hydroxide (Green and Manahan, 1978). During the titration, the fly ash showed very strong buffering effect due to the alkaline ions like Ca, Mg, Hence, to achieve the stable pH values required long equilibrium times. The fly ash solutions were prepared at 2, 5, 10, 25 and 50 % in water. The suspensions were strirred overnight for equilibration. The prepared solutions were titrated with adjusted 1 N HCl solution. The solutions were titrated within 1-2 weeks with periodic agitation and addition of acid to ensure equilibrium. The titration behavior was shown in Figure 5.22. The consumed amounts of HCl to reach the pH 7.0 was recorded and showed linearity as it was seen in Figure 5.23. The linearity tells us that the existence of water in solution did not change the neutralization equilibrium. The other reason why to study with the diluted amounts is to be sure of the theoretical S/L ratios and to check the consumed amounts by seeking a linear relationship. Fly ash contains many non-homogenous spheres and other mineral compounds in its structure. Finding the linearly correlated data with the added amounts provides to understand the properly prepared samples before the analysis. As it was demonstrated in Figure 5.22 and Figure 5.24, an increase in the fly ash amount in the mixture directly affected the amount of acid required for neutralization. The curves in Figures 5.23 and 5.25 can be used to plot the HCl amounts to reach the neutral pH of 7.0 as a function of solid concentration. It can be seen that there is a very strong linear correlation between the required HCl amount for neutralization and the fly ash content of the slurry. Hence, the

slope of the graphs presented in Figures 5.23 and 5.25 directly give the amount of fly ash required to neutralize 1 gram of 100% purity HCl.

Both set of experiments yielded nearly identical neutralization potential of 8.3 which means 8.3 grams of Soma fly ash is required for the neutralization of 1 g of 100% concentrated HCl..This corresponds to around 303 grams of fly as to neutralize 1 mol of 100% HCl.
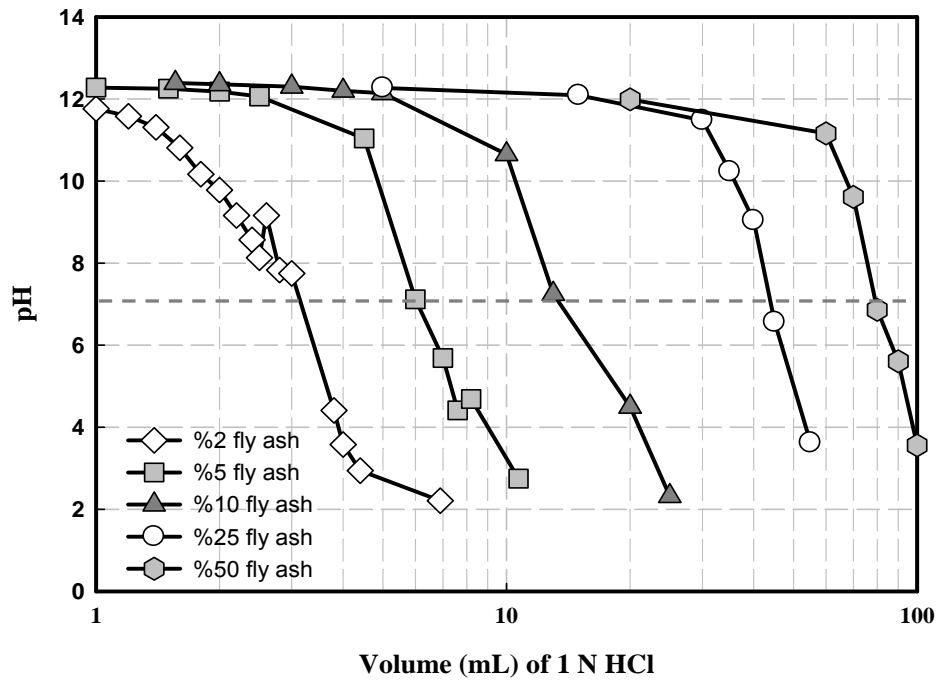
Figure 5.22. Titration of different concentrations of fly ash-water mixtures with HCl (1)
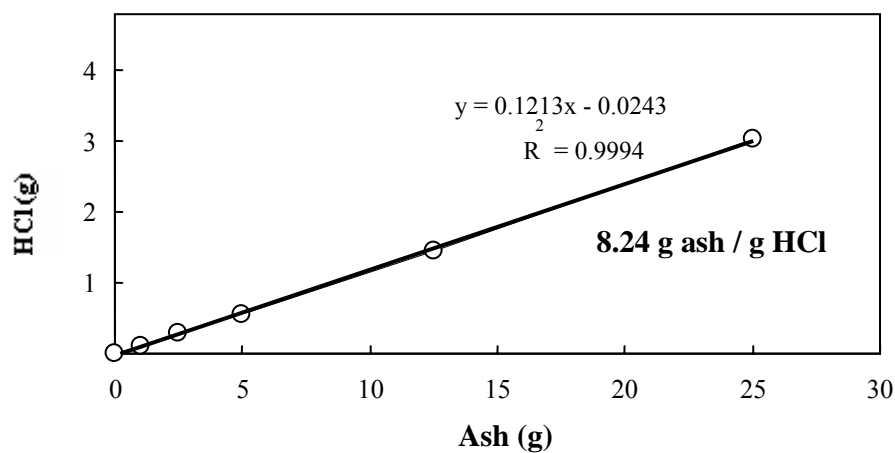
Figure 5.23. Linearity of titration of different concentrations of fly ash-water mixtures with HCl (1)
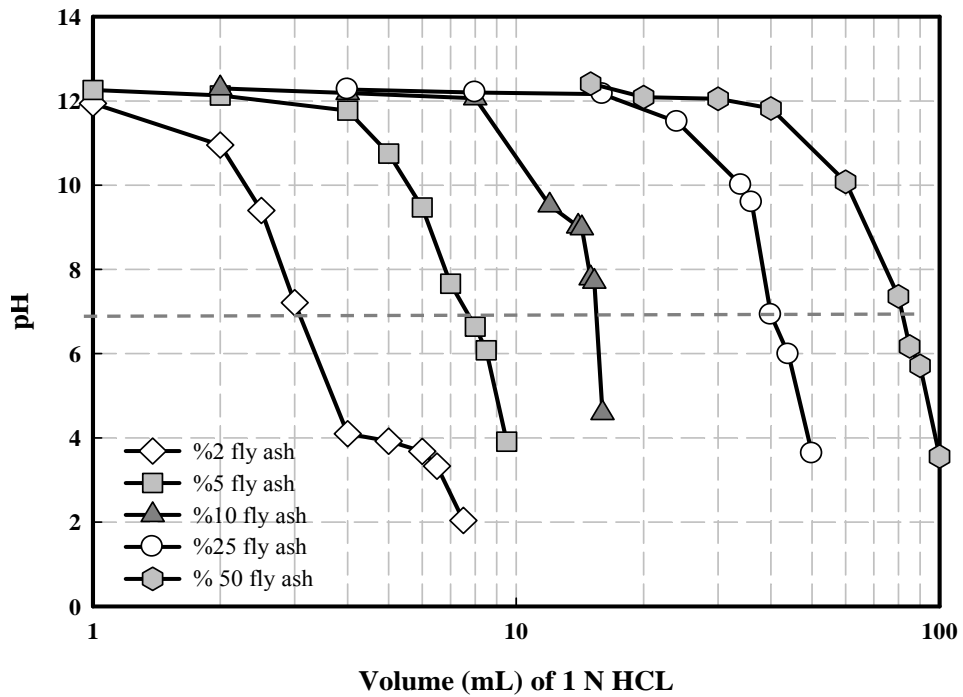
Figure 5.24. Titration of different concentrations of fly ash-water mixtures with HCl
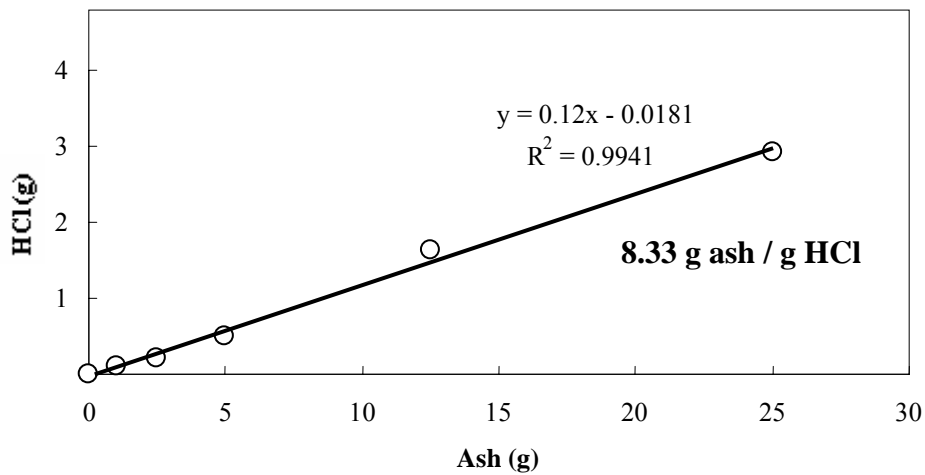
Figure 5.25. Linearity of titration of different concentrations of fly ash-water mixtures with HCl (2)

In the second part, the neutralization of the fly ash slurries was carried out not with HCl solutions, but with the actual acidic waste using fly ash amounts of 2.5 g, 12.5 g, 25 g and 50 g. In these experiments, the fly ash samples were directly acidified with acidic waste with no water present in the system. The titration behavior is presented in Figure 5.26. Again, the required amount of titrant (in this case acidic waste) to reach a

neutral pH of 7 was plotted against the solid content of the system is presented in Figure 5.27. The figure shows that the same linear attitude was observed with the added amount of acidic waste much like the case with the HCl. The slope of the curve in Figure 5.27 demonstrates that the amount of fly ash required to neutralize 1 gram of acidic waste was nearly 2.93 g.

This fly ash/acidic waste ratio of 2.93 is an important experimental parameter since the following aggregate production studies will be developed around it. The same number also gives a rough idea about the required amounts of the wastes if this process was used in the industry. If AW decided to neutralize its wastes using fly ash, they would need a fly ash amount of around 195 tons (50,000 liters of acidic waste, 64.9 tons, is produced by the company yearly). Such amounts can be transported and handled quite easily between Soma and Izmir.
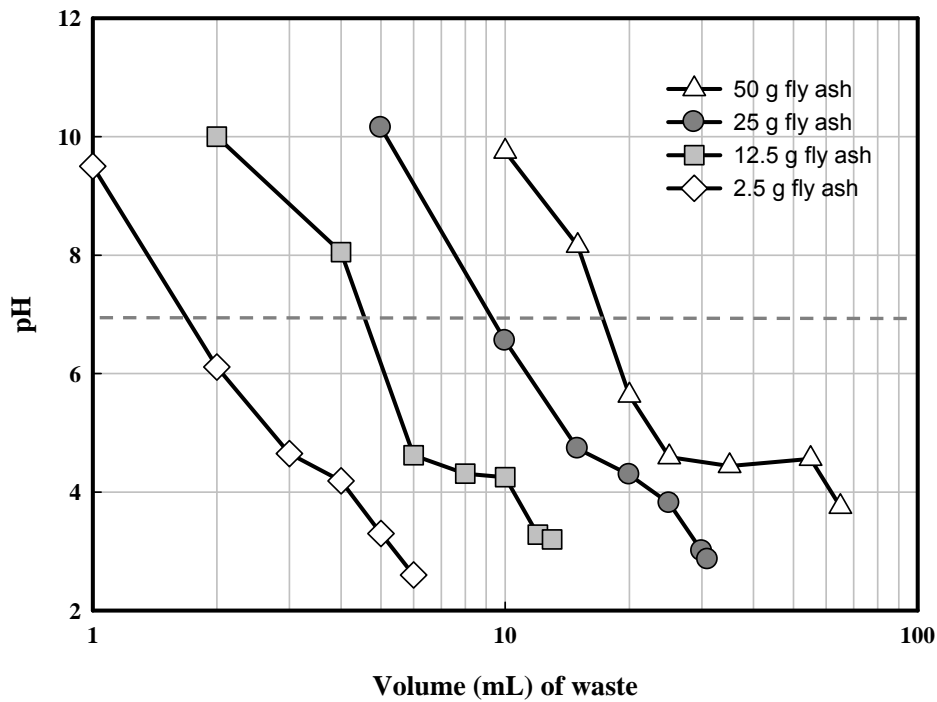
Figure 5.26. Neutralization of fly ash with acidic waste in different concentrations

$$y = 0.3406x + 0.2096$$
$$R^2 = 0.9979$$

2.93 g ash / g acidic waste
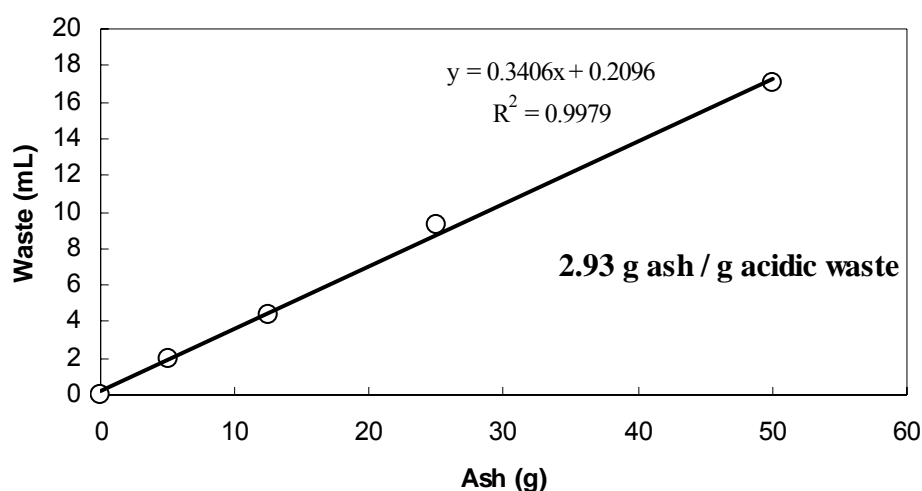
Figure 5.27. Linearity of titration

Neutralization of constant amounts of fly ash (5 g and 12.5 g) with acidic waste in different amounts of water was also tested. The reason for testing the presence of different amounts of water was to see the effect of water as a convective medium in the neutralization and fixation studies. It was quite possible that presence of a third fluid medium such as water could enhance the encounters between the fly ash particles and acidic waste and improve the dissemination of the reaction products for better reaction rates or enhanced reaction products.

Soma fly ash in water mixtures were prepared at incremental fly ash weight percentages of 2.5%, 5%, 10% and 20% (5 gram fly ash was completed to 200 g, 100 g, 50 g and 25 g with ultra pure water, respectively). Figure 5.28 demonstrates that the titration behavior of a constant amount of fly ash in different concentrations of water was not considerably distinct. Namely, the fly ash/water ratio of the mixture was not very effective on the titration attitude. The reactions and the mass transfers in aggregate body between the fly ash particles and the acidic waste were affected from the convective media in small ratio. It was concluded that the concentration of ions in leachates is controlled by the solubility of particular minerals and chemical equilibrium models can be used to predict leachate concentration of elements whose dissolution is controlled by reaction kinetics (Iyer, 2002).
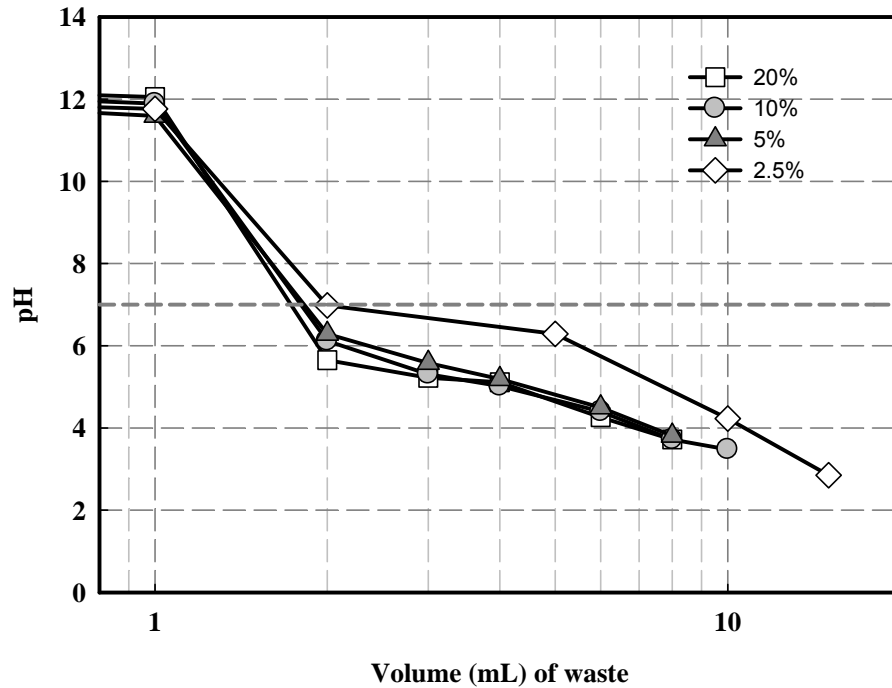
Figure 5.28. Neutralization of 5 g fly ash with acidic waste in different percentages of water

Figure 5.29 exhibits the titration of 2.5 times more fly ash (12.5 grams) in same fly ash/water ratios as in Figure 5.28 with acidic waste. That is, 12.5 g of Soma fly ash was prepared at incremental weight percentages of 2.5%, 5%, 10% and 20% in water. Weighed amount of fly ash was completed to 500 g, 250 g, 125 g and 62.5 g with ultra pure water, respectively. Here again no effect of fly ash/water ratio was observed.

Also, the graph in Figure 5.28 (5 grams of fly ash) shows that around 1.7 ml acidic waste was required to neutralize this 5 grams of fly ash. That is, the neutralization potential of fly ash was 2.40 grams for each gram of acidic waste lower than the no water case. Similarly, around 4 ml acidic waste was added to get the pH of the mixture to 7.0 in the case of 12.5 g ash was used. This also corresponds to a 2.26 g fly ash/ g acidic waste. Remember that the neutralization potential of fly ash was 3.80 grams for each gram of acidic waste. Hence, it can be concluded that the effect of water in the system or the size of the system has little affect on the neutralization potentials of the fly ash.

However, it should be noted that the equilibrium times in the above titration experiments were kept very long in order to allow sufficient reaction times between the ash particles and the acidic waste ions. This brings the mind the necessity of allowing

for the ash particles and the acidic waste enough time for the reactions. The dissolution of ions from charged fly ash particles as solid liquid mass transfer of ions across the diffuse double layer provides insights into the prolonged delay to achieve a steady state (Iyer, 2002).

A simple mixing of ash particles and acidic waste may not provide this time such that some "aging" of the fly ash-acidic waste mixtures (aggregates) may be required for letting the reactions to complete their courses in the solid phase in the aggregate structure. This will be an important experimental parameter in the following sections.
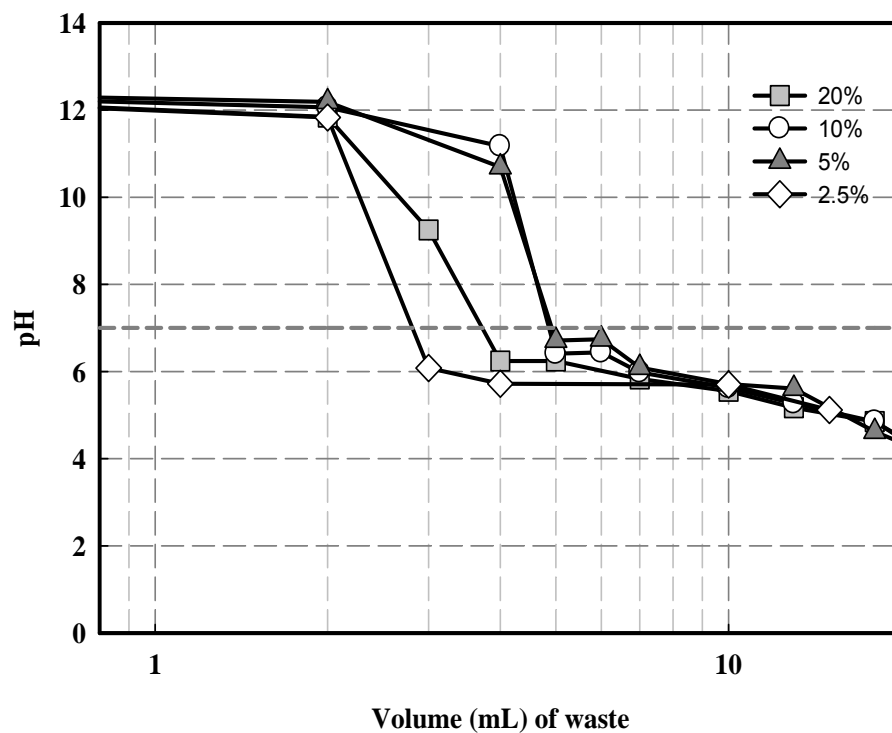
Figure 5.29. Neutralization of 12.5 g fly ash with acidic waste in different percentages of water

Using all calculated theoretical values we had to decide on the proportions for fixation and stabilization experiments. The theoretical values were figured out in Table 5.10.

Table 5.10. The theoretical neutralization potential

Method	Titrant	Fly ash
HCl titration (1)	1 g HCl (100%)	8.24 g
HCl titration (2)	1 g HCl (100%)	8.33 g
Acidic waste titration of SFA (no water)	1 g acidic waste	3.80 g
Acidic waste titration of SFA (small volume of water)	1 g acidic waste	2.40 g
Acidic waste titration of SFA (large volume of water)	1 g acidic waste	2.26 g

Finally, a kinetic study was performed using 12.5 g fly ash in different concentrations of water. As it was observed in Figure 5.30, same kinetic behavior was obtained in each case. The pH of the fly ash-water solution was rapidly decreased to neutral levels and remained relatively constant for long periods. The figure also shows that a time of around 2 minutes is sufficient to reach equilibrium in ash-water slurries. The pH dropped immediately below the 6 within 1 minute and then rised to 6.5; the neutralization reactions were completed and the solutions reached to equilibrium. The increase in pH after 1 minute was due to the continuing chemical reactions between fly ash and acidic waste components.
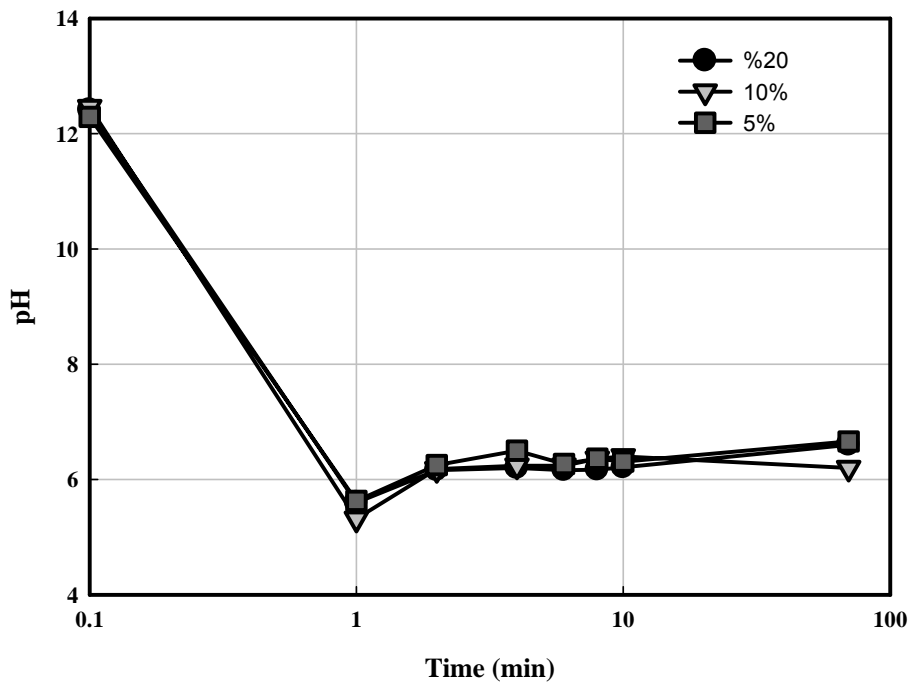
Figure 5.30. Kinetic neutralization of 12.5 g fly ash in different concentrations of water

5.3.2. The Results of Leaching Studies

Leaching studies are very important in predicting the environmental impacts associated with the disposal of fly ash at the dump. A series of leaching tests were carried out in order to simulate the different conditions fly ash is exposed to at the disposal scenario.

5.3.2.1. Effect of S/L Ratio and Aging Time on pH of Aggregates in Water

The results of the study contain the evaluation of the Soma fly ash as a potential chemical neutralization and fixation agent for industrial acidic waste. Effect of solid/liquid (S/L) (in other terms; fly ash/acidic waste) ratio, aging period and leaching time was investigated.

The aggregate samples obtained by a mixing process in pre-determined S/L ratios were dried within 2, 4 and 16 days at 25 ºC ambient temperature. After these aging periods the dried aggregates were placed in ultra pure water at a 1/10 aggregate

(A)/water (W) ratio to observe the pH and leaching kinetics of heavy metals. No water was added during aggregate production. The pH of the solutions prepared in different experimental conditions was given in Figure 5.31, 5.32 and 5.33. The pH of the solution was around 7.0 and did not exceed the 8.5 for pre-determined S/L ratios of 2, 3 and 4. The inadequacy of 2 days and 4 days aging periods for the neutralization of the constituents can be observed easily from these graphs. It was observed that in the pH graphics, the optimum pH value, in other words, the neutral pH (7.0) was obtained after 16 days aging periods. This verified the state that the least leaching condition, which was seen in the following graphs, was found in nearly neutral pHs.
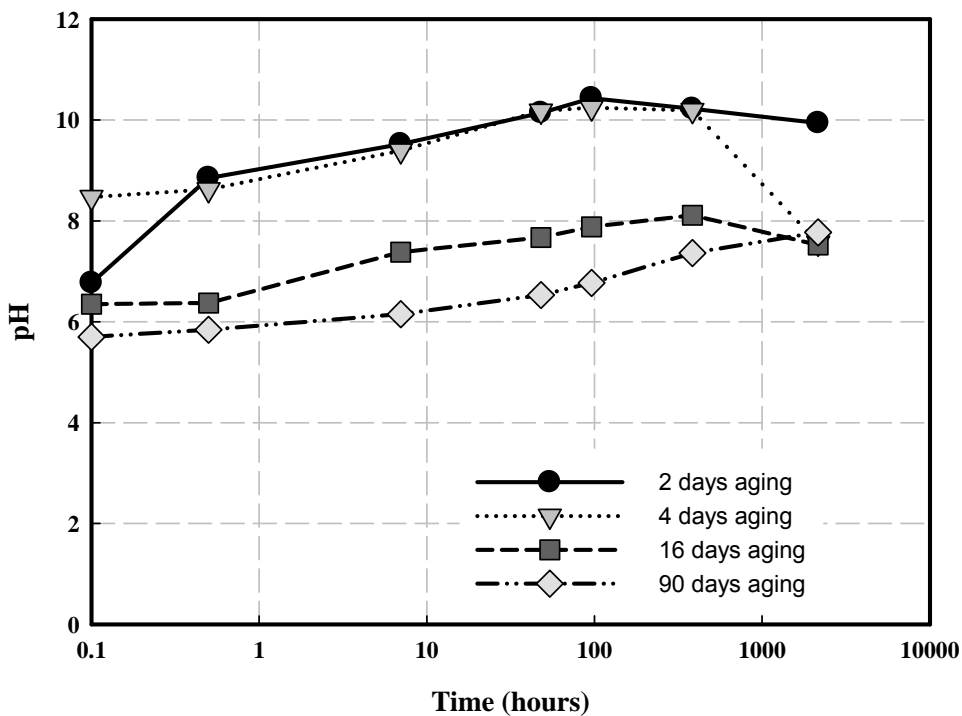
Figure 5.31. pH graph for S/L=2

Time-pH graphic in Figure 5.31 shows that the aggregates prepared at S/L ratio=2 , by increasing aging periods (4, 16, 90 days), pH of the solution were kept between 6-8 except the aggregates which were 2 days aged at the end of the 90 days leaching period of 90 days. Only the difference between the aggregates produced at 4, 16 and 90 days aging times were for 4 days aged samples. The pH of the solution increased like 2 days aged samples, but after a long leaching period, the ions were probably re-adsorbed and pH was decresed. So the aging periods of more than 16 days

and 90 days were enough due to the pH stability around neutral values. The noticable difference in the initial pH of the sample aged for 4 days was observed. The only thing that can cause the pH increase in the solutions can be the fast solubility of aluminium in 2 and 4 days aged samples as it is illustrated in Figure 5.36.
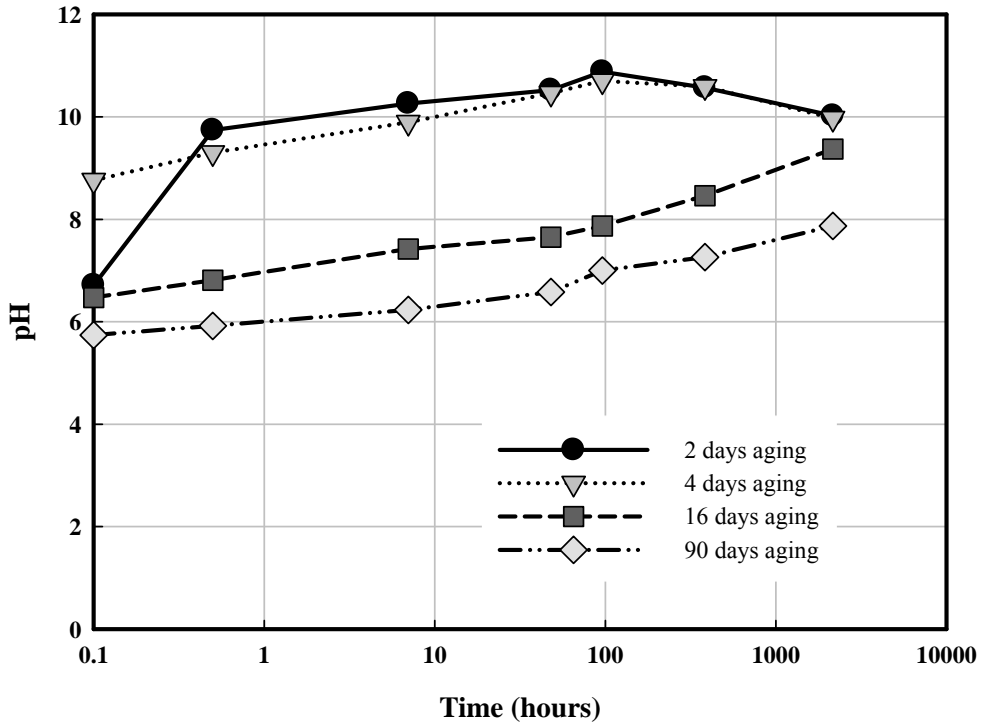
Figure 5.32. pH graph for S/L=3

Figure 5.32 illustrates the pH stability behavior of the aggregates which were prepared at S/L=3 ratio. The aggregates were subjected to 2, 4, 16 and 90 days aging periods, then put into deionized water in aggregate/water ratio of 1/10. The pH stability of the solution were controlled during 90 days leaching period again. And the results show that the almost same bahavior were observed with S/L=2 case. The pH of the solution were increased by the time, this means that solubility of some phases were occured in 16 and 90 days aged aggregates tests. But never the pH was far from 7.0. But the pH of the solution of 2 days and 4 days aged samples rapidly increased during the leaching period and a bit decreased after 4-5 days due to the re-adsorption of some ions. The pH of the solution reached to 10.
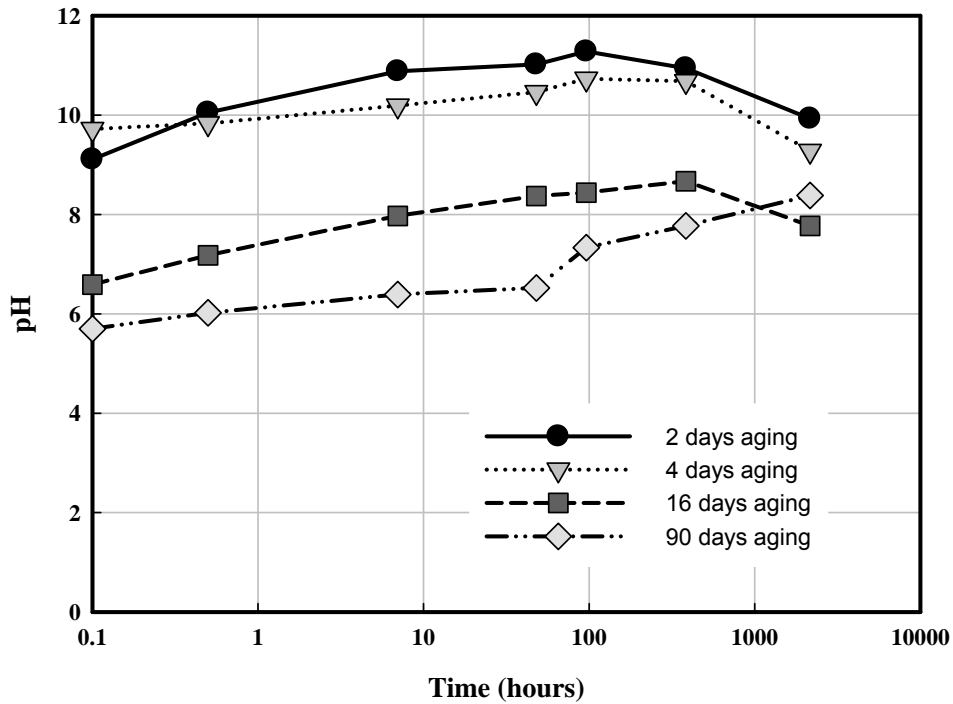
Figure 5.33. pH graph for S/L=4

The nearly same attitude was obtained for the aggregates produced at S/L=4 as seen in Figure 5.33. The 16 and 90 days aging of the aggregates were acceptable due to the pH stability. But the sharp increase in pH and a small decrease at the end of the long leaching period were observed for 2 and 4 days aging times in this case again.

5.3.2.2. Effect of S/L Ratio and Aging Time on Fixation of Metals

The dry aggregate were subjected to kinetic leaching test at an aggregate/water ratio (A/W) of 1/10. The solutions were analysed for 16 elements. The major elements; Na, Mg, Al, Si, K, Ca, Fe, Ba and the minor elements; Cr, Mn, Co, Ni, Cu, Zn, Cd, Pb in fly ash composition were studied. The group of graphs in each figure presents the leaching of indicated metal which was subjected to the kinetic leaching test at the end of a given aging period for different S/L ratios. The graphs in each figure explain the milligram of element passing into solution per 1 kg of aggregate at an aggregate/water ratio of 1/10. The horizantal line here is the element concentration of aggregate (mg/kg) averaging of that element in three S/L ratios (S/L=2,3,4).

There is not any discharge or hazardous limit for the major elements; Na, Mg, Al, Si, K, Ca and Fe except Ba. Figures 5.34, 5.35, 5.36, 5.37, 5.38, 5.39 and 5.40 illustrate the leaching of Na, Mg, Al, Si, K, Ca and Fe respectively. The leached amount of elements was shown in graphs per unit mass of aggregate into the water after 2, 4 and 16 days aging periods in predetermined S/L ratios (S/L=2,3 and 4). The S/L ratios were selected according to the neutralization study results which were discussed in section 5.31.

The group of graphs for each figure presents the leaching of indicated metal which was subjected to the kinetic leaching test at the end of a given aging period for different solid/liquid (S/L) ratios. The large amount of the major elements in fly ash (sodium, magnesium, aluminium, silicium, potassium, calcium and iron) was kept in the aggregate; however, a fixation was obtained directly related to the drying time. Namely, the aging time was directly proportional with the element fixation.

The graphics, presented in Figures 5.34, 5.35, 5.36, 5.37, 5.38, 5.39 and 5.40 gave the most intimate results for Na, Mg Al, Si, K, Ca, and Fe release. The leaching of the elements was proportional with the amount of the element that aggregate contained.

Figure 5.34. Effect of various parameters on the leaching of Na from the aggregate of Soma ash for A/W=1/10 *(Solid line=mg/kg element aggregate contained)*

Figure 5.34 shows that the release of Na element from the aggregate structure was not considerably obstructed for tested S/L ratios and aging times. Because the sodium ion is highly soluble in water in nearly all of its compounds and mostly counterbalanced by the chloride ion where the aggregates rich in this ion (Cl=248 g/L). Sodium is an essential element for living organisms and classified as a dietary inorganic

macro-mineral for animals (Aurie et al., 1998). Also, there is no any environmental limit or discharge standard for sodium in water in regulations. Therefore, the leaching of Na ion into water is not considered as a risk for living bodies.

Figure 5.35. Effect of various parameters on the leaching of Mg from the aggregate of Soma ash for A/W=1/10 *(Solid line=mg/kg element aggregate contained)*

— 2 days ⋯⋯▷⋯⋯ 4 days — ■ — — 16 days — ⋅◇ — ⋅⋅ 90 days aging

Magnesium release as shown in graphs in Figure 5.35 was hindered 10 times like sodium. There were disparities in leaching amounts among the different S/L ratios; for example the 2 days aging time seemed the least release providing element

surprisingly. This is the result of the rapid formation of the magnesium hydroxide which is the only insoluble form of magnesium. Most other magnesium compounds are soluble in water, providing the sour-tasting magnesium ion Mg^{2+}. Small amounts of dissolved magnesium ion contribute to the hardness and taste of natural waters (Baker and Avedesian, 1999). There was no any environmental risk limit or discharge standard for magnesium in Turkish regulations.

Figure 5.36. Effect of various parameters on the leaching of Al from the aggregate of Soma ash for A/W=1/10 *(Solid line=mg/kg element aggregate contained)*

As it was noticed in Figure 5.36 the release of aluminium into processed water was considerably prohibited in each tested S/L ratios. It was also indicated that the aging time was effective on the leaching leaching of Al, because for each S/L ratios the release of Al was at nearly zero levels which was determined below the detection limit. Stumm and Morgan (1996) defines that the Al solubility is a bit tricky and there are several curve fit variants used in modeling neutral capacity. Because of its strong affinity to oxygen, however it is almost never found in the elemental state; it is found in oxides or silicates The most abundant aluminium compounds are aluminium oxide and aluminium hydroxide in water. Feldspars are aluminosilicates (which was detected in both fly ash and aggregate structures) are the most common group of minerals in Earth's crust (Greenwood and Earnshaw, 1997). Aluminum naturally occurs in waters in very low concentrations. Although there is no discharge standard for aluminium in Turkish regulations, higher concentrations derived from mining waste may negatively affect aquatic biocoenosis. Within the tested operating parameters, this study prohibited to release of this metal into process water.

Si release of aggregates was not very high like Al compared to Mg and Na. 90 days aging of aggregates were enough to fix all the silicium inside the aggregate structure. S/L ratios were not affected the leaching of Si effectively (Figure 5.39). Water and water vapor probably have little influence upon silicon solubility, because a protective surface layer of silicon dioxide is rapidly formed. Silicon oxide is relatively water insoluble compared to other minerals Silicon dioxide has a water solubility of 0.12 g/L, whereas for example silicon carbide is water insoluble (O'Mara et al, 1990). Due to the low solubility of Si in water, the complexes formed as a result of the neutralization process are protected. The complexation reactions continues during the aging process and never released into the water during 90 days of leaching period.
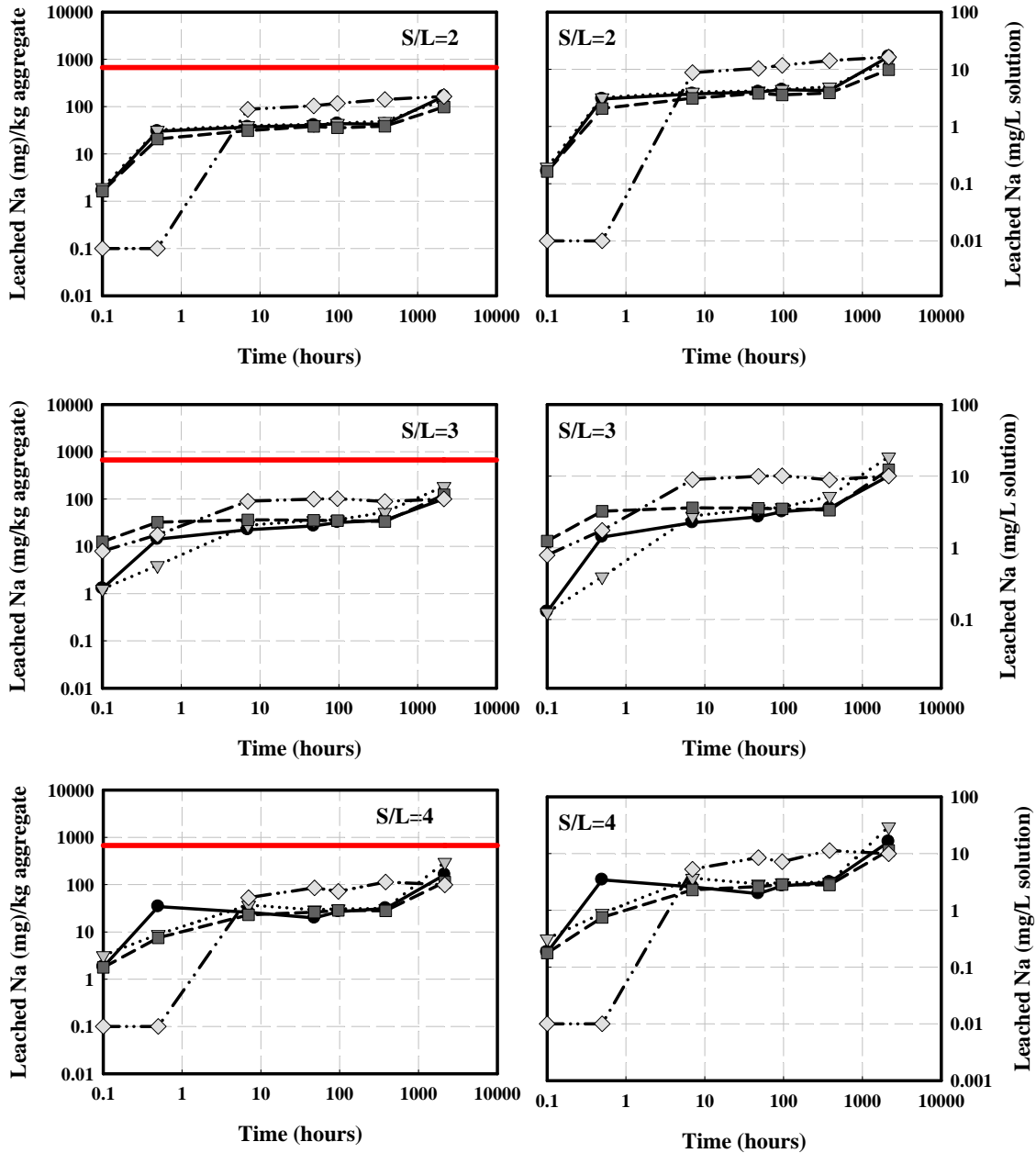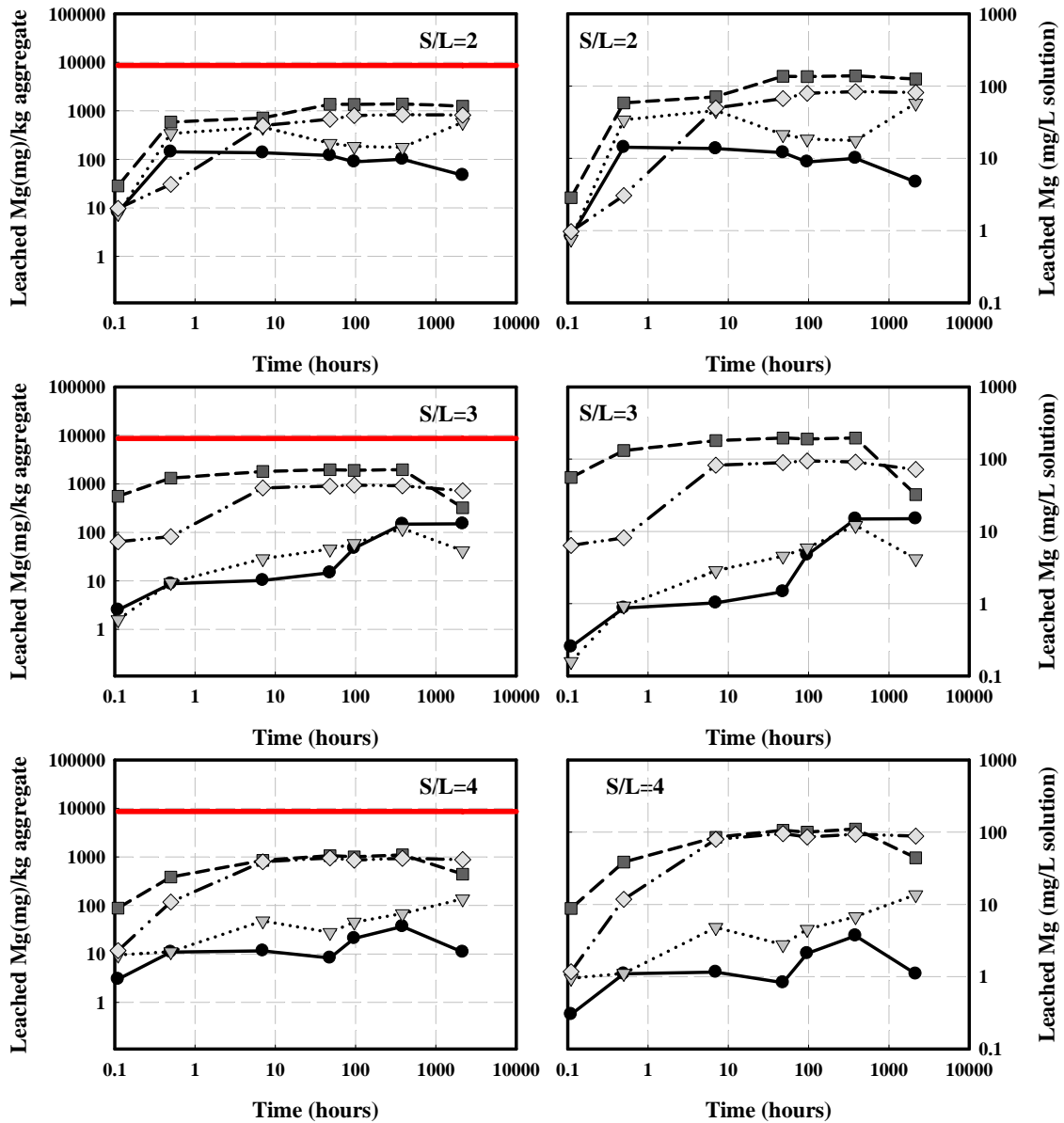
Figure 5.37. Effect of various parameters on the leaching of Si from the aggregate of Soma ash for A/W=1/10 *(Solid line=mg/kg element aggregate contained)*

——●—— 2 days ·······▷······· 4 days ——■—— 16 days —·—◇—·— 90 days aging

Figure 5.38. Effect of various parameters on the leaching of K from the aggregate of Soma ash for A/W=1/10 *(Solid line=mg/kg element aggregate contained)*

2 days ········▷········ 4 days ——■—— 16 days —··◇··— 90 days aging

There was no noteworthy impact of aging time on leachability of potassium (Figure 5.38). The aggregates prepared at three different S/L ratios (2,3 and 4) did not let out all of the potassium; 100 times of the total K content were encapsulated inside the aggregate structure. The possible form of K in aggregate structure is KCl due to the high chloride content of acidic waste. The solubility of KCl in water is 36 g/100 g water (Sigma-Aldrich, 2001).

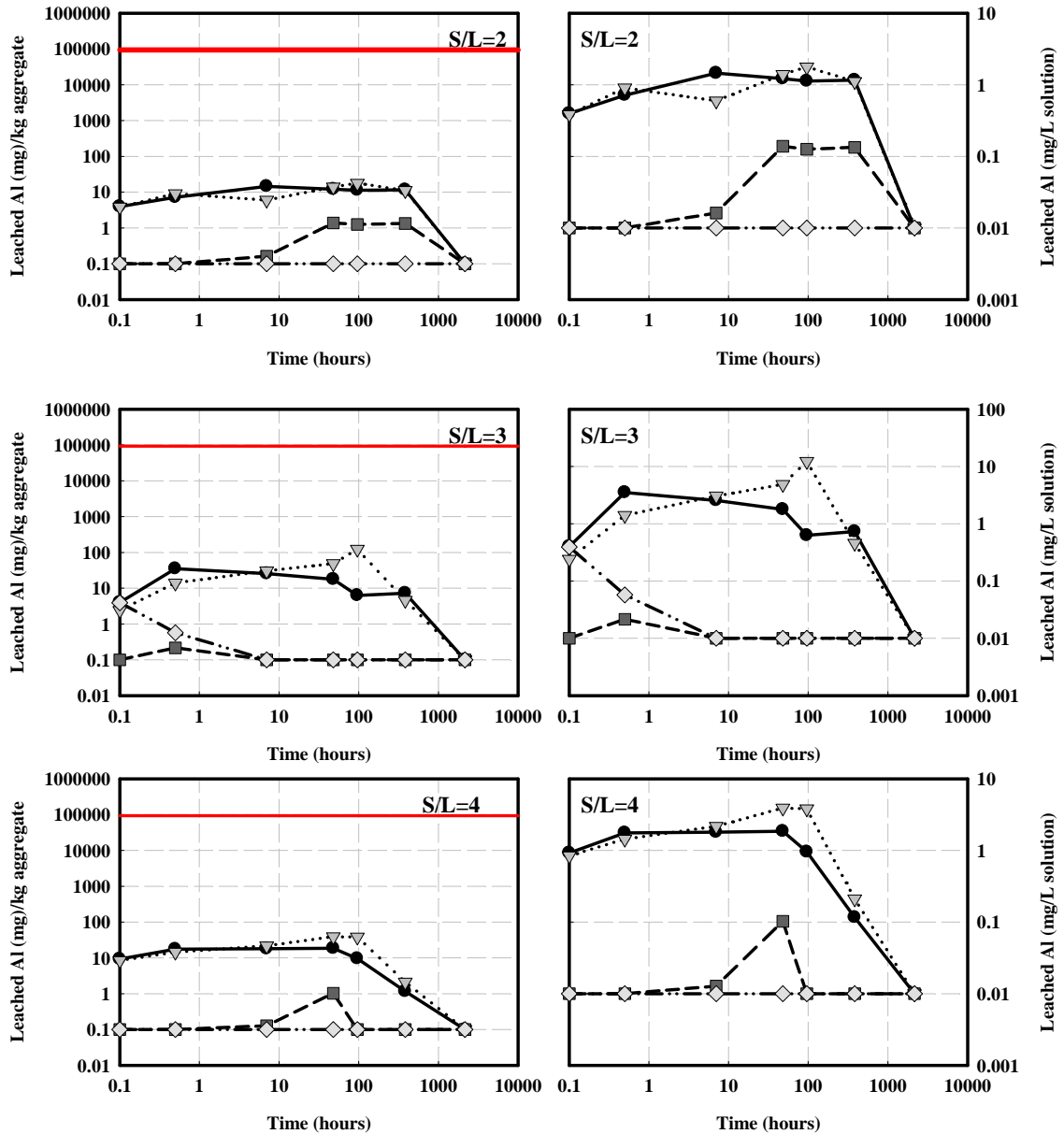Figure 5.39. Effect of various parameters on the leaching of Ca from the aggregate of Soma ash for A/W=1/10 *(Solid line=mg/kg element aggregate contained)*

In an aqueous solution calcium is mainly present as Ca^{2+} (aq), but it may also occur as $CaOH^+$ (aq) or $Ca(OH)_2$ (aq), or as $CaSO_4$ in seawater. Here also the $CaCl_2$ also possible form due to the high chloride content of acidic waste. Ca content of Soma fly ash was very high (CaO=21.3 %) and also acidic waste contains a considerable amount of Ca (400 ppm). So, the aggregates were extremely rich in calcium. Very large amount of calcium were released to processed water due to the high solubility of Ca

compounds in water. Calcium carbonate has a solubility of 14 mg/L, which is multiplied by a factor five in presence of carbon dioxide. calcium hydroxide 1.3 g/L (Patnaik et al., 2003). Solubility of calcium sulphate (anhydrite) and the solubility of calcium sulfate dihydrate (gypsum) is 2 g/L (Art Wilson Company, 2010). At long aging periods (90 days) the solubility of calcium as calcium carbonate is more possible. Other forms remain most stable and less amount of Ca releases at longer aging times.

Iron is very important element for this study because of the very huge Fe content of the acidic waste (88650 mg/kg) and fly ash (5.1 %). The results of the experimental studies in Figure 5.40 showed that a considerable amount of Fe was kept in aggregate body for each S/L ratios and aging time is effective on the fixation mechanism. The release of some Fe from the aggregate occurred but readsorbed at the end of the 90 days leaching period. Usually there is a difference between water soluble Fe^{2+} compounds and generally water insoluble Fe^{3+} compounds. The latter are only water soluble in strongly acidic solutions, but water solubility increases when these are reduced to Fe^{2+} under certain conditions. Elementary iron dissolves in water under normal conditions. Many iron compounds share this characteristic. Iron (II) carbonate has a water solubility of 60 mg/L, iron (II) sulphide of 6 mg/L. Iron is a dietary requirement for most organisms, and plays an important role in natural processes in binary and tertiary form (Raghavan, 2004). There is no Turkish Standard for discharge or hazardous limit of iron.
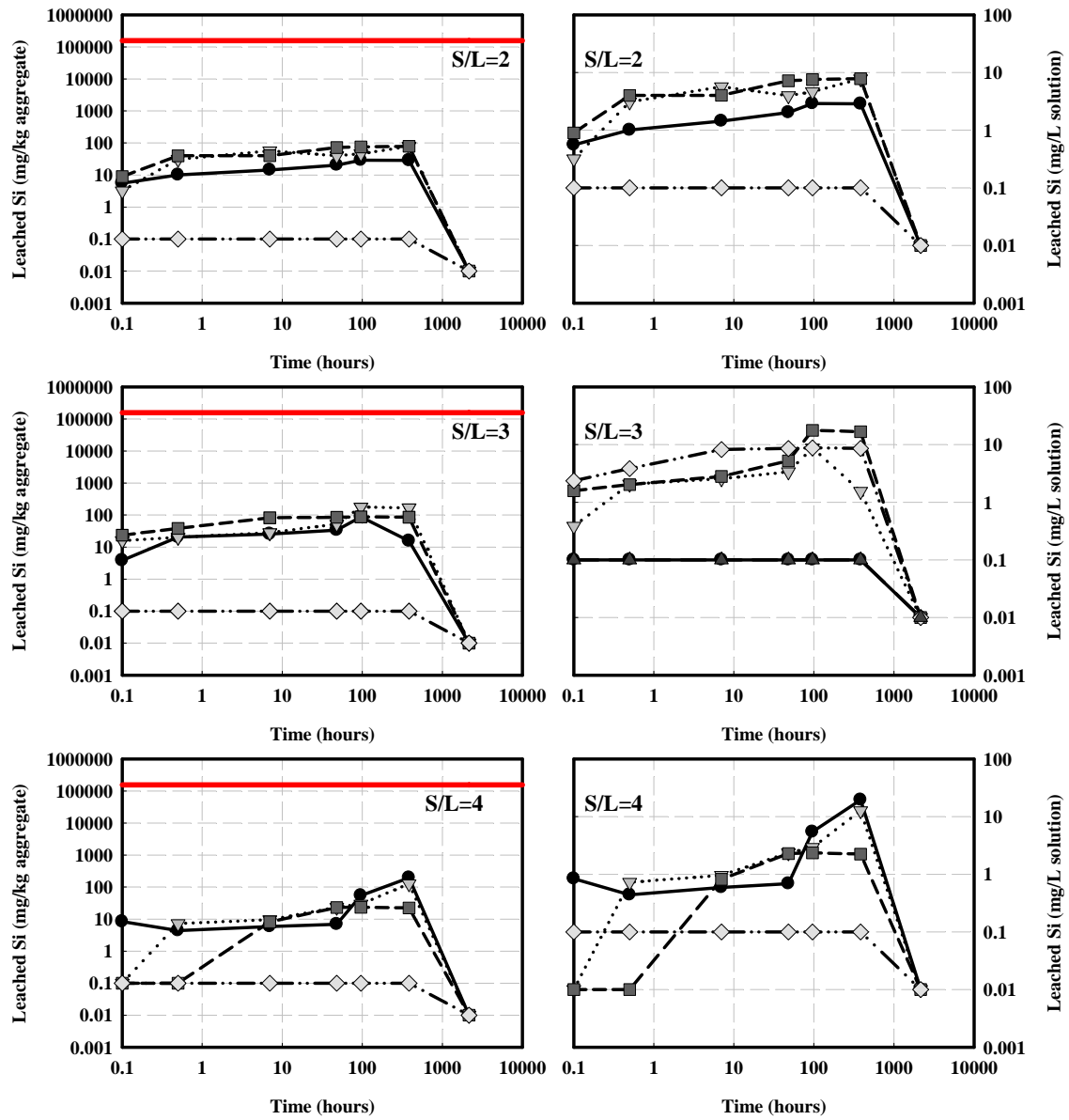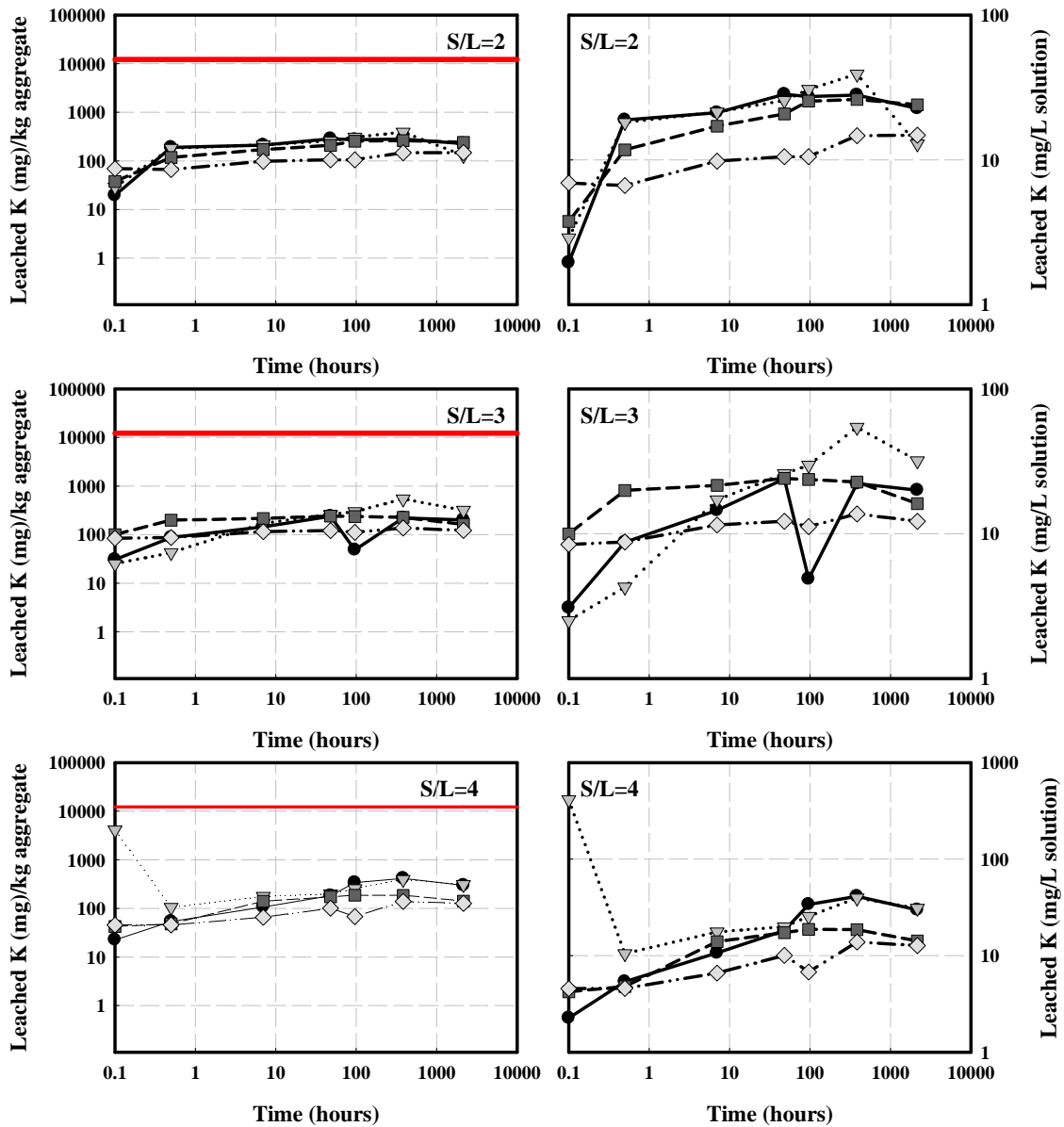
Figure 5.40. Effect of various parameters on the leaching of Fe from the aggregate of Soma ash for A/W=1/10 *(Solid line=mg/kg element aggregate contained)*

The concentration of elements, Ba, Cr, Ni, Zn, Mn, Co, Cu, Pb and Cd is very low in fly ash composition, but the release of these elements are very important due to their high toxicity. Moreover, the acidic waste in aggregate structure contains very large amounts of zinc element .The leaching of these elements especially zinc from aggregate was primarily important. The ICP-MS results displayed the release of Mn, Co, Cu and Pb concentrations were below the detection limits of equipment. Hence the leaching

kinetic graphs of these elements are not contained in this thesis. Figures 5.41, 5.42, 5.43, 5.44 and 5.45 point out the leaching of Ba, Cr, Ni, Zn and Cd ions into the water, respectively. The left side of graphs explains the milligram of element passing into solution per 1 kg of aggregate at an aggregate/water ratio of 1/10. The horizantal solid line here is the element concentration of aggregate (mg/kg) averaging of that element in three S/L ratios (S/L=2,3 and 4). The right side shows the concentration of the element leached into solution (mg/L). Two horizantal lines exist here; long dashed line shows the maximum level of that element to discharge the water into the environment as Class III (polluted water) according to the Turkish Regulation of Water Discharge, dotted line shows the maximum limit of that element to evaluate it as hazardous waste according to the TS EN 12457.

Left part of all graphs denote that the release of elements were at least 100 times lower than the amount of aggregate contained in mg element/kg aggregate. Especially in 16 days aged samples, the leaching of toxic metals are very low especially in Cr and Ni. Zn was the element which had the highest concentration in the aggregate and almost complete of its amount came from the acidic waste. The fixation of Zn element into the aggregate gave the acceptable results especially for S/L=4 ratio. As it was seen in Figure 6.33, only 1/10000 of Zn was leached into the solution at the end of the 2, 4 and 16 days leaching.

Right graphs in Figures 5.41, 5.42, 5.43, 5.44 and 5.45 showed that there was no element concentration in solution higher than hazardous limit according to the TS EN 12457. But a few is at around, a bit higher or lower than the discharge criterion for Class III water.

Ba concentration in aggregate structure comes from only the fly ash (BaO=0.1%) composition and especially found as $BaCl_2$ and $BaSO_4$ forms. All water or acid soluble barium compounds are poisonous (Patnaik, 2003). Therefore there are discharge and hazardous limits specified in regulations. The graphics at left side shows the considerable fixation and stabilization of Ba during the 90 days leaching conditions. 90 days aging period was better to complete all the complexation mechanism, because solubility of Ba ion seems lower than other conditions. At right side, graphics illustrates that 16 and 90 days aged aggregates were quite stable and the concentrations of Ba in processed waters were below both the discharge standard and hazardous limit. But short time aged samples were not fixed enough in terms of Ba element. But all the processed waters were below the hazardous limit of Ba (Figure 5.41).
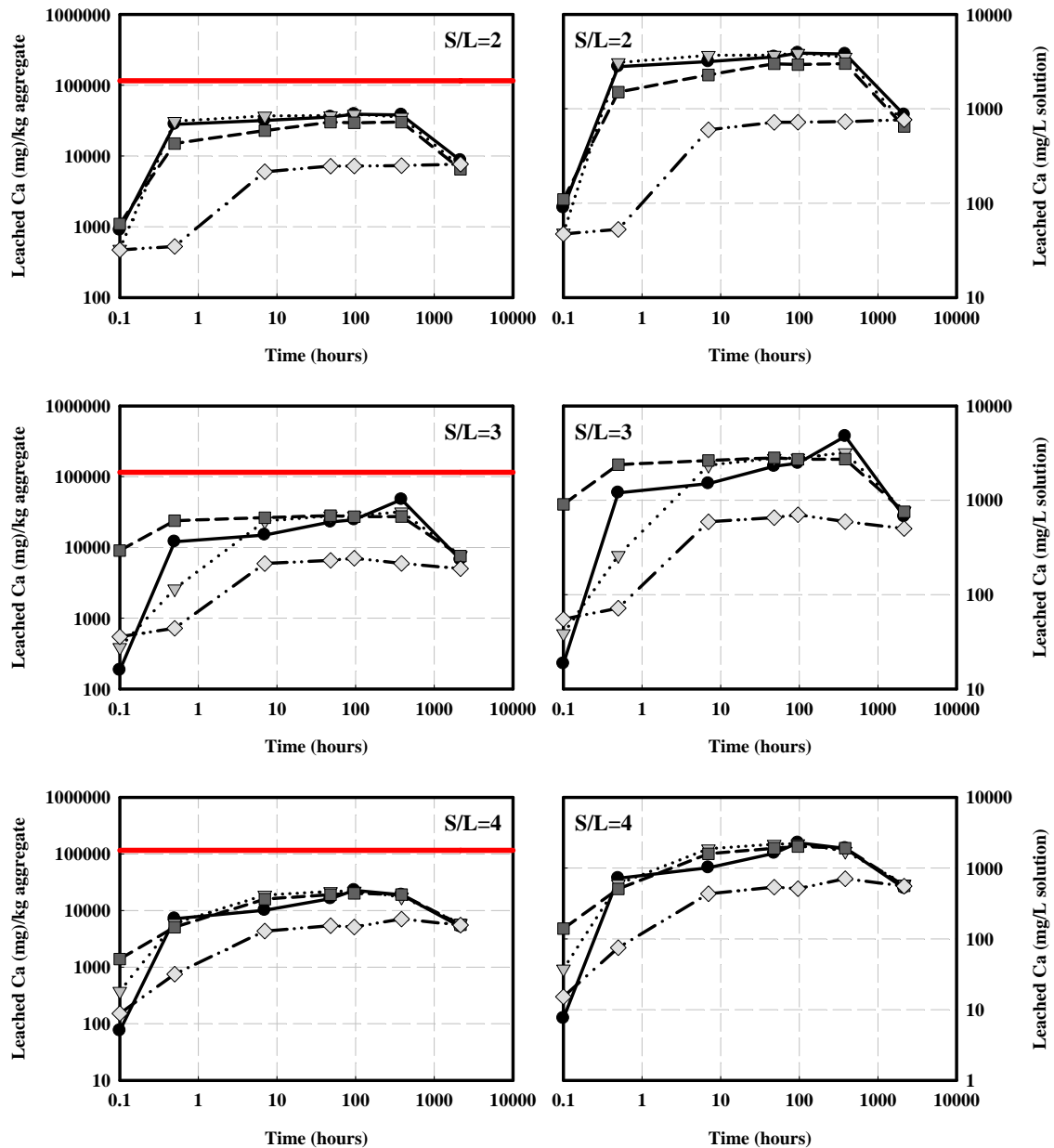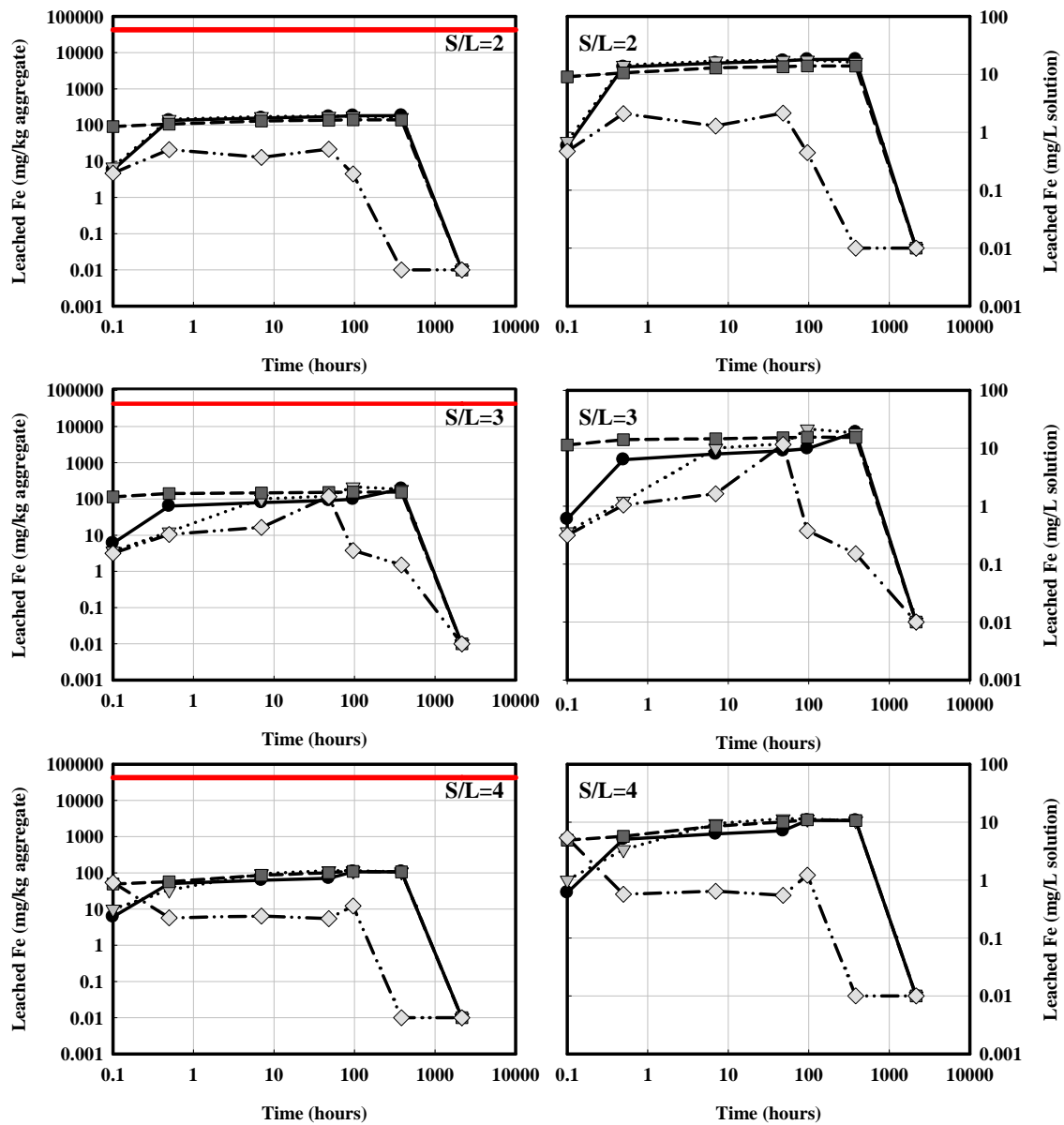
Figure 5.41. Effect of various parameters on the leaching of Ba from the aggregate of Soma ash for A/W=1/10 *(Solid line=mg/kg element aggregate contained, long dashed line=Turkish discharge standard for water quality III (mg/L), dotted line=Hazardous limit for TS EN 12457 (mg/L))*

2 days ········▷········ 4 days ——■—— 16 days —··◇··— 90 days aging

Chromium content of aggregate comes also from the fly ash (108 mg/kg) and acidic waste (55 mg/kg). Attitude of leaching of Cr was the same for all S/L ratios but aging time was again effective on the mechanism. 16 days and 90 days aging time were quite enough for complexation mechanism (Figure 5.42). While the leached amounts

are close to the limit values for 2 and 4 day aged samples, Cr content of processed water in which the aggregates waited was below the detection limit. Chromium ions tend to form complexes; chromium ions in water are usually octahedrally coordinated with water molecules to form hydrates (Dean and Tobin, 1999).

Figure 5.42. Effect of various parameters on the leaching of Cr from the aggregate of Soma ash for A/W=1/10 *(Solid line=mg/kg element aggregate contained, long dashed line=Turkish discharge standard for water quality III (mg/L), dotted line=Hazardous limit for TS EN 12457 (mg/L))*

2 days .... 4 days — — ■ — — 16 days — ·—◇—·— 90 days aging

Nickel in aggregate body comes from both fly ash (198 mg/kg) and acidic waste (50 mg/kg). Graphs in Figure 5.45 shows a considerable uptake of this toxic ion at tested S/L ratios. Especially at S/L=4 and partly at S/L=3, there was no leached amount of this element in processed water for 90 days aged aggregates. Aging time was definitely effective on release of Ni ion. Naturally, the composition of Ba in processed waters is under the environmental limits. Elementary nickel is water insoluble at T=20°C pressure = 1 bar. However, nickel compounds may be water soluble. Nickel chloride is most water soluble; 553 g/L at 20°C, to 880 g/L at 99.9^{o}C. Nickel carbonate has a water solubility of 90 mg/L, whereas other nickel compounds, such as nickel oxide, nickel sulphide and nickel tetra carbonyl are water insoluble. Nickel is a dietary requirement for many organisms, but may be toxic in larger doses (Greenwood and Earnshaw, 1997).

Zinc leachability of the aggregates were actually one of the major points in this part of the study. The Zn composition of aggregates were composed of fly ash (248 mg/kg) and acidic waste (54460 mg/kg). Elementary zinc does not react with water molecules. The ion does form a protective, water insoluble zinc hydroxide ($Zn(OH)_2$) layer with dissolved hydroxide ions, according to the following reaction mechanism:

$$Zn^{2+} + 2OH^- \rightarrow Zn(OH)_2(s) \qquad\qquad (5.2)$$

When the pH is fairly neutral, zinc in water insoluble. Solubility increases with increasing acidity.

As it was shown in Figure 5.44, there was no direct relationship between the operating factors (S/L ratio or aging time) and leaching amounts. But generally said that a considerable amount of this ion were encapsulated into the aggregate structure but at the end of the 16 days leaching periods all the values were above the limits. But readsorption of Zn occured at long leaching times and release amounts closed to zero level.
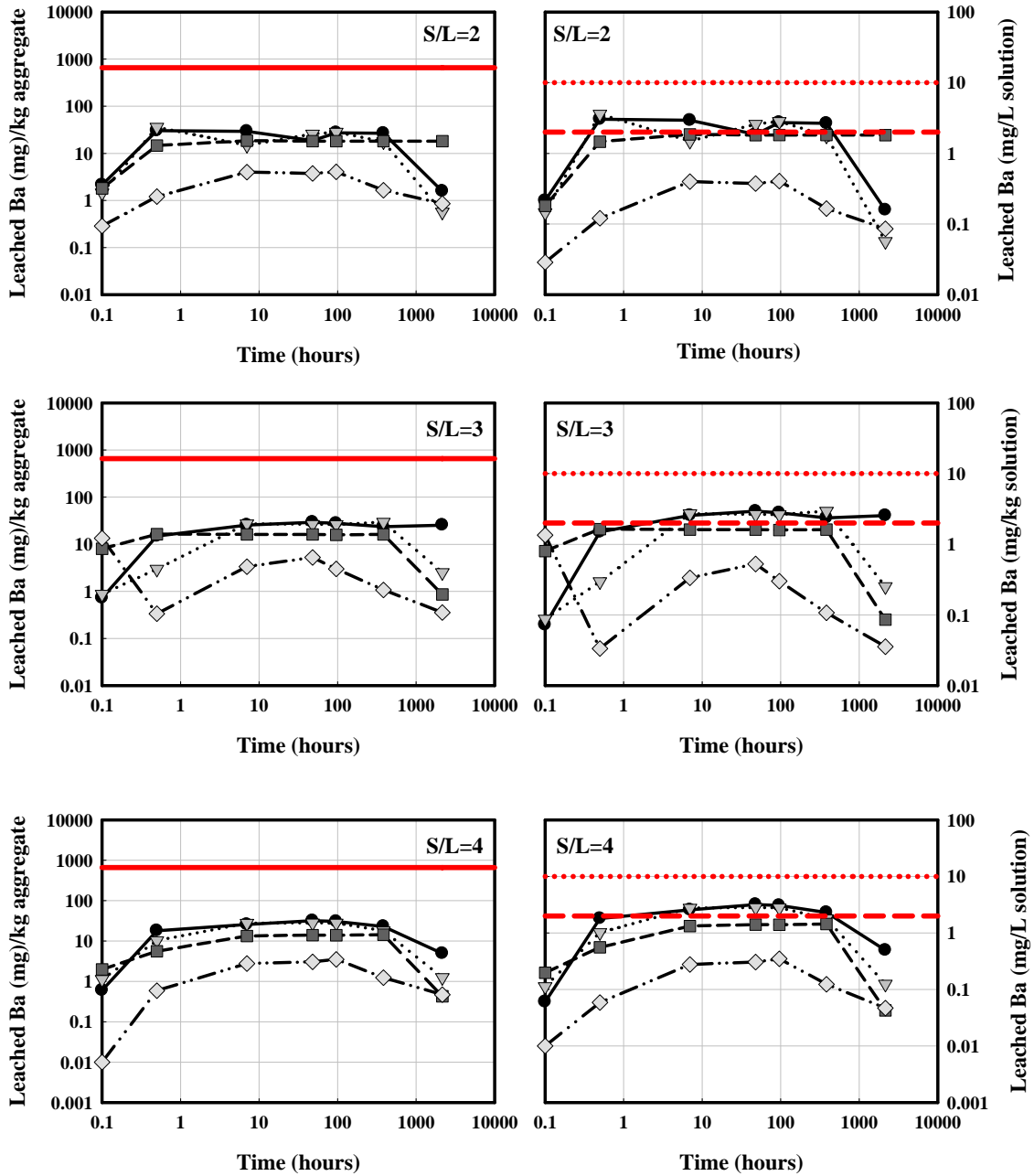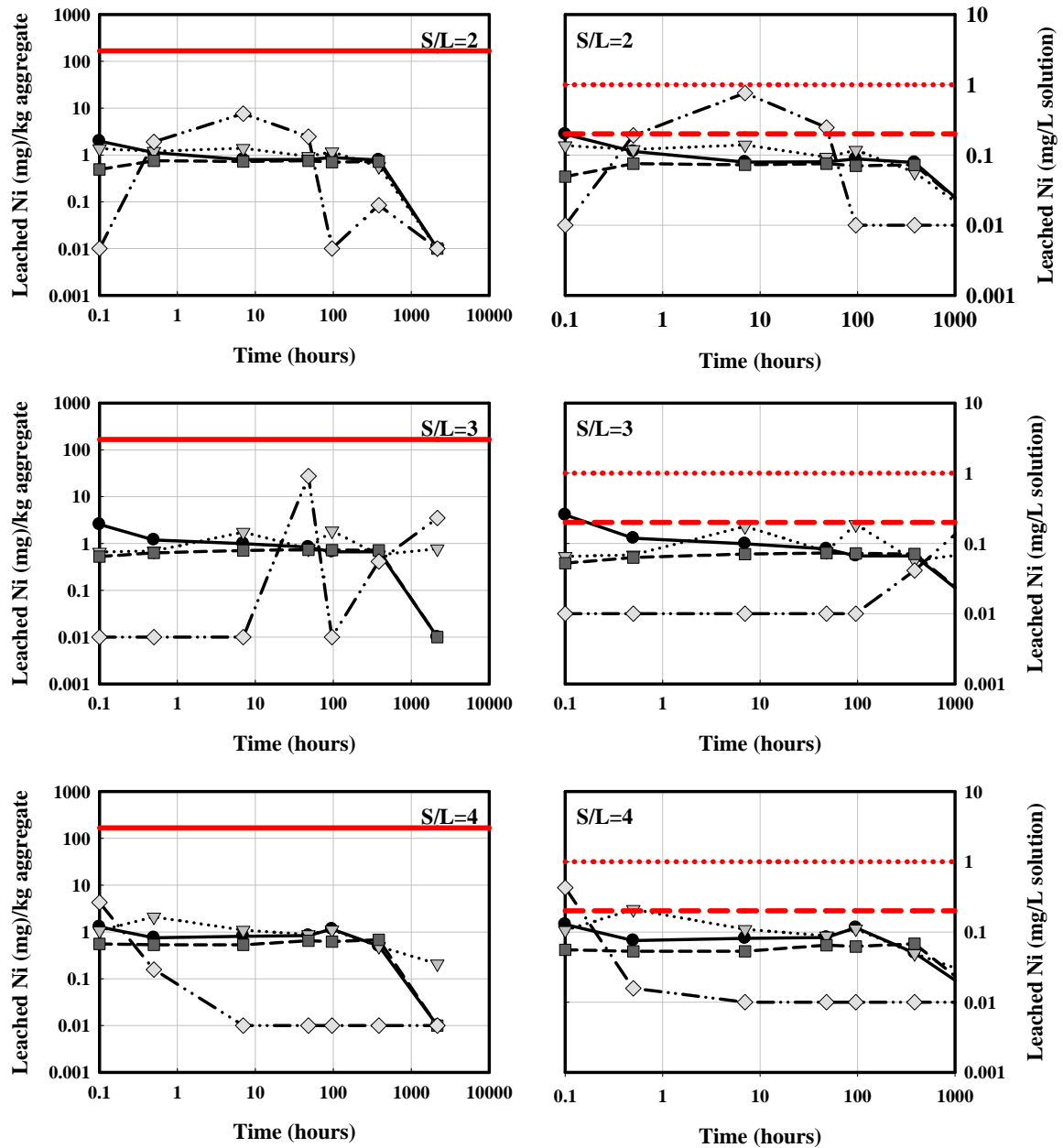
Figure 5.43. Effect of various parameters on the leaching of Ni from the aggregate of Soma ash for A/W=1/10 *(Solid line=mg/kg element aggregate contained, long dashed line=Turkish discharge standard for water quality III (mg/L), dotted line=Hazardous limit for TS EN 12457 (mg/L))*
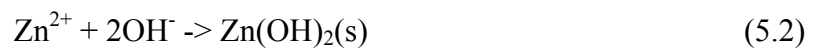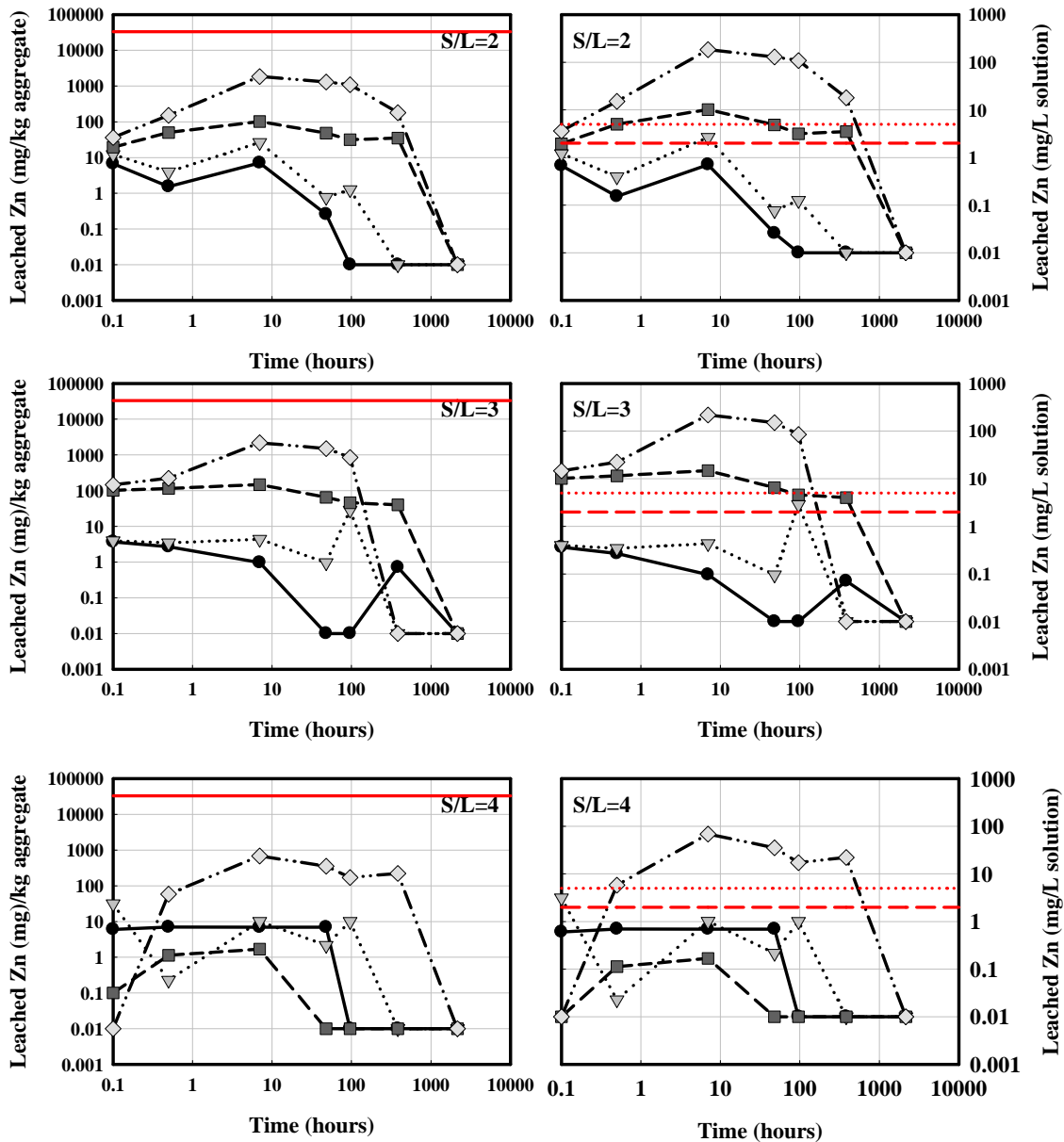
Figure 5.44. Effect of various parameters on the leaching of Zn from the aggregate of Soma ash for A/W=1/10 *(Solid line=mg/kg element aggregate contained, long dashed line=Turkish discharge standard for water quality III (mg/L), dotted line=Hazardous limit for TS EN 12457 (mg/L))*

As for the Cd leachability, the amount of this ion only comes from fly ash and very small amount, but we know that very small dose of Cd is also toxic. The Figure 5.45 illustrates the Cd concentraion of processed water is below the hazardous limit but above the envrionmental discharge limit for water quality III.
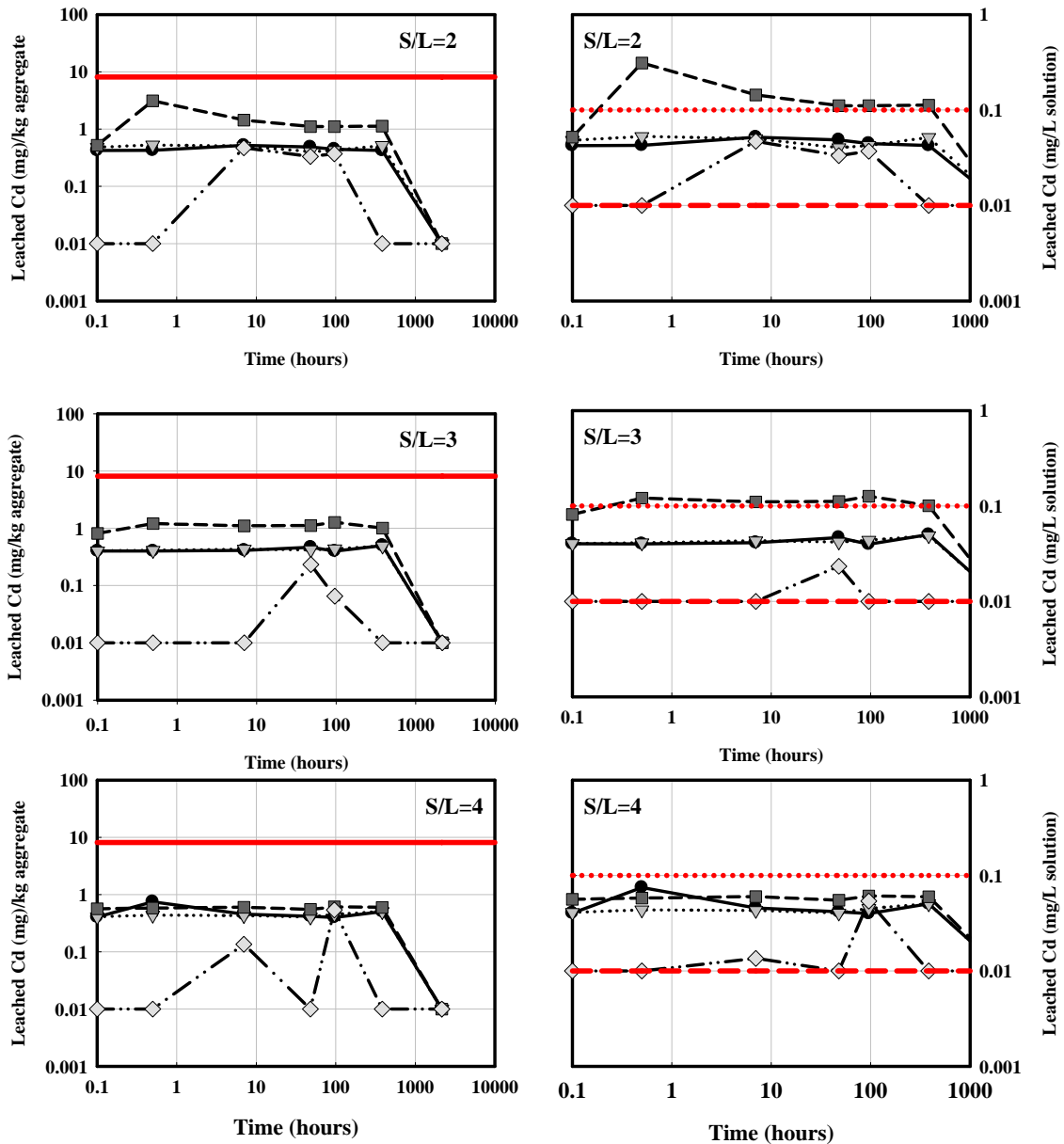
Figure 5.45. Effect of various parameters on the leaching of Cd from the aggregate of Soma ash for A/W=1/10 *(Solid line=mg/kg element aggregate contained, long dashed line=Turkish discharge standard for water quality III (mg/L), dotted line=Hazardous limit for TS EN 12457 (mg/L))*

5.3.3. Aggregate Testing Results

The aggregates prepared at S/L=4 ratio were subjected to 2 different processes. One group of aggregates were dried 16 days at ambient temperature which will be called as AG16, and the other group were subjected to 16 days leaching period after 16

days drying which will be called LAG16 in following discussions. In this part of the thesis, the testing results of Soma fly ash (SFA), AG16 and LAG16 will be compared. SEM, SEM-EDX, XRD, FTIR, TGA-DTA, BET analyses of fly ash and aggregates and the comparison of them will guide us to clarify the mechanism of fixation of heavy metals in aggregate body and stabilization of them over an extended period of time. Understanding the interaction between the metals in fly ash and aggregates and mineral phases being formed or to control their concentration in the neutralization process is significant to design a treatment process for acidic wastes with fly ash.

5.3.3.1. Composition of Aggregates

The results of XRF analysis of the Soma fly ash and aggregates at different S/L ratios were shown in Table 5.11. A comparison of the composition of SFA and aggregates indicates a decrease in SiO_2, Al_2O_3 and CaO. The decrease in SiO_2, Al_2O_3 and CaO generally reflects the dilution of these compounds due to the precipitation of many other metallic species. Otherwise, the decrease in CaO and MgO contents of aggregates display the dissolution of free lime and MgO which is responsible for the neutralizing capacity of the fly ash. An increase in Fe_2O_3 and ZnO in the aggregates indicates the removal of these elements from acidic waste as insoluble precipitates as the pH increases.

5.3.3.2. Neutralization Reactions

There are two opposing processes which establish the pH value for the solution in this neutralization process. The dissolution and hydrolysis of oxide components such as CaO and MgO from fly ash which contributes to an increase in solution pH;

$$CaO + H_2O \longrightarrow Ca^{2+} + 2OH^-$$
$$MgO + H_2O \longrightarrow Mg^{2+} + 2OH^- \tag{5.3}$$
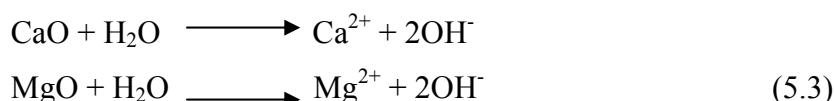
Offseting the pH increase is the hydrolysis of acidic waste constituents such as Fe^{2+}, Fe^{3+} and Zn^{2+}. The relative quantities of soluble bases (oxides) in fly ash and hydrolysable constituents in acidic waste dictate whether the final solution at a given

contact time will have a dominant acid or basic character. There are two factors that will finally dictate the nature of the leaching solution in these neutralization reactions; 1) solid/liquid ratios, and 2) aging time.

Table 5.11. Composition of Soma fly ash and aggregates for 2, 3 and 4 fly ash/acidic
waste (S/L) ratio

%	SFA	A (S/L=2)	A (S/L=3)	A (S/L=4)
SiO_2	45.9	30.2	33.4	34.6
Al_2O_3	23.3	15.4	16.9	17.8
CaO	17.2	11.2	12.4	12.9
Fe_2O_3	4.5	7.2	6.4	5.9
MgO	2.9	2.0	2.2	2.3
ZnO	0.02	2.0	1.5	1.3
Na_2O	0.5	1.2	0.9	0.4
K_2O	1.1	0.7	0.8	0.7
P_2O_5	0.2	0.2	0.2	0.2
TiO_2	0.7	0.5	0.6	0.6
CuO	0.3	0.3	0.3	0.5
SO_3	0.8	0.9	0.8	1.1
Cl	0.03	3.2	2.4	2.2
mg/kg				
Ba	1322	650	706	714
Cr	261	466	231	781
Pb	379	441	466	544
Sr	425	291	311	344
Cd	56	160	67	198
Zr	194	150	145	161
Ni	88	100	96	134

5.3.3.3. Calculation of Saturation States

Precipitation of solid phases may be the most important chemical processes influencing the fate of major (Fe^{3+}, Fe^{2+}, Zn^{2+}), minor (Ca^{2+}, Na^+, Mg^{2+}, Al^{3+}, Mn^{2+}, Pb^{2+}, Cr^{3+}, Ni^{2+}) elements and major anions (Cl^-) in acidic wastewater.

The acidic waste used in this study is highly acidic (pH=-0.017). Low pH of the acidic waste implies also the existence of ferrous minerals which give the acidity to solution.

Nordstorm et al. (2000) explained the pH-metal ion relationship of AMD which had the metal concentration range from 500 mg/L to 0.1 mg/L. If assuming the highest concentration allowed for each metal is 0.1 mmole/L, use metals' precipitation products, they calculated the criteria pH for each metal in water. During the titration

process Fe^{+2} ions are quickly oxidized into Fe^{3+} in the air and precipitate as more insoluble $Fe(OH)_3$. This lowers Fe^{2+} ions precipitation pH. The Table 5.12 below shows the experimental and theoretical pH criteria of metals in AMD.

Table 5.12. Experimental and theoretical pH criteria of metals

Metal	Fe^{+3}	Al^{+3}	Cu^{+2}/Mn	Zn^{+2}/Ni^{+2}	Fe^{+2}
pH (experimental)	<3.2	3-4.5	5-6.5	6.5-8	5.5-6.5
pH (theoretical)	2.93	4.43	6.60/9.33	7.83/8.22	8.95

Activities of aqueous species and mineral saturation indices of selected mineral phases were calculated using MINTEQ visual software. Saturation index (SI) is used when large deviations from equilibrium are observed. For SI=0, there is equilibrium between the mineral and the solution; SI<0 reflects subsaturation, and SI>0 supersaturation. For a state of subsaturation, dissolution of the solid phase is expected and supersaturation suggests precipitation is possible.

The comparison of the mineral phases or phase transformations could only be carried out by considering only the major ions which constitute the fly ash and aggregate (Si, Al^{3+}, Ca^{2+}, Fe^{3+}, Zn^{+2}, SO_4^{2-}, Cl^-) structure. According to the MINTEQ-Visual database, major possible precipitated phases calculated for aggregate prepared at S/L=4 ratio are hematite, kaolinite, halloysite, imogolite, quartz, goeethite etc. (Table 5.13). Hematite and quartz were detected amply by XRD of aggregates. Unsaturated phases which could possibly generated were lime, zinc compounds and portlandite. Due to the less than zero saturation indices of than zinc compound than zero, zinc minerals could not be detected in XRD, suggesting that they were in the amourphous phase. The SI values indicate that $Al(OH)_3$, Al_2O_3, boehmite, diaspore and gibbsite controls the Al^{3+} concentration while $Al_4(OH)_{10}SO_4$ and $AlOHSO_4$ controls the concentration of both Al^{3+} and SO_4^{2-}. Gypsum or anhydrite was observed to be controlling the Ca^{2+} and SO_4^{2-}. Fe^{3+} concentrations are in the forms of maghemite, goethite and magnesioferrite.

Table 5.13. Saturation indices and possible mineral phases for aggregate prepared at S/L=4 ratio

Phases	Saturation Indices	Phases	Saturation Indices
Al(OH)$_3$ (am)	2.97	Lepidocrocite γ-FeO(OH))	8.567
Al(OH)$_3$ (Soil)	5.48	Lime (CaO)	-20.989
Al$_2$O$_3$(s)	7.888	Maghemite (Fe$_2$O$_3$)	13.491
Al$_4$(OH)$_{10}$SO$_4$(s)	14.655	Magnesioferrite (MgFeO)	14.164
AlOHSO$_4$(s)	-0.726	Mg(OH)$_2$ (active)	-7.647
Anhydrite (CaSO$_4$)	-1.656	Mg$_2$(OH)$_3$Cl:4H$_2$O(s)	-13.312
Bianchite (Zn,Fe^{++})(SO$_4$)•6H$_2$O	-5.387	Periclase (MgO)	-10.437
Boehmite (γ-AlO(OH))	5.192	Portlandite (Ca(OH)$_2$)	-10.993
Brucite (Mg(OH)$_2$)	-5.953	Quartz (SiO$_2$)	2.46
Chalcedony (Si)	2.01	Sepiolite Mg$_4$Si$_6$O$_{15}$(OH)$_2$·6H$_2$O	1.914
Chrysotile Mg$_3$(Si$_2$O$_5$)(OH)$_4$	-1.839	Sepiolite (A)	-1.106
Cristobalite SiO$_2$	1.81	SiO$_2$ (am,gel)	1.17
Diaspore (AlO(OH))	6.897	SiO$_2$ (am,ppt)	1.2
Epsomite MgSO$_4$	-4.453	Spinel (MgAl$_2$O$_4$)	1.84
Ettringite (CaO)$_6$(Al$_2$O$_3$)(SO$_3$)$_3$ 32 H$_2$O	-12.225	Zincite (ZnO$_4$)	-0.656
Fe(OH)$_2$.7Cl (s)	10.096	Zincosite	-11.082
Fe$_2$(SO$_4$)$_3$(s)	-29.568	Zn(OH)$_2$ (am)	-1.9
Ferrihydrite (5Fe$_2$O$_3$•9H$_2$O)	6.738	Zn(OH)$_2$ (beta)	-1.18
Ferrihydrite (aged)	7.248	Zn(OH)$_2$ (delta)	-1.27
Gibbsite (Al(OH)$_3$)	6.03	Zn(OH)$_2$ (epsilon)	-0.96
Goethite ((FeO(OH)))	9.447	Zn(OH)$_2$ (gamma)	-1.16
Goslarite ZnSO$_4$·7H$_2$O	-5.141	Zn$_2$(OH)$_2$SO$_4$(s)	-4.078
Gypsum CaSO$_4$·2H$_2$O	-1.406	Zn2(OH)3Cl(s)	-3.649
Halloysite Al$_2$Si$_2$O$_5$(OH)$_4$	14.886	Zn$_3$O(SO$_4$)$_2$(s)	-22.643
Hematite (Fe$_2$O$_3$)	21.295	Zn$_4$(OH)$_6$SO$_4$(s)	-3.829
H-Jarosite KFe$_3$3(OH)$_6$(SO$_4$)$_2$	-0.248	Zn$_5$(OH)$_8$Cl$_2$(s)	-4.841
Imogolite Al$_2$SiO$_3$(OH)$_4$	13.001	ZnCl$_2$(s)	-15.688
Kaolinite Al$_2$Si$_2$O$_5$(OH)$_4$	17.026	ZnSO$_4$:1H$_2$O(s)	-6.514

5.3.3.4. Mineralogical Characterization of Aggregates with XRD

X ray diffraction data were recorded by a powder diffractometer using CuKα radiation. The aggregate pellets were cut horizontally and the XRD measurements were done at both surface and cross sectional part of them. Figures 5.46 and 5.47 shows the comparisons of XRD of SFA with cross-sectional and surface parts of AG16 and LAG16. As it was shown in XRD diagrams, in $2\theta=11$ region, there is a definite peak in surface part of 16 days aged aggregate and surface part of 16 days aged and 16 days leached aggregate. But there is not a related peak in this region of cross sectional layers of 16 days aged and 16 days leached aggregates and original fly ash. At $2\theta=21$, 22, 26, 27, 28, 32, 39, 41 and 50 regions there are peaks for both fly ash and each side of the aggregates. The peak of fly ash at $2\theta=27$ is nearly two fold of the corresponding aggregate peaks. At $2\theta=23$, 33, 34 and 54 regions XRD of fly ash gives peak but there is not any peak in aggregates in these regions. Especially the peak at $2\theta=54$ is a very definite. Table 5.14 shows the determined mineral phases by the scientists in the literature at specified 2theta regions.

Analysis of the aggregating fly ash spheres indicates an increase in Fe and Zn, suggesting that iron-rich and zinc-rich phases are being formed (Table 5.15). The formation of an iron-rich phase was observed by Gitari et al., (2008) in solid residues obtained from South African fly ash and AMD. They showed the formation of new phases by EDX spot analysis suggesting some kind of Al, O, Si mineral formation encapsulating or incorporating Fe, Ti, Mg, Ca and P in the structures. Gitari et al., 2008 also suggested the formation of gypsum as the only new mineral phase by XRD at 2 theta=11 region. Also in this study, the only new peak observed in aggregate structure was at 2 theta=11 region. It could be the gypsum here because the sulfate content of the aggregates was around 1% (Gitari et al. has 3.52 % SO_3 in solid residues) which was not very small percentage.

Table 5.14. Presence of the peaks in XRD of fly ash and aggregates

2θ	Determination of peak (literature data)
11	Gypsum (Gitari et al., 2008)
12	Feldspar (Karayiğit et al., 2001)
21	Quartz (Penthamkeerati etal.,2008, Criado et.al., 2007)
22	Quartz (Karayiğit et al., 2001, Ward et al., 2006)
23	Anhydrite (Karayiğit et al., 2001)
26	Mullite (Criado et al., 2007, Penthamkeerati et al., 2008, Gitari et al., 2008), Anhydirite (Karayiğit et al., 2001)
27	Quartz (Gitari et al., 2008, Criado et al., 2007)
28	Quartz (Karayiğit et al., 2001)
30	Feldspar (Karayiğit et al., 2001), Iron oxide (Penthamkeerati et al., 2008), Mulltite (Gitari et al., 2008)
32	Feldspar (Karayiğit et al., 2001), CaO (Penthamkeerati et al., 2008),
33	Mullite (Criado et al., 2007, Gitari et al., 2008)
34	Lime (Karayiğit et al., 2001), Hematite(Penthamkeerati et al., 2008)
38	Hematite(Karayiğit et al., 2001), CaO(Penthamkeerati et al., 2008),
39	Lime (Karayiğit et al., 2001), Quartz (Penthamkeerati et al., 2008, Gitari et al., 2008)
41	Quartz(Karayiğit et al., 2001), Hematite (Penthamkeerati et al., 2008), Mullite (Gitari et al., 2008, Criado et al., 2007)
50	Anhydrite(Karayiğit et al., 2001),Quartz(Gitari et al., 2008)
54	Gehlenite (Karayiğit et al., 2001)

Table 5.15. EDX of soma fly ash and aggregates processed 16 days

wt%	SFA	AG16	LAG16
Si	22.61	13.03	13.09
Al	12.42	8.30	7.44
Ca	11.29	18.08	15.43
Fe	5.15	12.00	6.30
Zn	1.20	2.37	4.21

The XRD of aggregates revealed gypsum as the only new mineral phase formed at the surface analysis of 16 days leached aggregate (Figure 5.46 and 5.47). X-ray diffraction analysis can detect crystalline phases present at concentration >5% (Gitari et al., 2008). Non-detection of other mineral phases in the aggregates by XRD could

probably due their amorphous nature, low concentration or dilution by the mullite, quartz and the aluminosilicate matrix present in the aggregates.

Analysis of the aggregates cementing the reacted fly ash particles by SEM-EDX indicated an increase in Fe, suggesting that an iron-rich phase was being formed that was amorphous to XRD.

The elements which are evident from the concentration profiles obtained for the three ratios; S/L=2, 3 and 4. For the fly ash/acidic waste reactions Al, Cr, Ni and Cd do not show increase of the concentration in solution. The other groups of elements Na, Mg, K, Ca, Ba, Zn and Fe show an increase in solution. This indicates development of solubility controls through dissolution kinetics or equilibrium precipitation (Gitari et al., 2008). The main feature prevalent in this group of elements is the increase of concentration in the first 1 hour of contact with water. This observation indicates that these elements could be present initially as readily soluble mineral phases or salts. As the dissolution increases and their concentration builds up in reaction mixture, their interaction with species in acidic waste results in precipitation of new mineral phases that control their concentration in solution. The introduction of chemical species in high concentration by the acidic waste seems to dictate the reaction paths in the neutralization process.
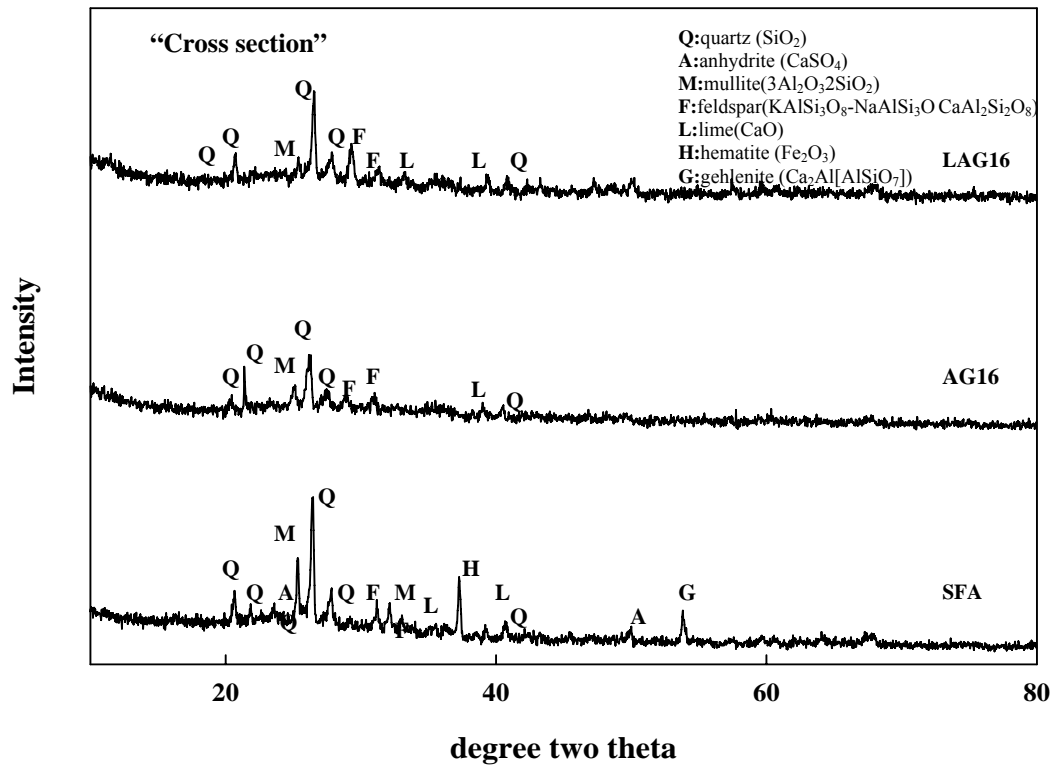
Figure 5.46. XRD graphs of Soma fly ash (SFA), aggregate 16 days aged (AG16) and aggregate 16 days aged and 16 days leached (LAG16) from cross section

As it was seen in Figure 5.46 and 5.47 the phase indicating the control of Si concentration is quartz, the phase indicating the control of Ca^{2+} concentration is anhydrite, lime and gehlenite, the phase indicating the control of Al^{3+} concentration is mullite, the phase indicating the control of Fe^{3+} concentration is hematite. The formation of feldspar controls the mineral phases formed by other elements by connecting to Al and Si.

The peak formed at 2theta=11 in Figure 5.47 illustrates the formation of gypsum as a new phase. But it can only be detected in surface of 16 days leached samples. The reason of this could be the solubility of $CaSO_4$ in water, precipitated again on the surface then was appeared as a new peak. In other situations, gypsum is in amorphous phase.In literature, **Gypsum** at fly ash-AMD mixture permeates was determined by Gitari et al., (2008) and Solem-Tishmack et al.(1995) at *2theta=12*. **Ettringite** ((CaO)3(Al2O3)(CaSO4)3 · 32 H2O) was also detected at fly ash-AMD mixtures by Solem-Tishmack et al.(1995) and at fly ash-water pastes by Yeheyis, (2010) at *2theta=10*. Ettringite, a naturally-occurring mineral, is formed in hydrated Portland

119

cement system as a result of the reaction of calcium aluminate with calcium sulfate, both present in Portland cement.
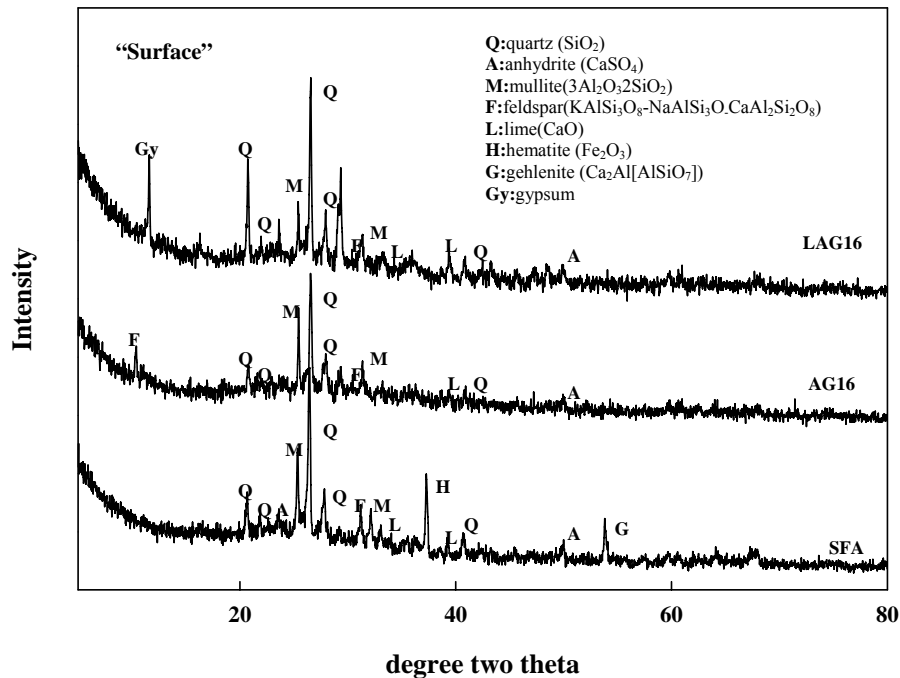
Figure 5.47. XRD graphs of Soma fly ash (SFA), aggregate 16 days aged (AG16) and aggregate 16 days aged and 16 days leached (LAG16) from surface

5.3.3.5. Aggregate Surface Characterization with SEM

According to the SEM-EDX analysis it can be deduced that the mechanism of the reaction could be dissolution of most of the surface soluble salts on contact with acidic waste. The dissolved salts then react with the acidic waste components in the bulk of the solution and the minerals either precipitate on the surface of the large spheres or fill in between the small spheres leading to aggregation (Figure 5.48, 5.49, 5.50). The SEM-EDX elemental profiles indicated a general decrease in content of Ca, Mg and Si in most of the areas analyzed. SEM analysis of aggregates shows needle like crystals dispersed over the residue material.
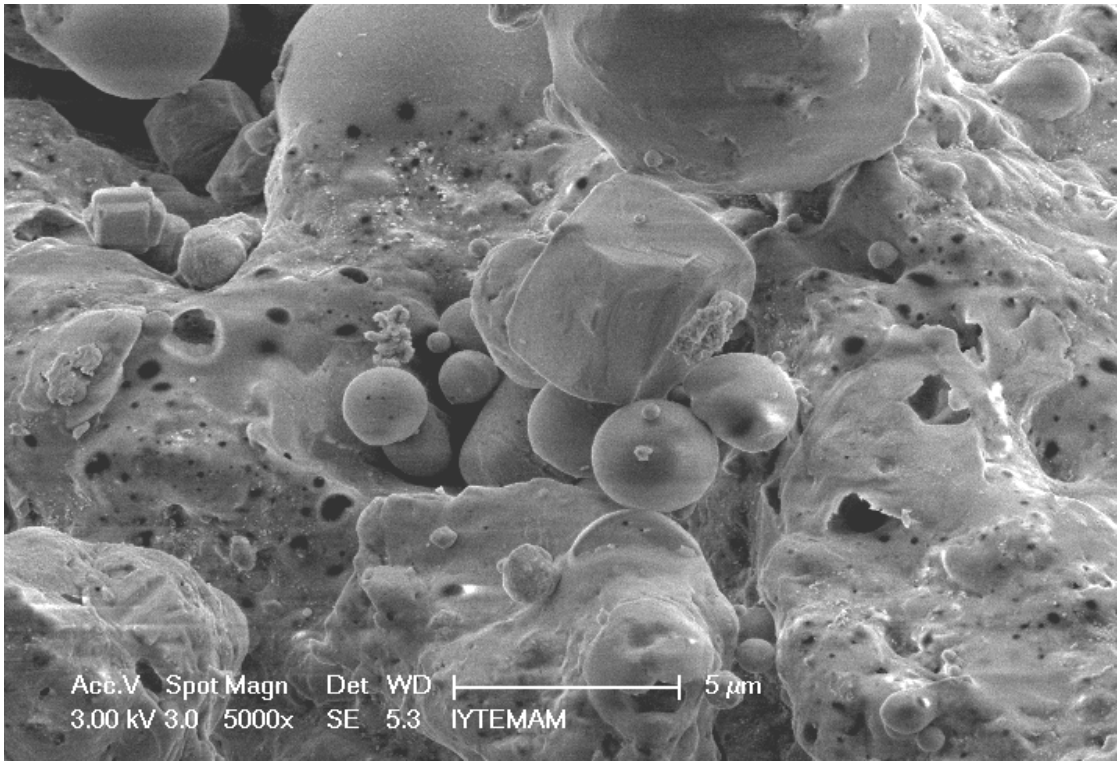
a)
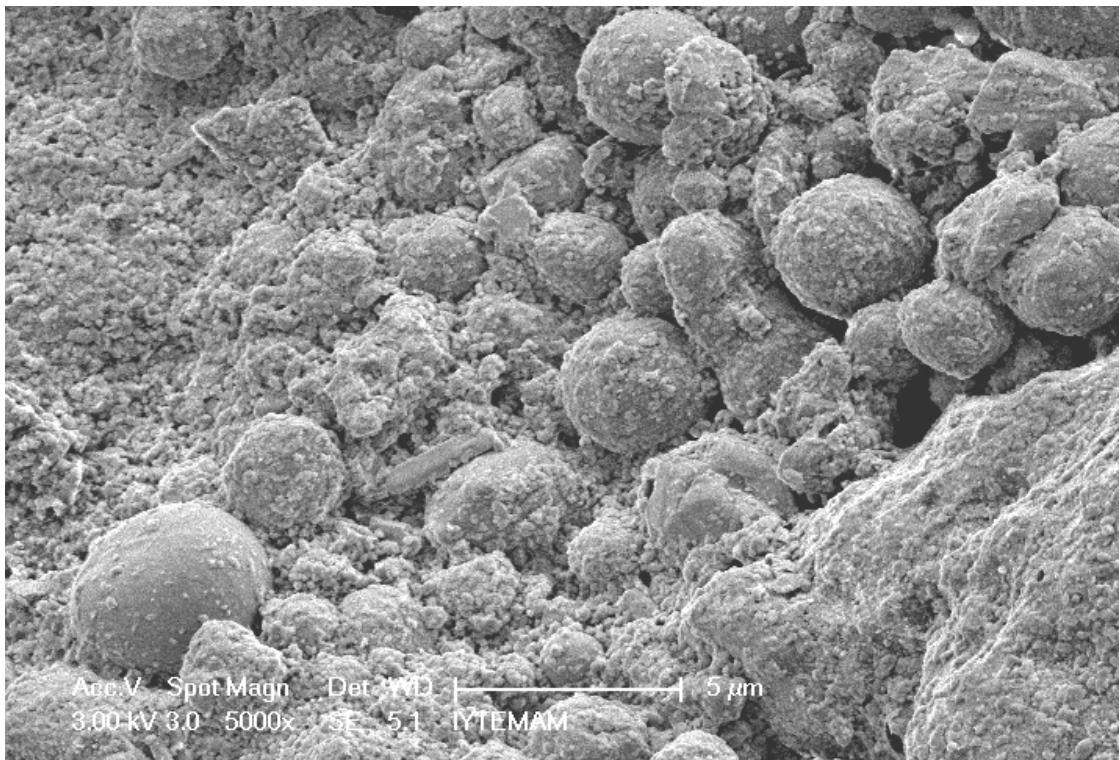
b)

Figure 5.48. SEM observations of a) untreated fly ash b) aggregate in 5 μm scale
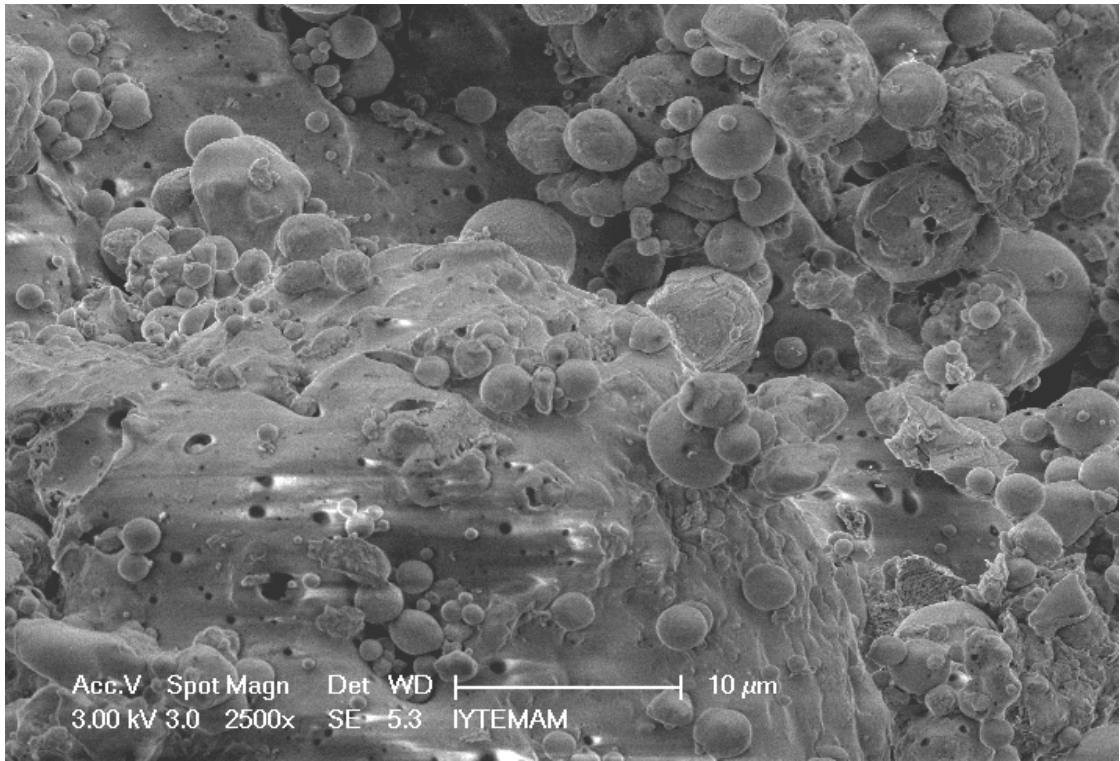
a)
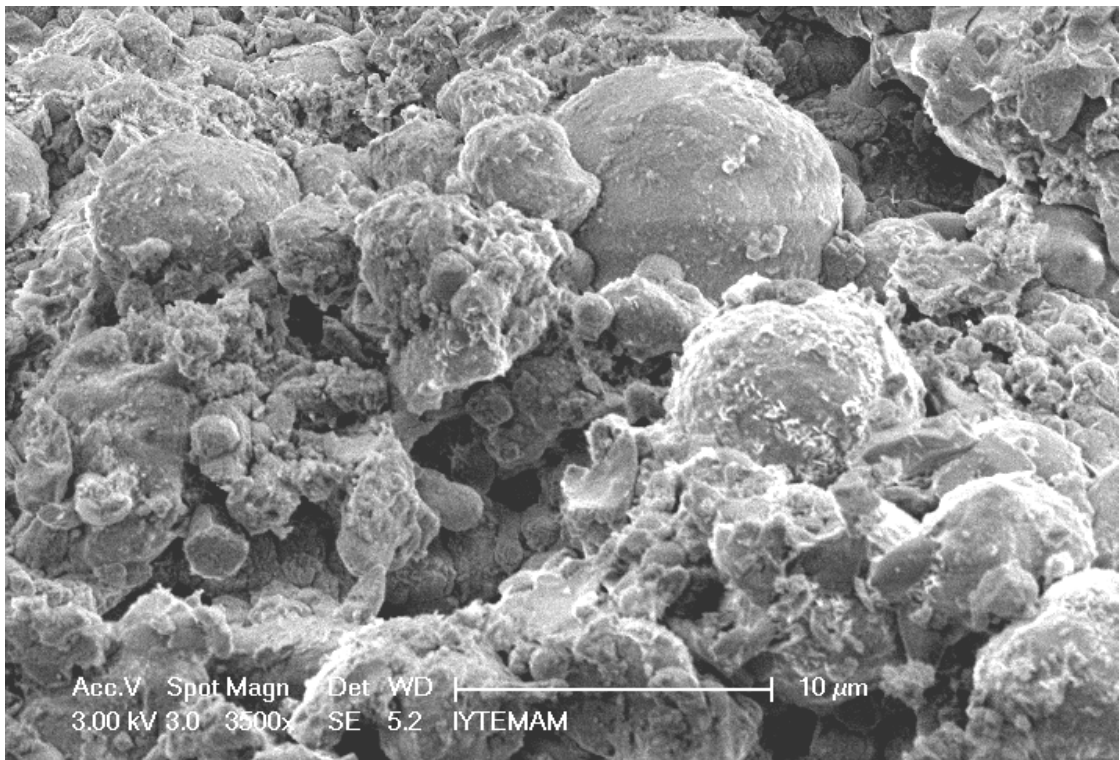
b)

Figure 5.49. SEM observations of a) untreated fly ash b) aggregate in 10 μm scale
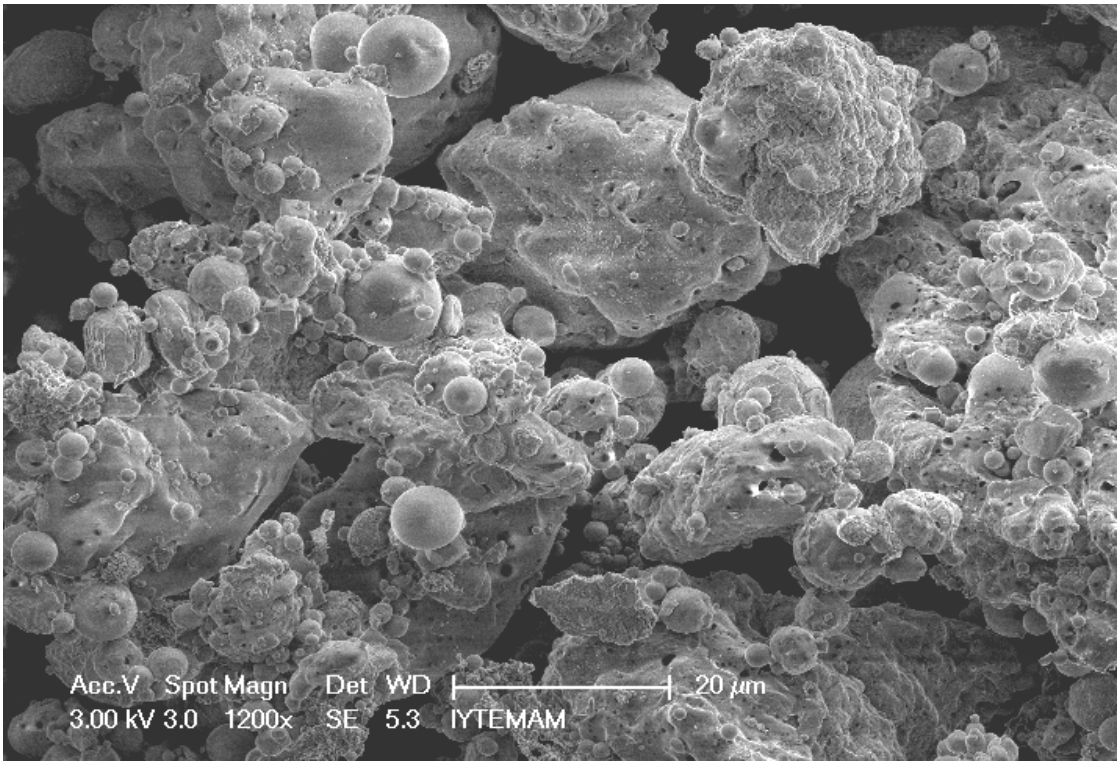
a)
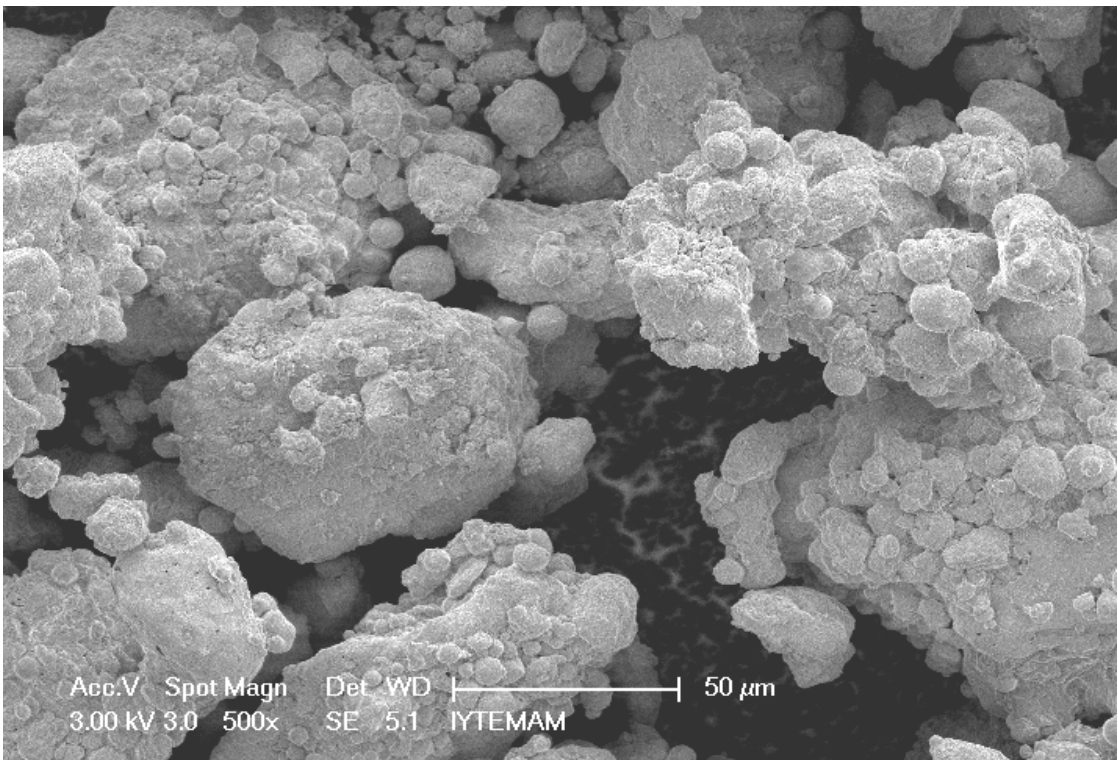
b)

Figure 5.50. SEM observations of a) untreated fly ash b) aggregate in 50 µm scale

5.3.3.6. Thermal Analysis of Aggregates

Thermogravimetric analysis was conducted on SFA, AG16 and LAG16 to determine the amount of weight loss from each sample at various temperatures. The samples were heated from 25 to 1000 ^{o}C at a rate of 10 ^{o}C per minute under a nitrogen atmosphere. Typical TGA curves for SFA, AG16 and LAG16 were shown in Figure 5.51. TGA-first derivative curves with TGA for SFA, AG16 and LAG16 were shown in Figure 5.52, 5.53 and 5.54, respectively. The results indicated that the temperature for maximum weight loss of SFA was around 545.99 ^{o}C, whereas the temperature of for the maximum weight loss of the AG16 sample was around 78.91 ^{o}C and the maximum weight loss for the LAG16 sample was around 85.42 ^{o}C.

The decreases below 545.99 ^{o}C, 78.91 ^{o}C and 85.42 ^{o}C attributed to the loss of the remaining adsorbed water for SFA, AG16 and LAG16, respectively. The loss of mass of SFA, AG16 and LAG16 was 5.312%, 16.731% and 30.625%, respectively. The dehydration of pure gypsum appeared also between 100-170 ^{o}C (TA Instruments, 2009).

It was expected to complete dehydration of the gypsum to the anhydrite form. In aggregate composition, sulfate content was higher than the fly ash sulfate content. Therefore, the water loss in AG16 and LAG16 was due to the both loss of free form of water and the loss of water of gypsum to degrade anhydrite form.
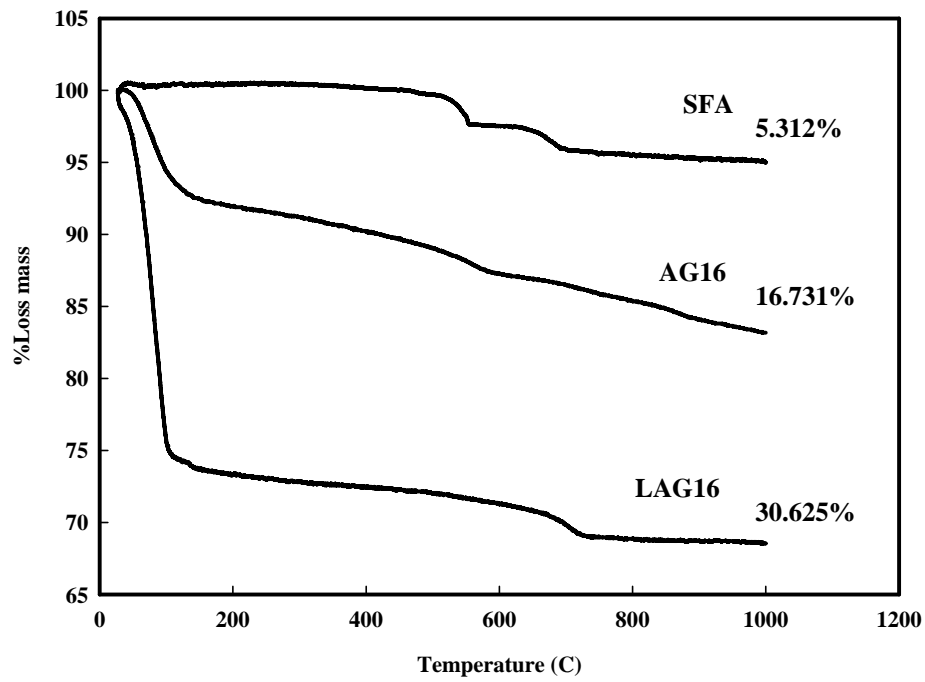
Figure 5.51. TGA of Soma fly ash
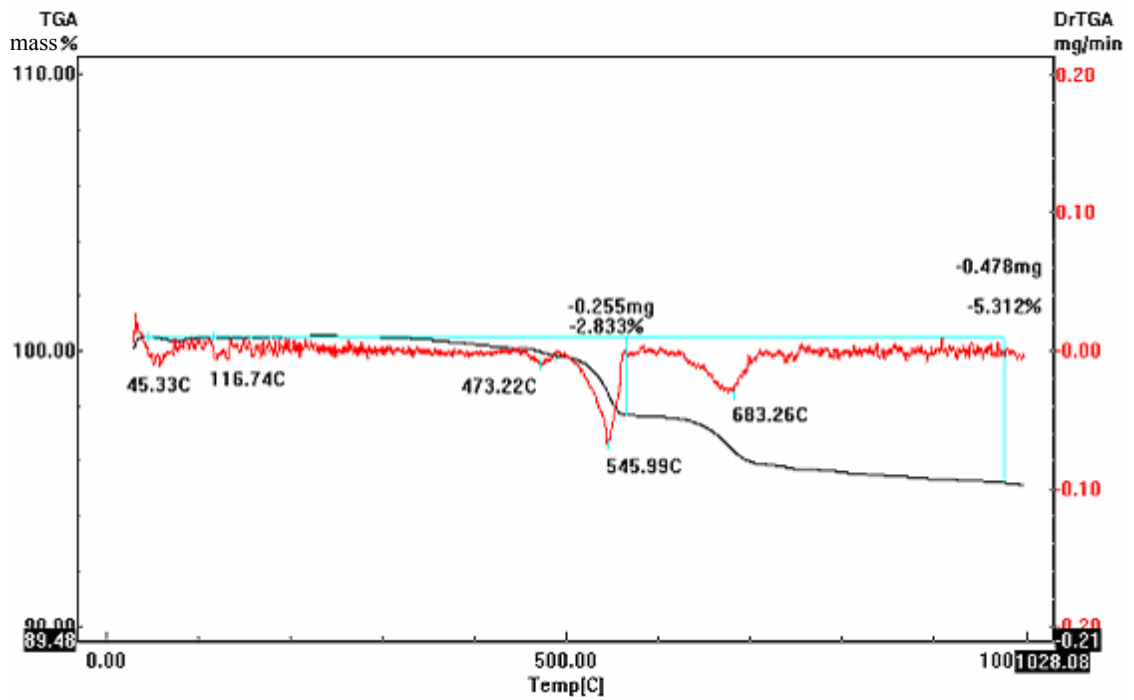
Figure 5.52. TGA and TGA-first derivative curve for SFA

125
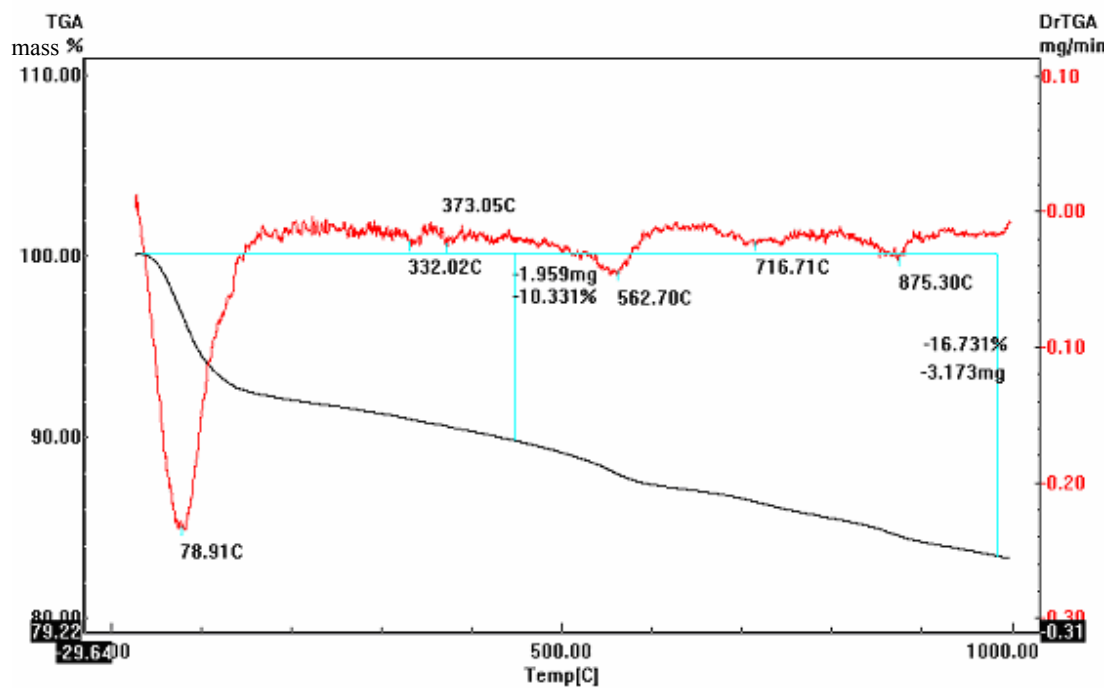
Figure 5.53. TGA and TGA-first derivative curve for AG16
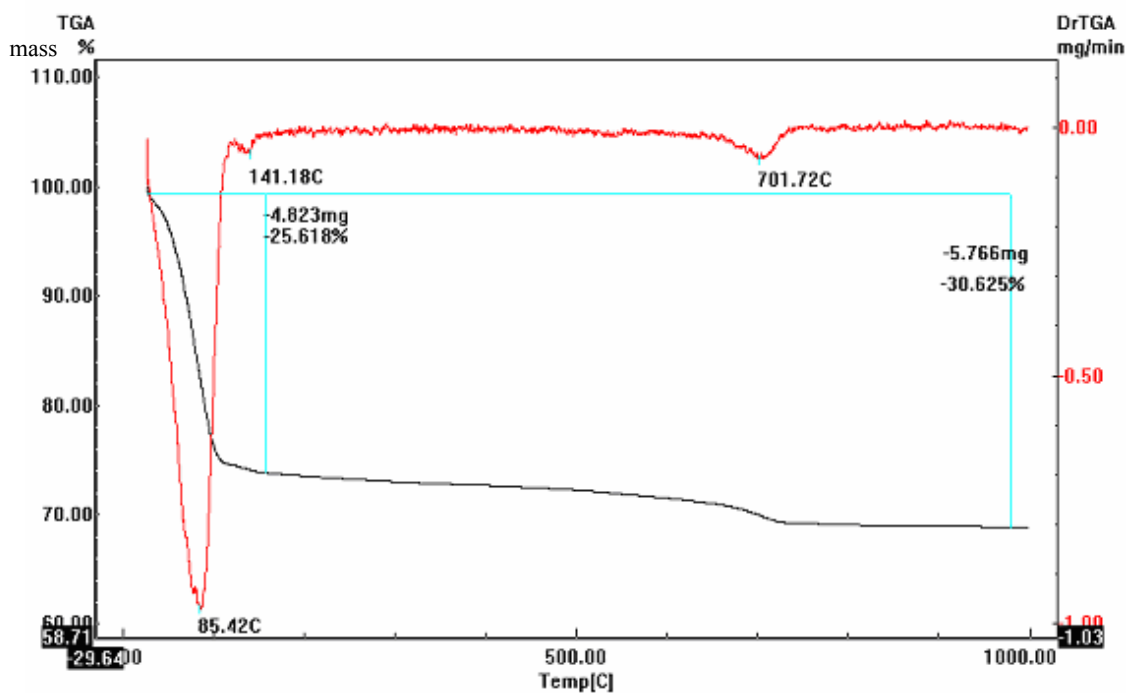
Figure 5.54. TGA and TGA-first derivative curve for LAG16

5.3.3.7. Infrared Spectra of Aggregates

FTIR analysis of the SFA revealed the presence of quartz as major crystalline phase and also mullite presents in XRD; the asymmetric stretching of Si-O-Si and Si-O-Al groups is assigned at between 947 and 1077 cm^{-1} and symmetric stretching of Si-O-Si and Al-O-Si are assigned at 463 and 947 cm^{-1} (Figure 5.55). The same bands were also observed which represent the existence of quartz and mullite determined in XRD of AG16 and LAG16 were also obtained in IR spectra of AG16 ang LAG16. The band at 590-670 cm^{-1} was attributed to SO_4^{2-} and the ionic sulfate was at 1100 cm^{-1} band. For both fly ash and aggregates contained the SO_4^{2-} bands in their IR spectra. CO_3^{2-} band was also determined at 1417 cm^{-1} and the symmetric band of carbonate at 860 and 880 cm^{-1} region for fly ash and aggregates. The absorbances of -OH and H_2O bands of SFA, AG16 and LAG16 were different. The band at 3363 cm^{-1} has been attributed to the stretching vibration of (-OH and H_2O) band and the bending vibration (HOH) at 1650 cm^{-1}. SFA contained less amount of water than aggregates ($LOI_{SFA}=2.1\%$, $LOI_{S/L=2}=24.7\%$, $LOI_{S/L=3}=21.0\%$, $LOI_{S/L=4}=18.2\%$). The aggregates contained acidic liquid wastes which increased the H_2O content.
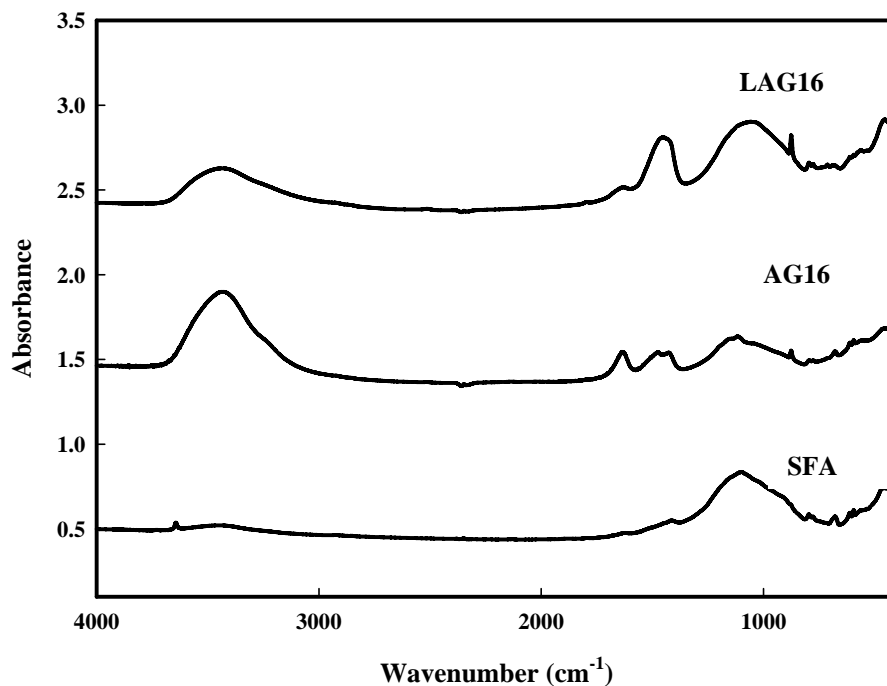
Figure 5.55. FTIR graphics of fly ash, 16 days aged and 16 days aged and leached aggregates

5.3.3.8. Surface Area Measurements with BET

Surface area measurements were analyzed by using N_2 adsorption technique. Table 5.18 shows the decrease in surface area after the aggregate formation from 7.3 to 1.7 m^2/g. The surface area of aggregates which were waited in deionized water after 16 days aging period increased 9 times and reached to 15.2 m^2/g, most probably due to dissolution-precipitation reactions which created a very small structures with a very large surface area (See Figure 5.48 to 5.50).

Table 5.18. Surface area measurements by BET

	SFA	AG16	LAG16
BET Surface Area (m^2/g)	7.3	1.7	15.2

5.3.3.9. Mechanical Test Results of Aggregates

The aggregate materials produced were suggested to use in some construction applications. For that reason, mechanical properties that is the response behavior to applied forces were important. In this part of the study, only the compression tests were carried out to determine somewhat the use of produced materials instead of low-strength or medium-strength materials.

A computer controlled compression test machine (Schimadzu AG-I 250 kN) was used to determine the mechanical properties of aggregates. After the compression test was performed, the output data were obtained as a computer file consisting of time, load and stroke. In order to convert from load-stroke data to engineering stress-strain data, load data were divided by the cross sectional area of the specimen (A=78.54 mm^2) to calculate engineering stress-compressive strength in N/mm^2 = MPa. Stroke data were divided by the original length (L_0 = 10 mm) to calculate engineering strain.

In Figures 5.56, 5.57 and 5.58 yield point is the point where the linear portion indicating the elastic region ends and the slope changes. Yield strength and yield strain were read by drawing perpendicular lines from the yield point to the axes. Tensile strength (ultimate stress, σ_u) is the maximum stress value reached in the stress-strain

curve. The corresponding strain value was marked as the tensile strain. Figure 5.56 shows the stress-strain curves for 2 days aged aggregates at three different S/L ratios. The slopes of the curves were very close to each other and the corresponding elastic modulus values are seen in Table 5.19. A definite decrease in elastic modulus can be noticed in Figure 5.57 (4 days aged samples) for S/L=4 ratio, but this did not repeat for the case of 16 days aging for S/L=4 (Figure 5.58). Generally said that, the increase of aging time caused also an increase in the Young's modulus of the prepared aggregates for each S/L ratios. But the increase in studied S/L ratios did not very effective on the mechanical properties excepting S/L=4 for 16 days aged case.
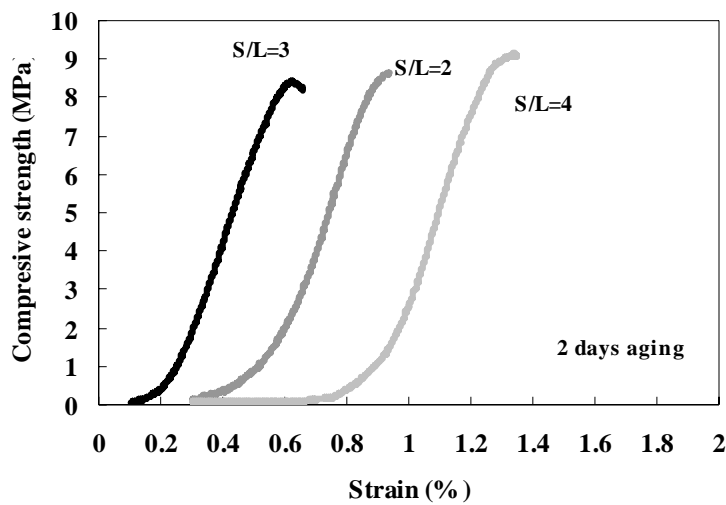
Figure 5.56. Compressive strength-strain curves for 2 days aged aggregates
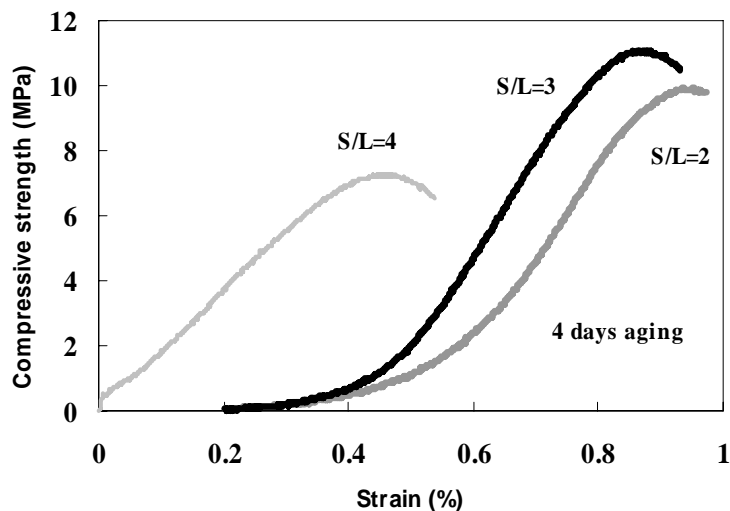
Figure 5.57. Compressive strength-strain curves for 4 days aged aggregates
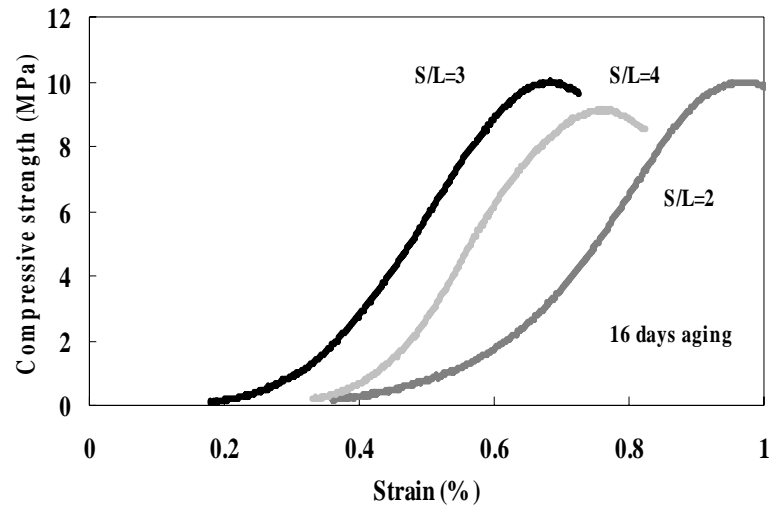
Figure 5.58. Compressive strength-strain curves for 16 days aged aggregates

Table 5.19. Mechanical properties of different aggregates

Process conditions		Tensile strength (max.stress) (σ_u) MPa	Modulus of Elasticity (Young's modulus) (E) MPa
Aging days	S/L		
2	2	8.54	2260.7
	3	8.42	2312.3
	4	9.12	2296.2
3	2	9.93	2613.4
	3	11.09	2830.9
	4	7.30	1767.3
4	2	9.98	2987.6
	3	10.02	3123.4
	4	9.13	3056.3
Controlled low strength material (CLSM) *Naik et al., 1991*		8 (Upper limit for CLSM)	2000
High strength concrete *Öztaş et al., 2006*		40	30,000

130

As it was seen in Table 5.19, the tensile strengths of produced aggregates are differed around the arithmetical mean of 9.28. For the evaluation, the compressive strength values were tabulated and compared with controlled low strength material (CLSM) and high strength concrete. CLSM is a self-compacted, cementitious material used primarily instead of compacted backfill and composed of water, portland cement, aggregate, and fly ash. Several terms are currently used to describe this material, including flowable fill, controlled density fill, flowable mortar, plastic soil-cement, soil-cement slurry, K-Krete, and other names. CLSM is defined as a material that results in a compressive strength of 1200 psi (8 MPa) or less (Portland Cement Association, 2010). The calculated tensile strength values of aggregates were generally above this limit. Öztaş et al., (2006) investigated the high strength concrete properties and declared the tensile strength of 40 MPa. Comparable with the lowest and the highest material properties it caould be said that, the produced aggregates were medium strength materials.

Figure 5.59 shows an increase in compressive strength value of the 16 leached aggregates at the end of the 16 days aging period. This could be the hydration of unreacted part of the fly ash and continuing cementitious reaction.
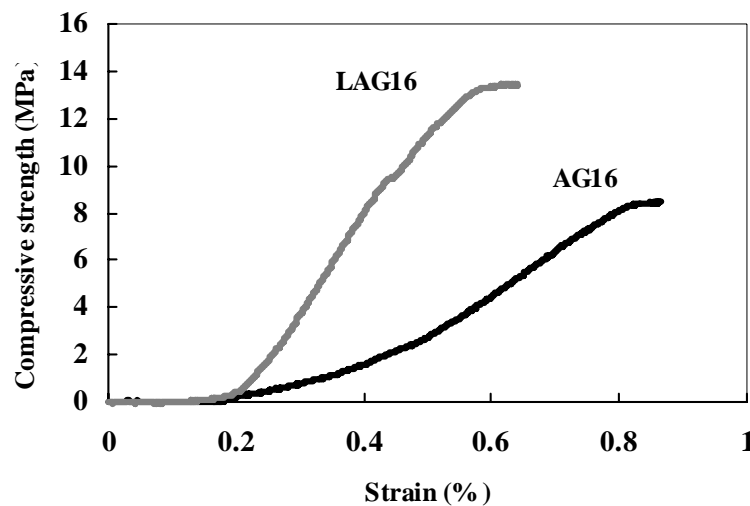
Figure 5.59. Comparison of stress-strain properties of leached and unleached aggregates

5.4. Statistical Evaluation of the Experimental Results with 2-Way ANOVA

Statistical evaluation of the test data were done by 2-Way ANOVA. Experimental results of leaching amount of elements at maximum leaching time (90 days) were evaluated by MINITAB Release 14. Statistical evaluations for each elements are below. The statistical values were shown in Tables 5.20 and 5.21.

Na; to change the S/L ratio and aging time is not statistically significant on Na concentration of the leachate at the end of the leaching period of 90 days. Because, P values for each variables are above 0.05.

Mg; to change the S/L ratio is not statistically significant on Mg concentration of the leachate at the end of the 90 days leaching period. Because P values for S/L factor is above 0.05. But the aging time is statistically significant on leaching of Mg ($P<0.05$).

K; to change the S/L ratio and aging time is not statistically significant on K concentration of the leachate at the end of the 90 days leaching period. Because, P values for each variables are above 0.05.

Al; to change the S/L ratio is not statistically significant on Al concentration of the leachate at the end of the 90 days leaching period. Because P values for S/L factor is above 0.05. But the aging time is statistically significant on leaching of Al ($P<0.05$).

Ca; to change the S/L ratio and aging time is not statistically significant on Ca concentration of the leachate at the end of the 90 days leaching period. Because, P values for each variables are above 0.05.

Ba; to change the S/L ratio and aging time is not statistically significant on Ba concentration of the leachate at the end of the 90 days leaching period. Because, P values for each variables are above 0.05.

Cr; to change the aging time is not statistically significant on Cr concentration of the leachate at the end of the 90 days leaching period. Because P values for S/L factor is above 0.05. But the S/L ratio is statistically significant on leaching of Cr ($P<0.05$).

Ni; to change the S/L ratio and aging time is not statistically significant on Ni concentration of the leachate at the end of the 90 days leaching period. Because, P values for each variables are above 0.05.

Table 5.20. P values for each element leaching

	P-values							
	Na	Mg	K	Al	Ca	Ba	Cr	Ni
S/L	0.556	0.181	0.856	0.095	0.110	0.691	0.008	0.303
Aging	0.204	0.042	0.242	0.047	0.387	0.523	0.626	0.641

Table 5.21. Statistical values for differing S/L ratio and aging time

Species	Sources	SS	df	MS	F	P value
Na	S/L	3391.0	2	1695.51	0.65	0.556
	Aging	16305.1	3	5435.02	2.08	0.204
Mg	S/L	328173	2	164087	2.30	0.181
	Aging	1103937	3	367979	5.16	**0.042**
K	S/L	1720.1	2	860.04	0.16	0.856
	Aging	29579.0	3	9859.68	1.83	0.242
Al	S/L	53.519	2	26.7596	3.56	0.095
	Aging	110.793	3	36.9309	4.92	**0.047**
Ca	S/L	33241669	2	16620835	3.26	0.110
	Aging	18351765	3	6117255	1.20	0.387
Ba	S/L	62.588	2	31.2939	0.39	0.691
	Aging	198.759	3	66.2532	0.83	0.523
Cr	S/L	1.84661	2	0.923303	11.71	**0.008**
	Aging	0.14708	3	0.049027	0.62	0.626
Ni	S/L	2.8390	2	1.41948	1.46	0.303
	Aging	1.7301	3	0.57669	0.59	0.641

CHAPTER 6

CONCLUSIONS

This study evaluated the alkaline coal fly ash from Soma Thermal Power Plant, Manisa for industrial acidic waste treatment. Highly acidic waste was obtained from a company in Atatürk Organized Industrial Zone at Çiğli, İzmir which produces light metal constructions and hot-dip galvanized cable trays. A detailed investigation was performed on the physical, chemical and mineralogical characteristics of Soma fly ash. The major properties of the coal fly ash for the neutralization of acidic waste were identified and possible environmental impacts under different environmental conditions during utilization were also evaluated.

The following conclusions could be drawn from this study;

i. The following conclusions are based on the characterization of Soma fly ash with respect to acidic waste water treatment;

    i. Physical, mineralogical and geotechnical characterization tests revealed that Soma fly ash has a unique structure that comes from the coal basin and many properties are in agreement with the references.

    ii. Soma fly ash had an alkaline properties and pH of the 30 times diluted solution was around 12.

    iii. Soma fly ash contains spherical cenospheres in its structure which was detected by SEM and the specific surface area was measured 7.26 m^2/g by BET. Large pores between the cenospheres caused to determine the larger surface area than calculated from the Malvern results. The most of the particles of Soma fly ash were under the 75 μm size.

    iv. X-ray analysis showed quartz is the first and mullite is the secondary predominant material in the Soma fly ash. The structure of the Soma fly ash contains of mainly Si-O-Si and Si-O-Al bands, H_2O and OH groups, SO_4^{2-} and CO_3^{2-} bands which are determined with FTIR. The results of thermal analysis agreed this.

v. The elemental composition of Soma fly ash contains mainly SiO_2, Al_2O_3 and CaO groups and also Fe_2O_3, MgO, K_2O, Na_2O, BaO and SO_3. This data is in correlation with XRD results. Some trace elements were also detected by ICP-MS. With this composition Soma fly ash shows both Class C and Class F properties.

vi. The acidic waste used in this study was a hydrochloric acid waste which has a very huge amount of zinci iron and chloride in its composition. And also it has a considerable amount of sulfate. The $[H_3O^+]$ concentration of it was calculated with different methods. The pH of acidic waste was around zero.

ii. The following conclusions are based on the fixation-stabilization experiments,

  i. The elemental composition of fly ash directly affects the neutralization potential.

  ii. The fly ash/acidic waste ratio in the aggregate determine the neutralization and fixation efficiency.

  iii. The decision of which fly ash/acidic waste ratio to be used has a significant effect on the aggregate properties.

  iv. The leaching of different metals from the product is affected by their acid-base properties.

  v. To obtain stable aggregates, appropriate fly ash/acidic waste ratio is 4 (S/L=4). For most of the elements, the reaction was completed within 16 days aging period. But 90 days aged aggregates seemed more stable than 16 days aged aggregates. Aging time is highly effective on aggregate properties.

  vi. In respect of Turkish environmental standards, leaching none of effluents of the metals was above their hazardous limits. Furthermore, the leachate quality was within the proper discharge limits for most of the elements.

iii. The following conclusions are based on the aggregate characterization and the fixation-stabilization mechanism;

     i. XRD peaks of fly ash and produced pellets are somewhat the same. But the formation of new peaks is observable in 16 days aged pellets. The formation of a new peak at 2theta=12 was discovered. The formation of gypsum as a new mineral phase was observed with XRD.

     ii. Most precipitates predicted by Minteq-Visual were not confirmed by XRD analysis, probably because they were present in amounts below the detection limits or were poorly crystallized.

     iii. Mechanical strength of the produced aggregate pellets can be considered as medium-strength and can be further developed by manipulating the experimental parameters.

Generally, the results of this study revealed that fly ash can be an alternative to manage to control the acidic wastes. Reuse of fly ash for this purpose has economical and environmental benefits. Utilization of fly ash also avoids the increasingly scarce landfill areas. The treatment of acidic wastes with fly ash could also be considered as a pretreatment. Produced aggregate properties should also be deeply investigated for future use in construction applications.

REFERENCES

Alderliesten, P.T.; Van der Sloot, H.A.; Plomp, A.; Christophe, J. Relation Between Pulverized Coal Particle Size Distribution and Fly Ash Quality as a Function of Coal Characteristics and Installation Performance.*Coal Sci. Technol.* **1987,** 11, 875-880.

Allen, S.J.; Brown, P.A. Isotherm Analysis for Single Component and Multi Component Metal Sorption onto Lignite, *J. Chem. Technol. Biotechnol. ,* **1995**, 62, 17.

Andini, S.; Cioffi, R.; Colangelo, F.; Grieco, T.; Montagnaro, F.; Santoro, L. Coal Fly Ash as a Raw Material for Manufacture of Geopolymer-Based Products. *Waste Management* **2008**, 28, 2, 416-423.

Apak, R.; Tütem, E.; Hügül, M.; Hızal, J. Heavy Metal Cation Retention by Unconventional Sorbents (Red Muds and Fly Ashes). *IVater Research* **1998,** 32, 2, 430-440.

Art Wilson Company. http://www.awgypsum.com/solubility.htm (accessed May 17, 2010)

Asan, T.; Levine, A.D.Wastewater Reclamation and Reuse: Past, Present and Future. *Water Science and Technology* **1996,** 33, 10-11, 1-14.

Ayala, J., Blanco, F.; Garcia, P.; Rodriguez, P.; Sancho, J. Austrian Fly Ash as a Heavy Metals Removal Material, *Fuel* **1998**, 77, 11, 1147-1154.

Baba, A. and Kaya, A. Leaching Characteristics Of Solid Wastes From Thermal Power Plants of Western Turkey and Comparison of Toxicity Methodologies. *Journal of Environmental Management* **2004a,** 73, 199–207.

Baba, A. and Kaya, A. Leaching Characteristics of Fly Ash from Thermal Power Plants of Soma and Tunçbilek, Turkey. *Environmental Monitoring and Assessment* **2004b**, 91, 1-3.

Baba, A.; Gurdal, G.; Sengunalp, F. Leaching Characteristics of Fly Ash from Fluidized Bed Combustion Thermla Power Plant: Case Study: Çan (Çanakkale-Turkey). *Fuel Processing Technology* **2010**, 91, 1073-1080.

Bada, S.O. and Vermaak, S.P. Evaluation and Treatment of Coal Fly Ash for Adsorption Application. *Leonardo Electronic Journal of Practices and Technologies* **2008,** 12, 37-48.

Baker, Hugh D. R. and Avedesian, M. *Magnesium and Magnesium Alloys*. Materials Park, OH: Materials Information Society, 1999.

Banerjee, K.; Cheremisinoff, P.N.; Cheng, S.L. *Water Reseach.* **1997,** 3, 2, 249-261.

Bayat, B. Combined removal of Zinc(II) and Cadmium(II) from aqueous solutions by adsorption onto high-calcium Turkish fly ash. *Water Air Soil Poll.* **2002a**, 136, 69–92.

Bayat, B. Comparative Study of Adsorption Properties of Turkish Fly Ashes I. The Case Of Nickel(II), Copper(II) And Zinc(II). *Journal of Hazardous Materials* **2002b,** B95, 251–273.

Bayat, O. Characterisation of Turkish Fly Ashes. *Fuel* **1998**, 77, 1059-1066.

Bergeson, K.L.; Schlorholtz, S. Physical Properties of Class C Fly Ashes Affecting Their Engineering Utilization, *Elem. Anal. Coal, 2nd Int. Conf. Proc.* **1992,** 232-251.

Berry, E.E.; Hemmings, R.T.; Cornelius, B.J. Speciation in Size and Density Fractionated Fly Ash III. The Influence of HCl Acid Leaching on the Glassy Constituents of a High Calcium Fly ash. *Mater Res. Soc. Symp. Proc.* **1988**, 113, 55-63.

Bettoli, M.G.; Cantelli, L.; Cecchini, M.; Lucchini, F.; Tositti, L.L.; Tubertini, O.; Valcher, S. Heavy Metals in Waste Materials: Leaching of Bottom Ashes by Coal Power Plants. *Ann. Chim.* **1995,** 85, 1-2, 41-53.

Bhattacharjee, U.; Kandpal, T.C. Potential of Fly Ash Utilisation in India. *Energy* **2002**, 27, 2, 151-166.

Boari, G. and Trulli, E. In *CIHEAM, IAMB,* Advance Short Course on Salinity and Pollution towards Sustainable Irrigation in the Mediterranean Region, 1997.

Bouzoubaâ, N., Zhang, M. H., Bilodeau, A., and Malhotra, V. M., "Effect of the Grinding on the Physical Properties of Fly Ashes," *Cement and Concrete Research* **1997**, 27, 12, 1861-1874.

Bruggen, B.V.; Vogels, G.; Kerck, P.V.; Vandecasteele, C. Simulation of Acid Washing of Municipal Solid Waste Incineration Fly Ashes in Order to Remove Heavy Metals. *J. Hazard. Mater.* **1998,** 57, 1-3, 127-144.

Brylicki, W. and Lagosz, A.. Utilization of Flue Gas Desulphurization By-products in the Cellular Concrete Technology. *Studies in Environmental Science,* 71, **1997,** 571-580.

Bulut, Y.; Karayigit, A.İ.; Hower, J.C. Sakulpitakphon, T.Characterization of Feed Coal, Fly Ash and Bottom Ash from the Soma Power Plant *The Nineteenth Annual International Pittsburgh Coal Conference*, September 23–27, **2002**, Radisson Hotel Green Tree, Pittsburgh, PA, USA.

Calesso, E.T.; Samama, J.; Brun, A. Study of Different Leaching Methods of Metallic Elements from Coal Fly Ash. *Environ. Technol.* **1992**, 13, 12, 1187-1192.

Camacho, L.M. and Munson-McGee, S.H. Statistical Analysis of Process and Leaching of Heavy Metals from Fly Ash Solidified/Stabilized Wastes, *Chemometr.* **2006,** 54, 9, 69–79.

Cho, H.; Oh, D.; Kim, K. A Study on Removal Characteristics of Heavy Metals from Aqueous Solution by Fly Ash. *J. Hazard Mater.* **2005**, 127, 1-3,187-195.

Ciccu, R.; Ghiani, M.; Serci, A.; Fadda, S.; Peretti, R.; Zucca, A. Heavy Metal Immobilization in the Mining-contaminated Soils Using Various Industrial Wastes. *Miner. Eng.* **2003**, 16**,** 187–192.

Corigliano, F.; Catalfamo, P.; Pasquale, S.D.; Mavilia, L. Influence of the Calcium Content on the Coal Fly Ash Features in Some Innovative Applications. *Resour. Conserv. Recy.* **1997**, 20, 119–125.

Cullity, B. D. *Elements of X-ray diffraction* 2nd ed; Addison Wesley, 1978.

Dai, S.; Zhao, L.; Peng, S.; Chou, C.; Wang, X.; Zhang, Y.; Li, D.; Sun, Y. Abundances and distribution of minerals and elements in high-alumina coal fly ash from the Jungar Power Plant, Inner Mongolia, China. *International Journal of Coal Geology* **2010**, 81, 320-332.

Das, H.A. and Sanden, C.M.V. Use of Radiotracer Experiments in the Study of the Transport of Trace Elements Between Fly Ash and Water. *J. Radioanal. Chem.* **1982** 75, 1-2, 17-25.

Dean, J.A. and Lange, N.A. *Lange's Handbook of Chemistry*, McGraw-Hill, 1998.

Dean, S.A. and Tobin, J.M. Uptake of Chromium Cations and Anions by Milled Peat. *Resources Conservation and Recycling* **1999**, 27, 151–156.

De Casa, G.; Mangialardi, T.; Paolini, A.E.; Piga, L. Physical-Mechanical and Environmental Properties of Sintered Municipal Incinerator Fly Ash. *Waste Management* **2007**, 27, 238–247

Demirbas, A.; Karshoglu, S.; Ayas, A. Utilization of lignite ash in concrete mixture. *Cement and Concrete Research* **1995,** 25, 1610-1614.

Deng, A. and Tikalsky, P.J. Geotechnical and Leaching Properties of Flowable Fill Incorporating Waste Foundry Sand. *Waste Management* **2008**, *28, 11, 2161-2170.*

Dermatas, D. and Meng, X. Utilization of Fly Ash for Stabilization/Solidification of Heavy Metal Contaminated Soils. *Engineering Geology* **2003**, 70, 3-4, 377-394.

Dogan, O. and Kobya, M. Elemental Analysis of Trace Elements in Fly Ash Sample of Yatagan Thermal Power Plants Using EDXRF. *Journal of Quantitative Spectroscopy & Radiative Transfer* **2006,** 101, 146–150.

Drakonaki, S.; Diamadopoulos, E.; Vamvouka, D.; Lahaniatis, M. Leaching Behaviour of Lignite Fly Ash. *J. Environ. Sci. Health* **1998**, 33, 2, 237-248.

EPA, *Industrial Waste Management Guide, 2002.*

Eren, Z.; Acar, F.N. Equilibrium and Kinetic Mechanism for Reactive Black 5 Sorption onto High Lime Soma Fly Ash. *Journal of Hazardous Materials* **2007**, 1-2, 226-232.

Fernandez-Jimenez, A. and Palomo, A. Mid-infrared Spectroscopic Studies of Alkali-Activated Fly Ash Structure, *Microporous and Mesoporous Materials* **2005**, 86, 207–214.

Fliszar-Baranyai, R.; Laszlo-Sziklai, I.; Rausch, H.; Zembplen- Papp, E. Leachability of Toxic Elements in Hungarian Fly Ash. *Acta Chim. Hung.* **1992,** 129, 3-4, 397-407.

Garavagila, R.; Caramuscio, P. Coal Fly Ash Leaching Behaviour and Solubility Controlling Solids. *Stud. Environ. Sci.* **1994**, 60, 87-102.

Gitari, W.M.; Petrik, L.F.; Etchebers, O.; Key, D.L.; Okujeni, C. Utilization of Fly Ash for Treatment of Coal Mines Wastewater: Solubility Controls on Major Inorganic Contaminants. *Fuel* **2008**, 87, 2450-2462.

Gitari, W.M.; Petrik; L.F.; Key, L.; Okujeni, C. Partitioning of Major and Trace Inorganic Contaminants in Fly Ash Acid Mine Drainage Derived Solid Residues. Int. *J. Environ. Sci. Tech.* **2010**, 7, 3, 519-534.

Graham, U.M. and Hower, J.C. Mineralogy and Petrology of Coal Combustion Byproducts at Kentucky Generating Stations Burning Southern Illinois Basin Coal, in Manage High Sulfur Coal Combust. Residues. *Issues Pract Conf Proc.*, **1994,** 80-90.

Greenwood, N.N. and Earnshaw, A. *Chemistry of the Elements*; 2nd ed; Butterworth-Heinemann: Boston, 1997.

Griest, W.H. and Tomkins, B.A. Carbonaceous Particles in Coal Combustion Stack Ash and Their Interaction with Polycyclic Hydrocarbons. *Sci. Total Environ.* **1984**, 36, 209-214.

Gupta, G. and Torres, N.Use of fly ash in reducing toxicity of and heavy metals in wastewater effluent. *J. Hazard. Mater.* **1998,** 57, 243–248.

Gupta, G.S.; Prasad, G.; Singh, V.N. *Water Res.***1990**, 24, 45.

Gupta, G.S.; Pandy, K.K.; Singh, V.N. *Water, Air, Soil Pollut.* **1988,** 37, 13.

Gupta, K.V. Utilization of Bagasse Fly Ash (a sugar industry waste) for the Removal of Copper and Zinc from Wastewater. *Separ. Purif. Technol.* **2000**, 18, 131–140.

Hall, M.L.; Livingston, W.R. Fly Ash Quality, Past, Present and Future, and The Effect of Ash on the Development of Novel Products. *J Chem Technol Biotechnol.* **2001**, 77, 234-239.

Hansen, L.D. and Fisher, G.L., Elemental distribution in coal fly ash particles. *Environ. Sci. Technol* **1980**, 14**,** 1111–1117.

Harris, W.R.; Silberman, D. Time Dependent Leaching of Coal Fly Ash by Chelating Agents. *Environ. Sci. Technol.* **1983,** 17, 3, 139-145.

Haynes, B.S.; Neville, M.; Quann, R.J. Factors Governing the Surface Enrichment of Fly Ash in the Volatile Trace Species. *J. Colloid Interface Sci.* **1992,** 87,1, 266-278.

Heebenik, L.V.; Hassett, D.J. In *University of Kentucky,* International Ash Utilization Symposium, 2001.

Hequet, V.; Ricou, P.; Lecuyer, I.; Le Cloirec, P. Removal of Cu^{2+} and Zn^{2+} in Aqueous Solutions by Sorption onto Mixed Fly Ash. *Fuel* **2001,** 80, 851–856.

Horiuchi, S., Kawaguchi, M. and Yasuhara, K.*J.* Effective Use of Fly Ash Slurry as Fill Material, *Hazard Mater.* **2000**, 76, 2-3, 301-337.

Huang, C.P.; Ghadrian, M. Physical-Chemical Treatment of Paint Industrial Wastewater. *J. Water Pollution Control Federation***, 1974,** 46, 10, 2340-2346.

Hytiris, N.; Kapellakis, I.E. The Potential Use of Olive Mill Sludge in Solidification Process. *Resour. Conser. Recycl.* **2004**, 40, 2, 129-139.

Inci, U. Depositional evolution of Miocene Coal Successions in the Soma Coalfield, Western Turkey, *Int. J. Coal Geol.* **2002**, 51, 1–29.

Iyer, R.S.; Scott, J.A. Power Station Fly Ash-A review of Value-added Utilization Outside of the Construction Industry Resources. *Conservation and Recycling* **2001***,* 31, 217–228.

Jaarsveld, J.G.S.; Deventer, J.S.J.; Lukey, G.C. The Characterisation of Source Materials in Fly Ash-Based Geopolymers, *Materials Letters*, **2003**, 57, 1272–1280.

Jackson, B.P.; Miller, W.P.; Schumann, A.W.; Suner, M.F. Trace element solubility from land application of fly ash/organic waste mixtures. *J. Environ. Qual.* **1999**, 28, 639–647.

Kalyoncu, R.S. *Coal Combustion Products*, US Geological Survey Minerals Yearbook, 2010.

Kao, P.C.; Tzeng, J.H.; Huang, T.L. Removal of chlorophenols from aqueous solution by fly ash**.** *Journal of Hazardous Materials* **2000**, 76, 237–249.

Karayigit, A.İ. Thermal Effects of a Basaltic Intrusion on the Soma Lignite Bed in West Turkey, *Energy Sources,* **1998***,* 20, 55–66.

Karayigit, A.İ. and Whateley, M.K. Properties of a Lacustrine Subbituminous (k1) Seam with Special Reference to the Contact Metamorphism, Soma-Turkey, *Int. J. Coal Geol.* **1997,** 34, 131–155.

Karayigit, A.İ.; Bulut, Y.; Querol, X.; Alastuey, A.; Vassilev, S. Variations in Fly Ash Composition from Soma Power Plant, Turkey. *Energy Sources* **2005**, 27, 1473–1481.

Karayiğit, A.İ.; Spears, D.A.; Booth, C.A. Distribution and Environmental Sensitive Trace Elements in the Eocene Sorgun Coals, Turkey. *International Journal of Coal Geology* **2000***,* 42, 4, 297-314.

Kawfherr, N.; Lichtman, D. Comparison of Micron and Submicron Fly Ash Particles using SEM and X-ray Elemental Analysis. *Environ. Sci. Technol,* **1984**, 18, 7, 544-547.

Khandekar, M.P.; Olaniya, M.S.;Bhide, A.D. A New Approach for Fly Ash Leachate Evaluation. *J. Inst Eng* **1996**, 76, 33-39.

Koukouzas, N.; Papanikolaou, D.; Tourunen, A. Mineralogical And Elemental Composition Of Fly Ash From Pilot Scale Fluidised Bed Combustion Of Lignite, Bituminous Coal, Wood Chips And Their Blends *Fuel* **2007,** 86, 2186–2193.

Kozar, S.; Bilinski, H.; Branica, M.; Schwugar, M.J. Adsorption of Cd(II) and Pb(II) on Bentonite Under Estuarine and Seawater Conditions, *Sci. Total Environ.* **1992**, 121, 203.

Krishnamoorthy, T.S.; Gopalakrishnan, S.; Balasubramanian, K.; Bharatkumar, B.H.; Mohan Rao, P.H. Investigations on the Cementitious Grouts Containing Supplementary Cementitious Materials . *Cement and Concrete Research* **2002**, 32, 9, 1395-1405.

Krauskopf, K.B.. Factors Controlling the Concentrations of Thirteen Rare Metals in Sea-water. *Geochim. Cosmochim. Acta* **1956,** 9, 1-32.

Kumar, S.; Upadhyay, S.N.;Upadhyay, Y.D. J. *Chem. Tech. Biotechnol.* **1987**, 37, p 281

Kumpiene, J., Ore S. and Lagerkvist, A. Stabilization of Pb- and Cu-Contaminated Soil Using Coal Fly Ash and Peat. *Environ Pollut.* **2007**, 145, 1, 365-373.

Landman, A.A.. Aspects of Solid State Chemistry of Fly Ash And Ultramarine Pigments. PhD Dissertation, University Of Pretoria, 2003.

Landman, A.A. and Waal, D.D. Fly Ash as A Potential Starting Reagent For The Synthesis Of Ultramarine Blue. *Materials Research Bulletin* **2004,** 39, 655–667.

Lee, W.K.W., Deventer, J.S.J., Structural Reorganisation of Class F Fly Ash in Alkaline Silicate Solutions, *Colloids and Surfaces A: Physicochem. Eng. Aspects* **2002,** 211, 49-66.

Leim, H.; Sandstroem, M.; Wallin, T.; Carne, A.; Rydevik, U.; Thurenins, B.; Moberg, P.O. Studies on the Leaching and Weathering Processes of Coal Ashes. *Water Sci. Technol.* **1983,** 15, 139-145.

Leroy, C. and Ferro, M.C. Production of Glass-Ceramics from Coal Ashes, *Journal of European Ceramic Society* **2001**, 21, 2, 195–202.

Lima, A.T.; Ottosen, L.M.; Pedersen, A.J.; Ribeiro, A.B. Characterization of Fly Ash from Bio and Municipal Waste, *Biomass and Bioenergy* **2008,** 32, 277 – 282

Lin, C.J. and Chang, J.E.. Effect of Fly Ash Characteristics on the Removal of Cu(II) from Aqueous Solution. *Chemosphere* **2001,** 44, 1185–1192.

Lo, S.L. and Lin, C.F. Evaluating an iron coated sand for removing copper from water, *Wat. Sci. Technol.* **1994**, 30, 175.

Malek, R.I.A.; Roy, D.M. Electrokinetic Phenomena and Surface Characteristics of Fly ash Particles. *Mater. Res. Soc. Symp. Proc.* **1985**, 43, 41-50.

Manz, O.E. Coal Fly Ash: A Retrospective And Future Look, *Fuel* **1999**, pp 133–136.

Martell, A.E. and Motekaitis, R.J. Determination and Use of Stability Constants; *Texas A&M University, VCH Publishers Inc.,* 1988.

Maruyama, T.; Hannah, S.A.; Cohen, J.M. Metal removal by physical and chemical treatment processes. *Water Pollution Control Federation* **1975,** 47, 5, 962-975.

Mathur, R.; Chand, S.; Tezuka, T. Optimal Use of Coal for the Power Generation in India. *Energy Policy (India)* **2003,** 31, 3, 319–331.

Matsumoto, M.R.; Weber, A.S.; Kyles, J.H. Use of Metal Adsorbing Compounds (MAC) to Mitigate Adverse Effects of Heavy Metals in Biological Unit Processes. *Chem. Eng. Commun.* **1994**, 86, 1.

McCarthy, G.J.; Swanson, K.D.; Keller, L.P.; Blatter, W.C. Mineralogy of Western Fly Ash. Cement and Concrete Research, **1984**, 14, 4, 471-478.

Metcalf&Eddy. *Waste Water Engineering: Treatment and Reuse,* 4th edition.; McGraw Hill Higher Education, 2002.

Miwa, T.; Kitagawa, K.; Mizuta, M. Characterization of Coal Fly Ash Particles. *Nippon Kagaku Kaishi* **1991**, 5, 439-441.

Mohapatra, R.; Kanungo, S.B.; Physico-Chemical Characteristics of Fly Ash Samples from Thermal Power Plants of Orissa. *Indian J. of Eng. & Mat. Sci.* **1997,** 4, 271-281.

Mohapatra, R.; Rao, J.R. Some Aspects of Characterisation, Utilisation and Environmental Effects of Fly Ash. J. Chem. Technol. Biotechnol. **2001**, 76, 9-26.

Mollah, M.Y.A.; Promreuk, S.; Schennach, R.; Cocke, D.L.; Güler, R., Cristobalite Formation from Thermal Treatment of Texas Lignite Fly Ash, *Fuel* **1999**, 78, 1277–1282

Mott, H.W. and Weber, W.J. *Environ. Sci. Technol.* **1992,** 26, 1234.

Murugendrappa, M.V.; Khasim, S.; Ambika Prasad; M.V.N. Synthesis, Characterization and Conductivity Studies of Polypyrrole–Fly Ash Composites. *Bull. Mater. Sci.,* **2005**, 28, 6, 565–569.

Naegele, E. The Zeta-Potential of Cement, Part-II, Effect of pH Value. *Cem. Concr. Res.* **1986,** 16, 6, 853-863 .

Naegele, E.; Schneider, V. The Zeta-Potential of Cement, Pt.V, Effect of Surfactants. *Cem. Concr. Res.* **1988,** 18, 2, 257-264.

Naik, T.R., Ramme, B.W. and Kolbeck, H.J., In Ash Utilization Conference. Proceedings: Shanghai,Electric Power Research Institute, Palo Alto, CA, Project 2422, Vol. 3, 110-111, 1991.

Nathan, Y., Dvoracheka, M., Pelly, I., Mimran, U., Characterization of Coal Fly Ash from Israel, *Fuel,* **1999,** 78, 205–213.

NEQS. National Environmental Quality Standards for Municipal/Industrial Effluent and Gaseous Emission, 1995. SRO. 742(I)/93, dated: 24th August, 1992.

Nordstrom, D.K.; Alpers, C.N.; Ptacek, C.J.; Blowes, D.W. Negative pH and Extremely Acidic Mine Waters from Iron Mountain, California. *Environmental Science & Technology,* **2000***,* 34, 2, 254–258.

Nugteren, H.W.; Janssen-Jurkovicova, M.; Merkus, H.G.; Scarlett, B. Coal Fly Ash: Threatening Waste or Promising Product. *World Congr. Part. Technol.* **1998**, 3, 4027-4036.

O'Mara, W. C. *Handbook of Semiconductor Silicon Technology*; William Andrew Inc., 1990.

Öztaş, A.; Pala, M.; Özbay, E.; Kanca, E.; Çağlar, N.; Bhatti, M.A. Predicting the Compressive Strength and Slump of High Strength Concrete Using Neural Network.*Construction and Building Materials*, **2006**, 20, 9, 99 769-775.

Papandreou, A.; Stournaras, C.J.; Panias, *D.* Copper and Cadmium Adsorption on Pellets Made from Fired Coal Fly Ash, *J. Hazard. Mater*. **2007**, 148, 538-547.

Palmer, B.G.; Edil, T. B, Benson. Liners, C.H. Liners for Waste Containment Constructed with Class F And C Fly Ashes. *Journal of Hazardous Materials* **2000,** 76, 193–216.

Pandian, N.S. Fly Ash Characterization with Reference to Geotechnical Applications. *J. Indian Inst. Sci.* **2004**, 84, 189–216.

Patnaik, P. *Handbook of Inorganic Chemical Compounds*; McGraw-Hill, 2003.

Peloso, A.; Rovatti, M.; Ferraiolo, G. *Resources and Conservation* **1983,** 10, 211-220.

Pengthamkeerati, P.; T. Satapanajaru and P. Chularuengoaksorn, Chemical Modification of Coal Fly Ash for the Removal of Phosphate from Aqueous Solution. *Fuel* **2008**, 87, 2469–2476.

Polat, M.; Guler, E.; Akar, G.; Mordogan, H.; Ipekoglu, U.; Cohen, H., Neutralization of Acidic Mine Drainage by Turkish Lignitic Fly Ashes: Role of Organic Additives in the Fixation of Toxic Elements. *J. Chem. Technol. Biotechnol.* **2002a.,**77, 3, 372–376.

Polat, M.; Lederman, E.; Pelly, I.; Cohen, H. Chemical Neutralization of Acidic Wastes Using fly ash in Israel. *Journal of Chemical Technology and Biotechnology* **2002b**, 77, 377-381.

Polat, M.; Güler, E.; Lederman, E.; Cohen, H. Neutralization of an Extremely Acidic Sludge and Stabilization of Heavy Metals in Flyash Aggregates. *Waste Manag.* **2007**, 27, 4, 482-489.

Portland Cement Association. http://www.cement.org (accessed Feb 12, 2010).

Potgieter-Vermaak, S.S.; Potgieter, J.H.; Kruger, R.A.; Spolnik, Z.; R. Van Grieken. A Characterization of the Surface Properties of Ultra Fine Fly Ash (UFFA) Used in the Polymer Industry, *Fuel* **2005**, 84, 2295–2300.

Pradas, E.G.; Sanchez, M.V.A.; Perez, M.F.; Viciana, M.S. Adsorption of Malathion from Aqueous Solution on Homoionoic Bentonite Samples. *Agrochimica,* **1993**, 37, pp 104–110.

Puertas, F. and Fernandez-Jimenez, A., Mineralogical and Microstructural Characterisation of Alkali-activated Fly Ash/Slag Pastes, *Cement & Concrete Composites* **2003**, 25, 287–292.

Querol, X.; Whateley, B.J.L.; Fernfindez-Turiel, A.; Tuncali, E. Geological Controls On The Mineralogy And Geochemistry Of The Beypazari Lignite, Central Anatolia, Turkey. *International Journal Of Coal Geology* **1997**, 33, 255-271.

Querol, X.; Alastuey, A.; Plana, F.; Lopez-Soler, A.; Tuncali, E.; Toprak, S.; Ocakoglu, F.; Koker, A. Coal Geology And Coal Quality Of The Miocene Mugla Basin, Southwestern Anatolia, Turkey. *International Journal of Coal Geology* **1999,** 41, 311–332.

Raghavan, V. *Materials Science and Engineering*; PHI Learning Pvt. Ltd., 2004.

Reardon, E.J.; Czank, C.A.; Warren, C.J.; Dayal, R.; Johnston, H.M. Determining Controls on Element Concentrations in Fly Ash Leachate. *Waste Manag. Res.* **1995,** 13, 5, 435-450.

Reuss, M. Comparison of different methods for estimating the leaching of heavy metals from coal combustion waste. *Water Sci. Technol.* **1983**, 15, 11, 193-205.

Ricou, P., Lecuyer, I., Le Cloirec, L.P.,. Experimental design methodology applied to adsorption of metallic ions onto fly ash. *Water Res.* **2001**, 35, 965–976.

Roode, V.; Douglas, E.; Hemmings, R.T. X-ray diffraction measurement of glass content in fly and slags. *Cement and Concrete Research* **1987**, 17, 2, 183-197.

Rovatti, M.,Bisi, M., Ferraiolo, G. High Value Added Products from Difficult Wastes. *Resour. Conser. Recycl.* **1992**, 7**,** 271–283.

Roy, W.P. and Griffin, R.A. Illinois Basin Coal Fly Ashes. 2D Equilibria Relationships and Qualitatives Modeling of Ash/Water Relations. *Environ. Sci. Technol.* **1984,** 18, 1, 739-742.

Sarkar, A., Rano, R.; Mishra, K.K.; Sinha, I.N. Particle Size Distribution Profile of Some Indian Fly Ash-A Comparative Study to Assess Their Possible Uses. *Fuel Process. Technol.* **2005**, 86:11, 1221–1238.

Sarkar, A.; Rano, R.; Udaybhanu, G.; Basu, A.K. A Comprehensive Characterization of Fly Ash from a Thermal Power Plant in Eastern India. *Fuel Processing Technol.* **2006,** 87, 3, 259–277.

Schwab, A.P. Application of Chemical Equilibrium Modelling to Leachates from Coal Ash. *SSSA Spec. Pub.* **1995**, 42, 143-161.

Scheetz, B.E.; Earle, R. Utilization of Fly Ash. *Sol. State Mater. Sci.* **1998,** 3, 510–520.

Shackelford, C.D.; Benson, C.H.; Katsumi, T.; Edil, T.B.; Lin, L. Evaluating the Hydraulic Conductivity of GCLs Permeated with Non-standard Liquids *Geotextiles and Geomembranes* **2000,** 18, 2-4, 133-161.

Shan, X.Q.; Ni, Z.M.; Zhang, L. Determination of Arsenic in Soil, Coal Fly Ash and Biological Samples by Electrothermal Atomic Absorption Spectrometry with Matrix Modification. *Analytica Chimica Acta* **1983**, 151, 179-185.

Sheng, J., Huang; B. X.; Zhang, J.; Zhang, H.; Sheng, J.; Yu, S. and Zhang, M. Production Of Glass From Coal Fly Ash. *Fuel* **2003**, 82, 181–185.

Sigma–Aldrich. Material Safety Data Sheet - Potassium Chloride. July 2001.

Singh, S.P.; Tripathy, D.P; Ranjith, P.G. Performance Evaluation of Cement Stabilized Fly ash–GBFS Mixes as a Highway Construction Material. *Waste Management* **2008**, 28, 1331–1337.

Small, J.A. and Zoller, W.H. Single-Particle Analysis of the Ash from the Dickerson Coal-Field Power Plant, *NBS Spec Publ.* **1977**, 5, 651-658.

Solem-Tishmack, J.K.; McCarthy, G.J. High Calcium Coal Combustion By-products:Engineering Properties, Ettringite Formation, and Potential Application in Solidification and Stabilization of Selenium and Boron. *Cement and Concrete Research* **1995**, 25,v3, 658-670.

Stumm, M.; Morgan, J.J. *Aquatic Chemistry, John* Wiley & Sons, Inc., New York, 1996.

Sun B, Jia C and Shui C, Particle Morphology of Pulverized Fly ash (PFA) and its Physical Properties. *Guisuanyan Xuebao 1982,* 10, 1, 64-69.

Sushil, S. and Batra, V.S. Analysis of Fly Ash Heavy Metal Content and Disposal in three thermal power plants in India. *Fuel,* **2006,** Volume 85, Issues 17-18, 2676-2679.

Swaine, D.J. *Trace Elements in Coal,* Butterworths: London, England ,1990.

Swanepoel, J.C. and Strydom, C.A. Utilisation of Fly Ash in a Geopolymeric Material. *Applied Geochemistry* **2002,** 17, 1143–1148.

Sykorora, I., Smolik, J.; Schwarz, J.; Kerkkone, O; Kucera, J.; Havranek, V. Composition and Morphology of Fly Ash from Fluidized Bed Combustion of Brown Coal, *Proc. ICCS* **1997**, 2, 1187-1190.

Tahir, S.S. and Rauf, N. Removal of Fe (II) from the Wastewater of a Galvanized Pipe Manufacturing İndustry By Adsorption onto Bentonite Clay. *Journal of Env. Manag.* **2004**, 73, 285–292.

TA Instruments: Thermal Analysis and Rheology http://www.tainstruments.co.jp/application/pdf/Thermal_Library/Thermal_Solutions/TS029 (accessed March 13, 2009)

Talbot, R.W.; Anderson, M.A.; Andren, A.W. Qualitative Model of Heterogeneous Equilibria in a Fly Ash Pond. *Environ. Sci. Technol.* **1978**, 12, 1056–1062.

Tamimi A. *Class Notes.* Hebron University, Hebron, West Bank, Paletsine, 2003.

Theis, T.L. and Wirth, J.L., Sorptive Behavior of Trace Metals on Fly Ash in Aqueous Systems. *Environ. Sci. Technol.* **1977**, 11, 1096–1100.

Ural, S. Comparison of Fly Ash Properties from Afsin–Elbistan Coal Basin, Turkey. *Journal of Hazardous Materials* **2005***,* B119, 85–92.

Ülkü, B.Ü.; Polat, M.; Polat, H. In 2nd Int. Conf. on Eng. for Waste Vol., Patras, Greece, 3-5 June 2008.

Üzelyalçin, B. and Polat. M. In *Xth International Mineral Processing Symp., Çeşme, TURKEY,* Oct 5-7, 2004.

Vassileva, C.G.; Karayigit, A.I.; Bulut, Y.; Alastuey, A.; Querol, X. Phase–Mineral And Chemical Composition of Composite Samples from Feed Coals, Bottom Ashes And Fly Ashes At The Soma Power Station, Turkey, *International Journal of Coal Geology* **2005**, 61, 35– 63

Vassilev, S.V.; Menendez, R.; Somoano, M.D.; Tarazona, M.R.V. Phase-Mineral And Chemical Composition Of Coal Fly Ashes As A Basis For Their Multicomponent Utilization. 2. Characterization Of Ceramic Cenosphere And Salt Concentrates. *Fuel* **2004**, 83, 585-603.

Viraraghavan, T. and Demaria Alfaro, F. Adsorbtion of Phenol from Wastewater by Peat, Fly Ash and Bentonite. *Journal of Hazardous Mat.* **1998***, 57,* 59-70.

Viraraghavan, T. and Rao, G.A.K., Adsorption of Cadmium and Chromium from Wastewater by Fly Ash. *J. Environ. Sci.-Health Part A* **1991,** 26, 5, 721–753.

Wang, S. and Viraraghavan, T. Wastewater Conditioning by Fly Ash. *Waste Manage.* **1997,** 17, 7, 443–450.

Wang, L.K.; Hung, Yung-Tse; Nazik, K. *Handbook of Advanced Industrial and Hazardous Wastes Treatment,* CRC Press, 2009.

Ward, C.R.; Jankowski, A.J.; French, D. B.; Groves, S. Mobility Of Trace Elements from Selected Australian Fly Ashes and its Potential Impact on Aquatic Ecosystems. *Fuel* **2006***,* 85, 243–256.

Wasay, S.A. Leaching Study of Toxic Trace Elements from Fly Ash in Batch and Column Experiment. *J. Environ. Sci. Health Part-A* **1992,** A27, 697-712.

Weng, C.H. and Huang, C.P. Treatment of Metal Industrial Wastewater by Fly Ash and Cement Fixation. *J. Envir. Engrg.* **1994,** 120, 6, 1470-1487.

White, S.C. and Case, E.D. Characterization of fly ash from coal-fired power plants. *J. Mat. Sci.,* **1990**, 5215-5219.

Woolard, C.D.; Strong, J.; Erasmus, J.R. Evaluation of The Use Of Modified Coal Ash As A Potential Sorbent For Organic Waste Streams. *Applied Geochemistry* **2002,** 17, 1159–1164.

Yeheyis, M.B.; Shang, J.Q.; Yanful, E.K. Feasibility of Using Coal Fly Ash for Mine Waste Containment. *J. Envir. Engrg.* **2010**, 136, 7, 682-690.

Zhou, Y., Levy, J. I., Evans, J. S.; Hammitt, J. K. The influence of geographic location on population exposure to emissions from power plants throughout China. Environment International **2006**, 32, 365-373

Zoorob, S.E. and L.B. Suparma. Laboratory Design and Investigation of the Properties of Continuously Graded Asphaltic Concrete Containing Recycled Plastics Aggregate Replacement (Plastiphalt). *Cement Concrete Comp.* **2000**, 22, 233–242.

Zwozdziak, J.W.; Jagiello, R.; Kowalski, M.; Zwozdziak, A.B.; Lisowski, A. Identification of Coal Fly Ash Particles in Ambient Aerosols. *Environ. Prot. Eng.* **1989,** 14, 1, 23-37.

VITA

Name: **Berna ÜZELYALÇIN ÜLKÜ**

Date / Place of birth: 22.07.1975 / Manisa

Education and degrees: **Ph.D. (Chemical Engineering) [2002-2010]**
İzmir Institute of Technology, İzmir, Turkey.
Dissertation: *"Fixation and Stabilization of Heavy Metals in a Product Composed of Fly Ash and Industrial Acidic Wastes"*. Advisor: Prof.Dr. Mehmet Polat, Co-advisor: Prof.Dr. Hürriyet Polat.
M.Sc. (Biotechnology) [1999-2002]
İzmir Institute of Technology, İzmir, Turkey.
Dissertation:*"Effects of Trace Elements on the Production of Baker's Yeast"*. Advisor: Prof.Dr. Şebnem Harsa, Co-advisor: Prof. Dr. Ulgar Güvenç.
B.Sc. (Food Engineering) [1992-1998]
Ege University, İzmir, Turkey.

Related work experience: **Research assistant**
Biotechnology and Bioengineering, İzmir Institute of Technology, İzmir, Turkey [1999-2002].
Research assistant
Department of Chemical Engineering, İzmir Institute of Technology, İzmir, Turkey [2002-2010].

Selected publications:

B.Üzelyalçın, M.Polat. *"Use of low-cost materials for heavy metal removal in wastewater"*. X[th] International Mineral Processing Symposium, Çeşme, Türkiye, (5-7 October 2004).

B.Ü.Ülkü, M.Polat, H. Polat. *"Evaluation of the use of fly ashes for industrial wastewater utilization"* 2nd Int. Conf. on Eng. for Waste Vol., Patras, Greece, (3-5 June 2008).

B.Ü.Ülkü, M.Polat, H.Polat, K.Sekeroglu. *"Characterization of fly ashes and the aggregates produced from ash-waste mixtures"* XIth International Mineral Processing Symposium, Antalya, Türkiye, (21-23 October 2008).

B.Ü.Ülkü, M.Polat. *"An economical chemical neutralization method for the destruction of industrial acidic wastes"*.EMCC6-6th Chem. Eng. Conf. for Collaborative Research in Eastern Mediterranean Countries, Antalya-Türkiye, (7-12 March 2010).